Identifying cellular and molecular mechanisms controlling lineage fate of lymphoid-primed multipotent progenitors and alterations in aging

Sneha A. Borikar

in partial fulfillment of the requirements for the degree of

PhD

in

Genetics

Tufts University, Sackler School of Graduate Biomedical Sciences

May 2017

Adviser: Jennifer Trowbridge, PhD

Abstract

Hematopoiesis is a dynamic process responsible for producing the cellular components of the blood system for the life of an organism. With aging, the robustness and function of the immune system is compromised, in part caused by a general shift in cell production towards the myeloid cell types at the expense of the lymphoid and erythroid cell types. This bias can be seen in the clinical manifestations of increased risk of myeloid proliferative disorders and leukemias as well as susceptibility to anemias and infection in older adults. While hematopoietic stem cells (HSCs) have long been considered to be the foundation of hematopoietic cell production, recent *in vivo* lineage tracing studies have shown that the contribution of multipotent progenitors (MPPs) to long-term, steady-state hematopoiesis is greater than previously thought. However, how changes in the composition and function of the MPP compartment contribute to age-related phenotypes such as myeloid skewing were unknown. To interrogate functional changes of MPP cells in a high-throughput assay, I developed a novel *in vitro* culture system that was also adapted for single cell fate mapping. Using this assay and other techniques, I have discovered the frequency and function of a particular subset of MPP cells, lymphoid-primed multipotent progenitors (LMPP/MPP4), decreases with aging. These changes contribute to increased myeloid production and decreased B-lymphoid production with aging. In an independent study, I have utilized the high-throughput assay I developed to screen for epigenetic regulators controlling myeloid versus lymphoid cell production from LMPP/MPP4 cells. I have discovered that altered expression of

the histone lysine methyltransferase *Kmt5a* in LMPP/MPP4 cells causes expansion of myeloid cell production from these progenitors. This study suggests that specific epigenetic mechanisms regulate lineage production from MPP cells. Together, this work has direct implications for better understanding the molecular drivers of biased myeloid lineage production from lymphoid-primed multipotent progenitor cells and how this contributes to age associated myeloid skewing of hematopoiesis and malignancy.

Acknowledgements

First and foremost, I would like to thank my supervisor, Dr. Jennifer Trowbridge from the Jackson Laboratory (JAX; Bar Harbor, ME) for her support throughout the duration of my PhD study. I am truly honored to be her first graduate student. This thesis was not possible without her guidance both personally and professionally. I am grateful for being given the opportunity to work under her supervision.

I would like to thank current and former lab members of the Trowbridge Laboratory, including but not limited to, Rebecca Bell, Olivia Erickson, Eraj Khokar, Lauren Kuffler, Matthew Loberg, Vivek Philip, and Kira Young. I thank Will Schott and Ted Duffy from flow cytometry core services for their assistance in sorting and FACS analysis. I thank my committee, Dr. Robert Braun, Dr. Ewelina Bolcun-Filas, Dr. Kyuson Yun, Dr. Steven Munger, Dr. Gavin Schnitzler, and also past members Dr. Kevin Mills and Dr. Dave Harrison. Thank you to the Genetics Program at Tufts University and the Education Department at Jackson Laboratory.

I would like to acknowledge my incredible friends Leah Graham, Meagan Montesion, Mandy Hung, and Kaiden Waldron-Francis for being constant support and taking me in to their local families. Last but not least, I could not have continued my research without the unconditional and unwavering support and encouragement from my parents and my incredible brother. They motivate me everyday. I am completely indebted to them.

Table of Contents

List of Figures

List of Tables

List of Abbreviations

4', 6-diamidino-2-phenylindole.....DAPI
Analysis of variance.....ANOVA
Bone marrow.....BM
Burst Forming Unit-Erythroid.....BFU-E
Complementary DNA.....cDNA
Common lymphoid progenitors.....CLP
Common myeloid progenitors.....CMP
Colony forming unit.....CFU
Deoxyribonucleic acid.....DNA
Dimethylsulfoxide.....DMSO
Double Negative 2.....DN2
Dulbecco's Modified Eagle Medium.....DMEM
Ethylenediaminetetraacetic acid.....EDTA
Fetal bovine serum.....FBS
Fms-like tyrosine kinase 3.....FLT3
Forward scatter.....FSC
Gene set enrichment analysis.....GSEA
Granulocyte-macrophage progenitors.....GMP
Green fluorescent protein.....GFP
Hematopoietic stem cells.....HSC
Hematopoietic stem and progenitor cells.....HSPC
Interleukin.....IL
Iscove's Modified Dulbecco's Medium.....IMDM
Leukemia inhibitory factor.....LIF
Luria Bertani.....LB
Lymphoid-primed multipotent progenitors.....LMPP
Megakaryocyte-erythroid progenitors.....MEP
Messenger ribonucleic acid.....mRNA
Month old.....mo
Multipotent progenitors.....MPP
Phosphate buffered saline.....PBS
Phycoerythrin.....PE
Polymerase chain reaction.....PCR
Principal component analysis.....PCA
Propidium iodide.....PI
Reverse transcription.....RT
Ribonucleic acid.....RNA
Roswell Park Memorial Institute.....RPMI
Stem cell factor.....SCF
Transcripts per million.....TPM
T cell receptor.....TCR

List of Copyrighted Materials Produced By Author

Young, K., Borikar, S., Bell, R., Kuffler, L., Philip, V., & Trowbridge, J. J. (2016). Progressive alterations in multipotent hematopoietic progenitors underlie lymphoid cell loss in aging. *Journal of Experimental Medicine*, jem-20160168.

CHAPTER 1: INTRODUCTION

1.1 Hematopoiesis

Hematopoiesis refers to the process of generating all of the cellular components of the blood system. In developing mammalian embryos, blood formation occurs from clusters of angioblasts called “blood islands” in the yolk sac (mouse E7.5-E8.5), while hematopoietic stem cells (HSCs) originate in the aorta-gonadal-mesonephros (AGM) region of developing embryos (mouse E10.5) (Bertrand et al., 2005; Birbrair and Frenette, 2016; Dzierzak and Speck, 2008). Shortly after birth, HSCs home to the bone marrow which then becomes the primary location of blood formation for the entire organism (Coskun et al., 2014). However, maturation, activation, and proliferation of some mature cell types occurs in peripheral hematopoietic organs including the spleen, thymus, and lymph nodes (Fernandez and de Alarcon, 2013). Terminally differentiated hematopoietic cells can be divided into three distinct lineages- erythroid, myeloid, and lymphoid. The erythroid lineage includes red blood cells, megakaryocytes, and platelets. The myeloid lineage largely constitutes the innate immune system including macrophages and granulocytes (neutrophils, eosinophils, and basophils), and represents the first line of defense in a host’s immune system. The lymphoid lineage largely constitutes the adaptive immune system, including B cells, T cells, and natural killer cells, which identify and remove specific pathogens.

The accessibility and distinct morphology of many of the hematopoietic cell types has allowed this system to become one of most highly defined differentiation cascades in mammalian tissues. Technological advancements such as antibody-

based flow cytometry, *in vitro* culture propagation, *in vivo* transplantation, and genetically engineered mouse models have refined and continue to further our understanding of distinct cell identities, functional potential, and lineage relationships between hematopoietic cells.

1.1.1 Bone marrow hematopoiesis

In adults, hematopoiesis takes place in the bone marrow and derives from the long-term hematopoietic stem cell (LT-HSC). Located atop the hematopoietic hierarchy, LT-HSCs are marked by their life-long ability to reversibly switch from dormancy to self-renewal as well as the ability to differentiate into all of the cellular components of blood (Wilson et al., 2008). Short-term hematopoietic stem cells (ST-HSCs) and multipotent progenitors (MPPs), although still multipotent, have limited ability for self-renewal (Reya et al., 2001). While ST-HSCs and MPPs are capable of producing multilineage cell types, it remains to be resolved whether there is a defined sequential restriction of cell fate potential or whether there is continued plasticity of cell fate potential during differentiation.

In the classical model of hematopoiesis, each step in differentiation is made by a decision between two fates, thereby gradually diminishing lineage potential **(Figure 1.1A)**. Identification of the common myeloid progenitor (CMP) and common lymphoid progenitor (CLP) marked the differentiation branch of MPPs into the myeloid and lymphoid lineages, respectively. CMPs give rise to all myeloid cell types via the commitment to either megakaryocyte-erythroid progenitors (MEP) or granulocyte-macrophage (GMP) progenitors (Akashi et al.,

2000), while CLPs exhibited the potential to generate cells of B- ,T-, and natural killer cells (Kondo et al., 1997). More recently, this model has been contested with the identification of lymphoid-primed multipotent progenitors (LMPPs), marked by high Flk2 expression, which have both lymphoid and myeloid differentiation potential but have limited megakaryocyte and erythroid potential (Adolfsson et al., 2005). Revised models dictate early bifurcation of erythroid lineage cell types followed by later bifurcation of myeloid and lymphoid cell types (Notta et al., 2016) **(Figure 1.1B)**. Supporting this model, recent single-cell assays have demonstrated that the classically defined CMP is either highly transient or non-existent in normal, physiological hematopoiesis in mice and humans (Notta et al., 2016; Paul et al., 2015).

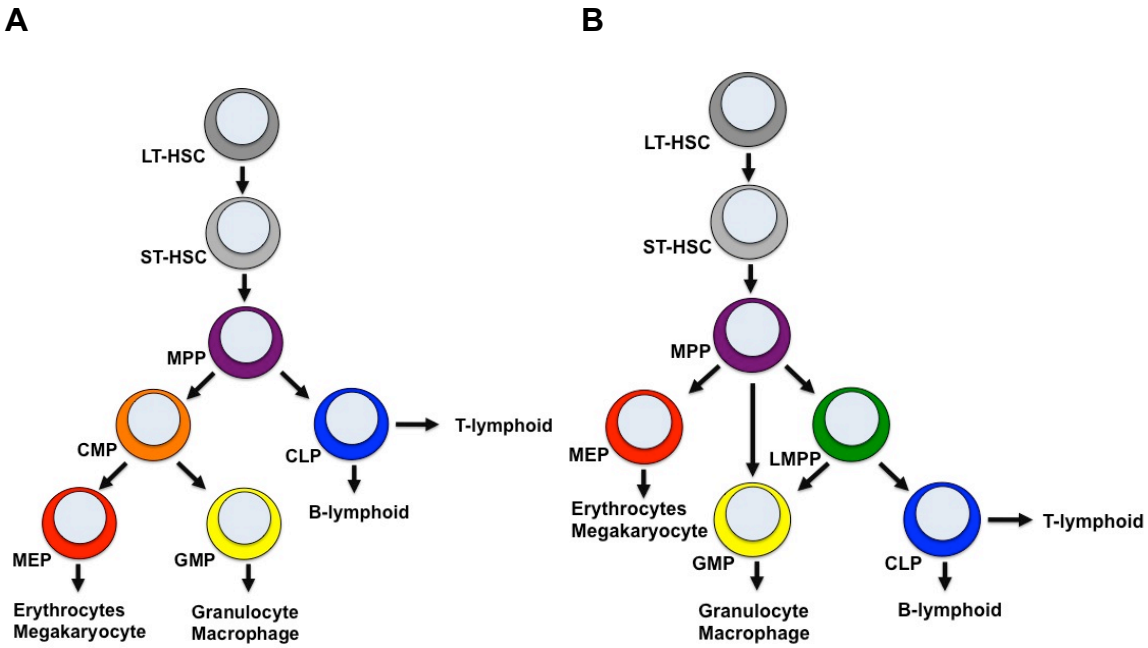

Figure 1.1 | Models of the hematopoietic hierarchy. (A) Classical model in which MPPs lose their multipotent capacity in a stepwise fashion as they differentiate into lineage-restricted progenitors (CMPs or CLPs) which in turn undergo further lineage commitment to produce mature cell types. **(B)** Revised model in which early bifurcation of erythroid committed progenitors (MEP) is followed by later birfurcation of myeloid and lymphoid lineage progenitors (GMP or CLP). LT-HSC, long-term hematopoietic stem cell; ST-HSC, short-term hematopoietic stem cell; MPP, multipotent progenitor; CMP, common myeloid progenitor; LMPP, lymphoid-primed multipotent progenitor; MEP, megakaryocyte-erythroid progenitor; GMP, granulocyte-macrophage progenitor; CLP, common lymphoid progenitor.

To define and interrogate functional heterogeneity in the multipotent progenitor compartment, expression of the cell surface markers CD150 and CD48 were found to separate functional sub-populations of MPPs; MPP2, MPP3, and MPP4 (Wilson et al., 2008). The MPP2, MPP3, and MPP4 subpopulations predominantly differentiate to give rise to erythroid, myeloid, and lymphoid cell types, respectively, although this is not found to be exclusive **(Figure 1.2)**.

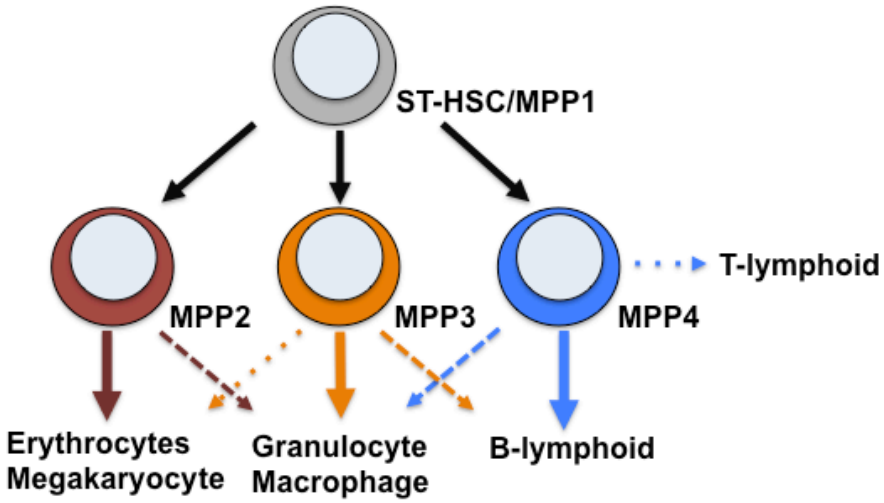

Figure 1.2 | Functionally defined subsets within the multipotent progenitor compartment. MPPs can be separated into three distinct lineage-primed populations derived from the ST-HSC (also termed MPP1). MPP2 predominantly generates megakaryocyte-erythroid cells, MPP3 predominantly generates granulocyte–macrophage cell types while MPP4 predominantly generates B-lymphoid cell types. Solid arrows represent dominant lineage output while dashed arrows represent cell potentials that are less robust.

1.1.2 Mature Hematopoietic lineages

1.1.2.1 Erythroid

Erythroid differentiation begins in the bone marrow from the MEP. The expression of *Gata-1*, the master regulator of erythropoiesis, begins to increase at this progenitor stage, likely priming it for erythroid differentiation (Hu et al., 1997). Expression of *Gata-1* peaks in late-stage erythroid progenitors, but decreases gradually with further differentiation. *Gata-1* regulates key erythroid target genes including *Epo* and the *Epo* receptor (*EpoR*) both of which are necessary for erythropoiesis (Ferreira et al., 2005). Megakaryocytes result from MEP differentiation induced by Thrombopoietin (*Tpo*) rather than *Epo* (Bunting et al., 1997). Once the cell has completed differentiation and become a mature megakaryocyte, it begins the process of producing platelets, which are needed for the formation of blood clots. The cell DNA is replicated up to four times and begins to become granular (Choi et al., 1995). The “proto-platelet” explosively breaks up into smaller platelets giving rise to up to 5000 new platelets. In a healthy adult, 1×10^{11} platelets are produced daily, highlighting the incredible scale of cell production from a single progenitor cell (Harker et al., 2000).

1.1.2.2 Myeloid

Production of monocyte or granulocyte cell types is termed myelopoiesis. These cell types constitute the innate immune system and the process of their terminal differentiation is highly conserved among species. Differentiation towards the macrophage or granulocyte cell fate requires two major transcription factors,

Pu.1 and *C/ebp*α. The expression of these factors increases from HSC differentiation through the CMP and GMP progenitor populations (Friedman, 2002). *Pu.1* is found to be expressed in both myeloid and lymphoid cells, while *C/ebp*α is found predominantly in myeloid cells (Friedman, 2002; Scott et al., 1994; Scott et al., 1992). Although *Pu.1* and *C/ebp*α are both required for macrophage and neutrophil specification, their relative levels regulate the macrophage or neutrophil cell fate choice from the GMP; *Pu.1* expression increases to promote neutrophil formation while *C/ebp*α expression increases to drive macrophage development (Dahl et al., 2003; Iwasaki et al., 2006; Laslo et al., 2006).

1.1.2.3 Lymphoid

Lymphoid lineage commitment begins in the bone marrow with the CLP defined by the increased expression of the Interleukin-7 receptor (*Il-7R*), essential for lymphoid development (Kondo et al., 1997). The CLP is capable of differentiating into the B-lymphoid committed pre-pro-B cell or colonize the thymus and differentiate into early thymocyte progenitors (ETPs). While ETPs retain myeloid and lymphoid potential as measured by *in vitro* studies, they exist transiently and rapidly differentiate into T-lymphoid and NK cells *in vivo* (Boehm and Bleul, 2006). ETPs undergo step-wise differentiation reaching the Double Negative 2 (DN2) thymocyte stage where they may mature into either NK cells or continue commitment by T-Cell Receptor (TCR) gene rearrangement and stringent processing into a CD4+ or CD8+ T cells (Rothenberg et al., 2008; Wu, 2006).

CLPs that do not migrate to the thymus begin differentiation towards B-lymphopoiesis. During several stages of maturation including V(D)J recombination and changes in gene expression patterns CLPs become immature B-cells (Loder et al., 1999; Pelanda and Torres, 2012). Immature B-cells complete development in the spleen and can be further activated in the spleen or the lymph nodes.

While mature cell types are highly committed and restricted to their lineage cell types, progenitors exhibit greater flexibility in their lineage potential, which may be influenced by extrinsic factors including cytokines. Although in GMPs with high levels of *Pu.1,* neutrophil formation is induced, in the presence of the granulocyte-colony stimulating factor (G-CSF), macrophage development is induced in the presence of Interleukin-3 (IL-3) (Dahl et al., 2003). Additionally, *in vitro* studies have found that GMPs in lymphoid culture conditions can produce mature B and T lymphoid cell types, although, their production *in vivo* is limited (Ng et al., 2009). Likewise CLPs and DN1s display surprisingly robust myeloid potential when plated with OP9-DL1 *in vitro* stromal co-cultures but display little myeloid potential *in vivo* as well as in methylcellulose cultures (Richie Ehrlich et al., 2011). This fluidity in cell output may be needed to meet the changing demands of the blood system in times of infection, injury, and regeneration.

1.1.3 Functional assays for hematopoietic stem and progenitor cells

Unlike many other tissue systems, hematopoietic stem and progenitor cells do not exist in a fixed location that can be easily histologically evaluated. Instead, examining prospective hematopoietic stem and progenitor cells using a series of cell surface markers remains the most reliable phenotypic assay, yet provides no functional data. To meet this need, multiple *in vitro* and *in vivo* assays have been developed to functionally evaluate immature hematopoietic cells.

In assays using an input of functionally heterogeneous cells, it is impossible to discriminate the progeny from each individual progenitor. Therefore, in these "bulk" assays, the precise number of cells contributing to a given end point cannot be inferred by only measuring the total number of cells or lineages recovered (Coulombel, 2004). Instead, a single cell assay, although less robust, can identify proliferative and lineage differentiation properties of individual cells. This type of precise evaluation of primitive hematopoietic stem and progenitor cells is essential to understand the mechanisms of cellular fate.

1.1.3.1 *In vitro* assays

In vitro colony formation assays are powerful tools to determine the functional potential of stem and progenitor cells, measuring both their proliferative and differentiation capacities **(Table 1.1)**. Semi-solid media, usually methylcellulose-based, is supplemented with growth factors that support the growth of each lineage cell type. The 3-dimensional nature of these assays allows the progeny of each progenitor to remain separated for easy quantification and the size of

each colony is roughly proportional to the proliferative potential of the progenitor (Bradley and Metcalf, 1966). Hematopoietic progenitor cell frequencies can be determined by performing colony forming cell assays (CFU) in as little as 7-10 days. Using these assays, progenitors such as colony forming unit erythrocytic (CFU-E), blast forming unit erythrocytic (BFU-E), colony forming unit granulocytic and monocytic (CFU-GM), colony forming unit granulocytic, erythrocytic, monocytic and megakaryocytic (CFU-GEMM), and pre-B lymphoid (CFU-preB) can be quantified. These assays provide some functional analysis, as the ability to form a multi-lineage colony requires both the ability to differentiate and limited self-renewal (Coulombel, 2004; Cumano et al., 1990).

It is known that stem and progenitor cells require highly specialized niches consisting not only of extracellular signals but also structural support. To replicate this environment *in vitro*, a stromal co-culture system can be used. The feeder layer can be either primary bone marrow stromal cells or an established cell line. The stromal cell line used defines the readout of the assay. For example, to assay the most primitive cell types, such as HSCs, the cobblestone area-forming cell (CAFC) and long-term culture initiating cell (LTC-IC) assays can be used with the M2-10B4 cell line to readout oligopotency and repopulation capacity (van Os et al., 2004). Both of these assays require more extensive self-renewal ability than the CFU assay and are thus more time-consuming (Ploemacher et al., 1989; Sutherland et al., 1989). For less primitive progenitors, the OP9 or the OP9-DL1 cell lines can be used for determining either B-lymphoid or T-lymphoid

potentials, respectively (Barker and Verfaillie, 2000; Cumano et al., 1990; Schmitt and Zuniga-Pflucker, 2002).

Assay	Duration	HSC readout	Lineage Potentials Assayed
CFU-Myeloid	7-14 days	×	Myeloid
CFU-Lymphoid	7-14 days	×	B-lymphoid
OP9-DL1	20 days	×	T-lymphoid
OP9 Stromal	20 days	×	B-lymphoid
Long-Term Culture Initiating Assay (LTC-IC)	2 months	✓	Myeloid

Table 1.1 | *In vitro* functional assays for hematopoietic stem and progenitor cells.

Although these *in vitro* cultures are strong measures of differentiation potential, there are many limitations to assaying HSCs and progenitors by *in vitro* methods. These assays cannot measure the true functional potential of HSCs to home and engraft in bone marrow or their ability for long-term self-renewal (Coulombel, 2004). These features make the HSC distinct from its progeny and are fundamental to its cell identity. Additionally, variations in procedures and stromal cell layers can result in different outcomes in different laboratory environments. Furthermore, re-isolating purified hematopoietic cells after a co-culture for downstream molecular applications or transplantation is challenging due to their tendency to strongly adhere to neighboring stromal cells.

1.1.3.2 *In vivo* transplantation assays

Similar to *in vitro* assays, *in vivo* bone marrow transplantation assays measure two cellular properties: longevity and multipotentiality. *In vivo* assays rely on the discrimination between donor and recipient cells, achieved by using congenic strains such as C57BL/6J and B6.SJL that express different isoforms of the CD45 receptor or a PCR-based method for male donor Y-chromosome in female recipients. Transplantation assays can range from short-term to those of many months **(Table 1.2)**. Short term *in vivo assays* are able to measure progenitor cells that are more immature than CFUs but more mature than HSCs. Colony-forming unit spleen cells (CFU-S) form mixed colonies in the spleen, while pre-CFU-S cells are able to produce CFU-S in secondary recipients (McCulloch et al., 1964). The ability of transplanted cells to home to the bone marrow is another quantifiable aspect of functionality not assayable *in vitro* (Purton and Scadden, 2007). Marrow-repopulating activity (MRA) is used to define production of differentiated cells of the lymphoid and myeloid lineages in the bone marrow for many months after transplantation (Bradley and Hodgson, 1979; Jordan et al., 1990; McCulloch and Till, 1964). While all of these assays measure functional capacity of a population of stem or progenitor cells, they cannot compute how many of the clones within the pool of cells are actually functional.

Assay	Duration	HSC readout	Stem Cell Properties Assayed			
			Homing to Bone Marrow	Multilineage Differentiation	Self-Renewal	Reference
CFU-S	12 days	×	×	✓	×	(McCulloch and Till, 1964)
Pre-CFU-S	1 month	×	×	✓	✓	(McCulloch and Till, 1964)
Marrow Repopulating Assay (MRA)	4 months	✓	✓	✓	×	(Bradley and Hodgson, 1979)
Competitive repopulation (CRU)	4 months	✓	✓	✓	×	(Harrison, 1980)
Limiting Dilution Assay (LDA)	4 months	✓	✓	✓	×	(Harrison, 1980)
Serial transplantation	6+ months	✓	✓	✓	✓	(Harrison, 1980)

Table 1.2 | *In vivo* functional assays for hematopoietic stem and progenitor cells.

The competitive repopulation unit assay (CRU) or limiting dilution assay (LDA) can quantify the proportion of single HSCs that will functionally read out as long term repopulating cells (LTRCs). Decreasing numbers of donor test cells are injected into conditioned mice with a defined competitive repopulating population, usually whole bone marrow, and the proportion of recipients positive for donor-derived repopulation is measured. Purified populations are coinjected with whole bone marrow to prevent radiation-induced lethality of the recipient mice (Harrison, 1980; Jones et al., 1990). While these assays measure long-term multilineage differentiation potential, the most stringent assay for stem cell self-renewal is the serial transplantation assay. Here, four months after transplantation, marrow from transplanted recipients is isolated and transplanted into secondary recipients (Lemischka et al., 1986). The long-term engraftment in secondary recipients is necessary to exclude any contribution from short-term

HSC and progenitors. Therefore, only primitive long-term stem cells with high self-renewal capacity will repopulate the secondary recipient.

In vivo assays remain the best ways to measure HSC content but exhibit many limitations. Readouts of lineage potential may be masked by donor cell defects in engraftment and homing to the bone marrow niche. Differentiation kinetics of test populations may be altered or even arrested, impacting readouts of multilineage differentiation and engraftment (Purton and Scadden, 2007). While each assay provides unique information about stem and progenitor cell properties, *in vivo* assays are costly and time-consuming, making preliminary *in vitro* screening prior to initiating *in vivo* assays appealing.

1.2 Aging Hematopoiesis

Hematopoietic aging is an evolutionarily conserved process in humans and mice that affects the balanced generation of all blood cell lineages. Similar features of aging mouse HSCs (20-24 months) are seen in older human HSCs (above 65 years); both human and mouse HSCs are increased in frequency but decreased in engraftment and lymphoid potential (Pang et al., 2011). The mouse is, therefore, a powerful model to study cellular and molecular alterations that occur in aging of humans **(Figure 1.3)**. The functional capacity and frequency of blood cells changes dramatically with age, and immune deficiency and anemia are considered major contributory factors to the increased morbidity and mortality in elderly populations.

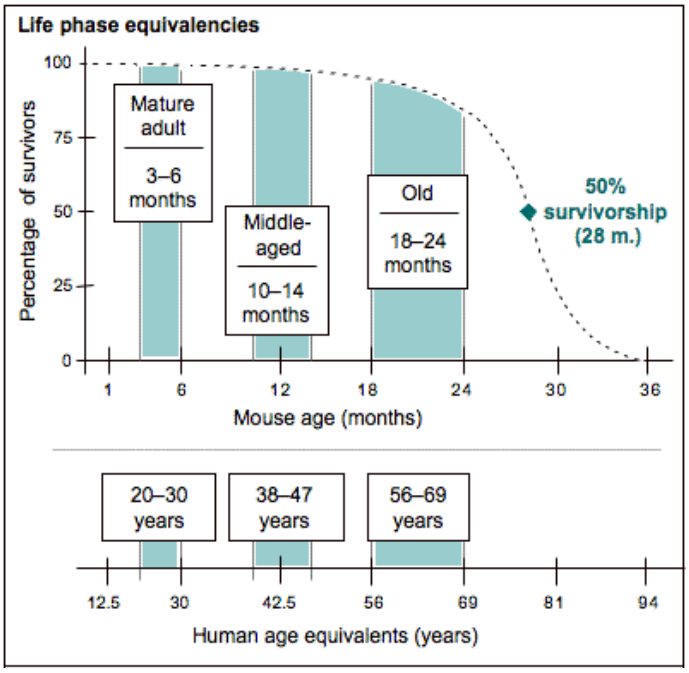

Figure 1.3 | The mouse as a model of aging. The equivalent ages of human development in mice are now well-defined and have made the mouse a powerful model organism to study aging phenotypes. (Copyright: Flurkey K, Currer JM, Harrison DE. 2007)

1.2.1 Cellular changes in aging

Aging causes alterations in cellular composition of the hematopoietic system, beginning with the most primitive cell type, the LT-HSC. The phenotypic HSC compartment expands in frequency and absolute number due to increased self-renewal (Rossi et al., 2005). However as mice age, HSCs exhibit reduced homing and engraftment capabilities (Dykstra et al., 2011; Liang et al., 2005; Morrison et al., 1996). Aged HSCs are also more easily mobilized into the peripheral blood (Xing et al., 2006). Despite having similar *in vitro* functionality, LT-HSCs from aged mice when measured in long-term transplantation assays were two-fold less capable of reconstituting lethally irradiated bone marrow compared to young HSCs (Morrison et al., 1996). In addition, HSCs exhibit diminished lymphoid differentiation potential and increased myeloid potential (Beerman et al., 2013; Rossi et al., 2005; Sudo et al., 2000; Sun et al., 2014a). Aged HSCs are enriched for the myeloid-biased cell surface marker CD41 (Gekas and Graf, 2013).

Under steady-state conditions in young mice, bone marrow hematopoiesis generates a balanced supply of each of the mature hematopoietic cell types that are essential for the maintenance of immune homeostasis. This balance is necessary as immune responses are induced by coordination of both the adaptive and the innate immune systems. With age, a dramatic decline in the production of naïve T cells as well as the clonal expansion of memory and effector T cells leads to decreased immune defense and increased autoimmunity (Dorshkind et al., 2009; Van Zant and Liang, 2012). The number of B cells

decreases with age and old B cells generate antibodies with less affinity and diversity (Han et al., 2003). Furthermore, other types of immune cells, such as natural killer and dendritic antigen-presenting cells, have been shown to diminish and functionally deteriorate with old age (Mocchegiani and Malavolta, 2004; Uyemura et al., 2002). In contrast to the lymphoid lineages, the mature myeloid compartment is expanded with aging inducing a proinflammatory environment in the body (Franceschi et al., 2007).

A majority of aging hematopoietic studies have focused on the role of the HSC in producing these downstream alterations. Two models are proposed for HSC aging at a population level- a classical population shift model and a clonal alteration model **(Figure 1.4).** The population shift model assumes a homogenous HSC population undergoing uniform change with aging, where aged stem cells are altered to differentiate towards the myeloid lineage at the expense of the lymphoid lineage (Cho et al., 2008) **(Figure 1.4A)**. However, in a clonal alteration model of HSC aging, the HSC compartment is heterogeneous and age-related hematopoietic phenotypes are derived from a changing composition of distinct classes of HSCs (Beerman et al., 2010; Cho et al., 2008; Dykstra et al., 2011; Morita et al., 2010) **(Figure 1.4B)**. Supporting this model, three functional classes of HSCs have been identified: balanced, lymphoid-biased, and myeloid-biased stem cells. All three subsets of HSCs exist in both young and old mice, but the composition shifts with aging such that the myeloid-biased HSC subpopulation is selectively expanded and causes downstream lineage skewing.

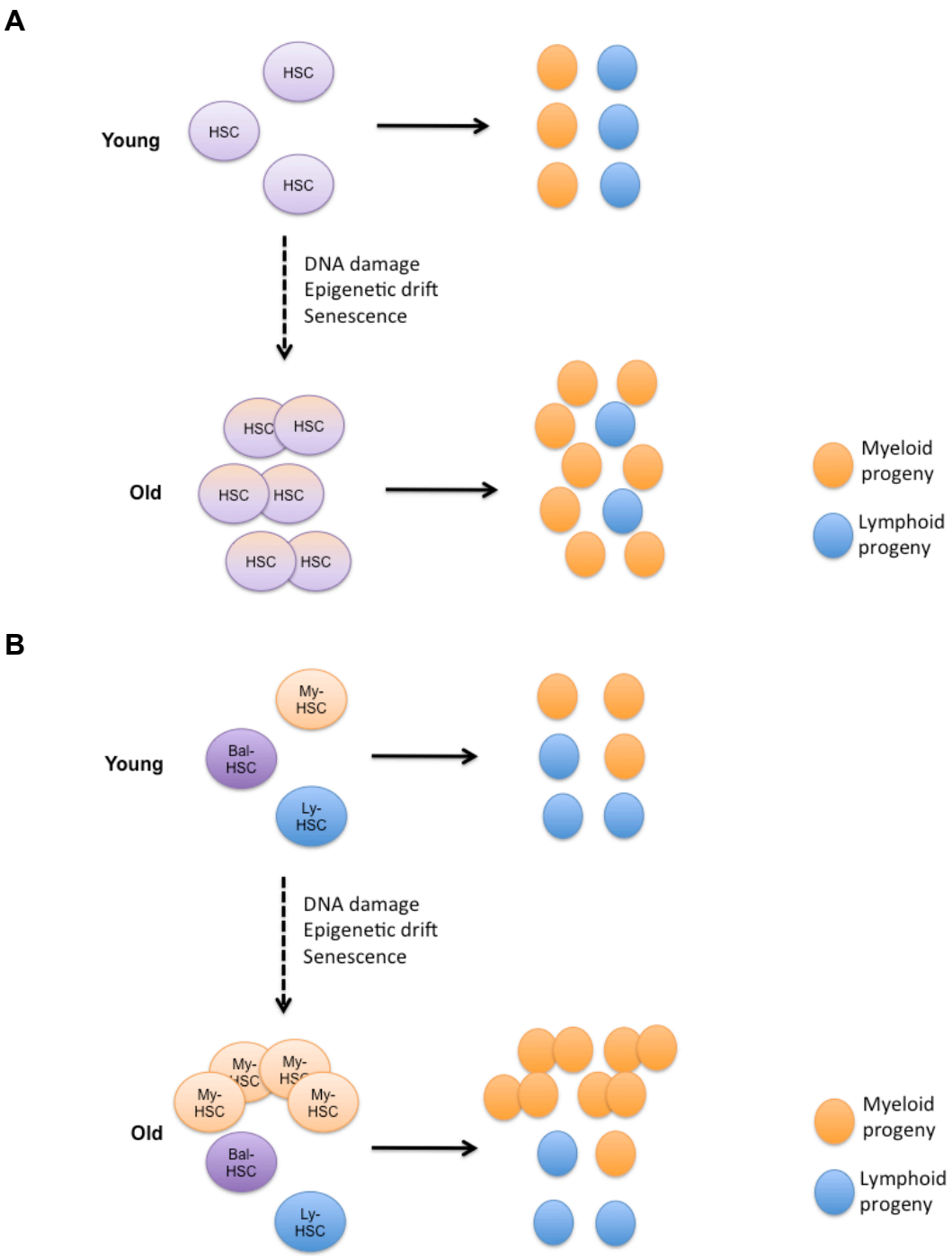

Figure 1.4 | Models of HSC aging. (A) In the population shift model, young HSCs produce a balanced output of lymphoid and myeloid progeny, but due to DNA damage, epigenetic drift, and other molecular changes that occur with aging, old HSCs expand as a population and are intrinsically altered to produce more myeloid progeny. **(B)** In the clonal model, HSCs are classified as myeloid-biased (My-HSC), balanced (Bal-HSC), and lymphoid-biased (Ly-HSC). The myeloid skewing seen in the mature compartment of old mice is due to an expansion of myeloid-biased HSCs.

Paradigm-shifting research on clonality and the heterogeneous contribution of HSC and progenitor clones to hematopoiesis has recently challenged the view that alterations of HSCs are entirely responsible for the phenotypic alterations in aging. Higher levels of clonality, where only a few clones actively contribute to the production of peripheral blood cells, has been observed with hematopoietic aging (Sun et al., 2014b). Recent barcoding experiments tracked mouse HSC clonality *and* monitored both steady-state and stress-induced hematopoiesis. These experiments found that multiple HSC clones contribute to hematopoiesis during development, however, later in adulthood, long-lived progenitors mostly contribute to hematopoiesis rather than HSC (Sun et al., 2014b). Additionally, with more refined isolation of HSC subsets, the short-term HSC population is now thought to have greater direct contribution of to adult hematopoiesis compared to long-term HSCs (Busch et al., 2015). Based on mathematical modeling, it has been suggested that aging-associated myeloid bias might be a consequence of reduced MPP differentiation to CLPs rather than a change in the HSC pool composition (Busch et al., 2015). As technological advances have made subpopulation-specific studies more possible, it becomes of great importance to determine how the progenitor populations, as well as HSCs, contribute to downstream alterations observed in aging.

1.2.2 Molecular changes in aging

Identifying the molecular events that regulate self-renewal and multipotency in stem and progenitor cells and how these are altered during aging is of importance for the discovery of the therapeutic targets to prevent or reverse

aging-associated hematopoietic conditions. Comparing microarray profiles of young and old HSCs has revealed increased expression of genes linked to oxidative stress, protein aggregation, and inflammatory responses with age, whereas genes involved with transcriptional regulation were repressed (Chambers et al., 2007; Pang et al., 2011; Wagner et al., 2009). Transcriptional regulation of genomic integrity in aged HSCs has also been found to be altered, specifically mediated by the increased expression of the tumor suppressor P53 (Asai et al., 2011). Aged hematopoietic stem cells exhibit an accumulation of genomic damage, telomere shortening, and an increase in metabolic byproducts (Hamilton et al., 2014). All of these cellular changes activate multiple signaling pathways and mechanisms that are involved in apoptosis, senescence, or impaired proliferation (Nijnik et al., 2007; Sahin and Depinho, 2010; Yahata et al., 2011). Cells that enter senescence as a consequence of DNA damage secrete pro-inflammatory cytokines and chemokines that might contribute to the chronic inflammation observed and known as “inflammaging” (Franceschi et al., 2007).

In addition, differential expression of genes associated with particular hematopoietic lineages (myeloid, lymphoid, and erythroid) has been found between old and young HSCs; aged HSCs exhibit an upregulation of myeloid differentiation-associated genes such as *Runx1*, *Hoxb6*, and *Osmr*, while genes involved in lymphopoiesis such as *Flt3* and *Il-7r* are downregulated (Akunuru and Geiger, 2016). These gene expression changes correlate with age-induced myeloid skewing, suggesting that aging-induced cellular changes may be mediated by these transcriptional alterations.

1.2.3 Alterations in the bone marrow microenvironment in aging

There is increasing evidence that changes in the bone marrow microenvironment also contribute to the aging-associated decline in stem cell function. The stem cell niche interacts chemically and physically with stem and progenitor cells to coordinate their survival, proliferation, and differentiation. Aging alters cellular composition and function of the microenvironment, as well as secreted niche factors. Circulating levels of pro-inflammatory cytokines such as CCL5 are increased in aged niches which may contribute to the myeloid skewing seen from HSCs (Ergen et al., 2012) while levels of secreted CXCL12, an osteoblast factor responsible for stem cell localization, is decreased (Tuljapurkar et al., 2011). Changes in cellular composition not only influences homing but also lineage potential. Decreased bone formation and enhanced adipogenesis is also seen in the aged niche (Bellantuono et al., 2009; Wagner et al., 2008), which contribute to a suppression of lymphopoiesis (Bethel et al., 2013).

Proof of concept that cell-extrinsic mechanisms contribute to age-related stem cell impairments was first demonstrated using parabiosis experiments. Young and old mice were surgically joined to share a common circulatory system and it was observed that cell-extrinsic factors from the young mice could restore stem cell function in the old mice (Conboy et al., 2005). Understanding the mechanisms by which these young factors were able to rejuvenate old stem cells could provide druggable targets and novel therapies to improve hematopoietic healthspan during aging.

1.2.4 Clinical conditions associated with aging hematopoiesis

Clinical conditions as a result of cellular changes in the hematopoietic system with aging may appear as multiple pathologies. The phenotypic shift in the mature compartment from erythroid and lymphoid lineages to the myeloid lineage is associated with immune dysfunction and the decline of adaptive immunity in old age. One of the more common medical conditions observed in elderly people, although usually mild, is anemia (Carmel, 2001). The risk factor for anemia doubles between the ages of 60 to 75 which poses an obstacle in most elderly patients in need of surgery (Carmel, 2001). The specific mechanism underlying the reduction of red blood cells with aging remains unclear but data suggests a highly depleted erythropoietic reserve with aging as well as abnormal cytokine profiles contribute to this phenotype. An additional major concern is reduced adaptive immunity in the elderly. With aging, the ability to maintain receptor diversity is reduced (Goronzy et al., 2007). Additionally, the number of naïve T cells in the periphery is significantly reduced, most likely due to thymic involution (Lynch et al., 2009). Decreased numbers of T-cells impairs an elderly person's ability to fight off infections and decreases his or her response to vaccines. These lymphoid deficiencies make the elderly especially vulnerable to infections such as influenza and pneumonia, making recovery time much longer and even sometimes incomplete (Alam et al., 2013).

A major consequence associated with myeloid imbalance with aging is an increased incidence of myeloid proliferative diseases. Aging HSCs exhibit a myeloid-biased shift in lineage potential, similarly leukemias that develop in

elderly patients are mostly myeloid, while pediatric leukemia tends to be lymphoid (Kim et al., 2003). Additionally, aged HSCs express elevated levels of genes involved in leukemic transformation such as *Aml1, Pml and Eto* (Rossi et al., 2005). The upregulation of such proto-oncogenes may act in concert with the myeloid bias of aged cells to predispose toward myeloid disease (Rossi et al., 2008). Whether upregulation of these proto-oncogenes in stem and progenitor cells with age increases their risk of cytogenetic translocations that drive leukemia remains to be determined.

1.3 Epigenetic regulation of hematopoiesis

Classes of epigenetic regulatory proteins comprise several families of related enzymes and chromatin-interacting proteins. These proteins deposit, remove, or bind acetyl and methyl groups on DNA or histone proteins **(Table 1.3)**. Histone marks and their bound complexes contribute to the physical structure of chromatin and are responsible for the accessibility of recruited transcription factors (Arrowsmith et al., 2012). The epigenomic landscape evolves during cellular differentiation and development. These epigenetic changes are in part responsible for cellular plasticity that enables cellular reprogramming and response to the environment (Goldberg et al., 2007). The dynamic and reversible nature of epigenetics means that it may be possible to alter disease-associated epigenetic states through direct manipulation of the molecular factors involved in this process.

Enzyme family	Class	Function	Example Enzymes
DNA methyltransferases	Writer	DNA methylation	DNMT1, DNMT3A, DNMT3B
Protein acetyltransferases	Writer	Histone/ non-histone acetylation	CREBBP, MYST4, ATXN7L1, EP300
Protein methyltransferases	Writer	Histone/ non-histone methylation	SETD7, KMT5A, SUV39H2, CXXC1
Protein deacetylases	Eraser	Histone/ non-histone de-acetylation	HDAC9, SIRT4, SIRT3
Protein demethylases	Eraser	Histone/ non-histone demethylation	KDM5B, PRDM9, PRDM16
Bromodomain-containing proteins	Reader	Targeting of chromatin-modifying enzymes to specific sites	BRD4
Methyl-lysine- methyl-arginine-binding domain-containing proteins	Reader	Targeting of chromatin-modifying enzymes to specific sites- Act in epigenetic complexes	TRDR3, PIWI
PHD-containing proteins	Reader	Targeting of chromatin-modifying enzymes to specific sites	DACH1

Table 1.3 | Classes of epigenetic regulatory proteins.

Epigenetic regulation is essential for the maintenance and differentiation of hematopoietic stem and progenitor cells. DNA methylation, mediated through Dnmt1, plays a significant role in the self-renewal and differentiation of adult HSCs (Trowbridge et al., 2009). Reduced Dnmt1 activity results in the differentiation of HSCs into myeloerythoid, but not lymphoid progeny (Broske et al., 2009). Histone modifications are present at lineage-specific loci in HSC and progenitor cells before high-level expression in mature subsets. The *B-globin* gene is highly transcriptionally expressed in mature erythroid lineage cells, but not stem and progenitor precursors. However, histone 3 of the *B-globin*

chromatin region is increasingly acetylated from MPP cells through mature erythroid cells, allowing access to transcription factors that will drive expression in mature erythroid cells (Bottardi et al., 2003). As low-level transcription of lineage-affiliated genes in progenitor cells has been observed, it is likely that epigenetic priming at lineage-specific genes in progenitor cells is responsible for this transcriptional priming (Mansson et al., 2007).

Loss of methylation of DNA and histone tails has been observed in hematopoietic stem and progenitor cells with aging and leads to the cumulative loss of epigenetic gene regulation over time (Fraga et al., 2005). With aging, regulatory gene regions associated with HSC differentiation are hypermethylated and exhibit decreased expression, while genes associated with regulating HSC maintenance are hypomethylated and exhibit increased expression, consistent with impaired differentiation potential and increased numbers of aged HSC (Bocker et al., 2011).

1.3.1 Lysine methyltransferases

Enzymes that add or remove the methylation mark on histone and non-histone protein lysine residues are classified as lysine methyltransferases (KMTs) and lysine demethylases (KDMs), respectively. KMTs catalyze mono-, di-, or tri-methylation by transferring one, two, or three methyl groups, respectively, from *S*-adenosyl-L-methionine to the ε-amino group of a lysine residue. Except for KMT4, all known KMTs contain a conserved SET (Su(var)3-9, Enhancer of Zeste, Trithorax) domain harboring the enzymatic activity (Qian and Zhou, 2006).

Besides the SET domain, most KMTs also contain other defined protein domains or homologous sequences that are used to classify KMTs into distinct subfamilies **(Table 1.4)** (Allis et al., 2007; Aravind et al., 2011).

Family	Enzyme	Alternate ID	Known Histone Substrate	Known Non-Histone Substrate
KMT1	KMT1A	SUV39H1	H3K9me3	
	KMT1B	SUV39H2	H3K9me3	
	KMT1C	EHMT2	H3K9me2, H3K27me2 H1K26me2, H1K187me2	P53, C/EBP*B*, DNMT1, CDYL1, WIZ, ACINUS
	KMT1D	EHMT1	H3K9me2	P53
	KMT1E	SETDB1	H3K9me3	TAT
	KMT1F	SETDB2	H3K9me3	
KMT2	KMT2A	MLL	H3K4me3	
	KMT2B	MLL2	H3K4me3	
	KMT2C	MLL3	H3K4me3	
	KMT2D	MLL4	H3K4me3	
	KMT2E	MLL5	H3K4me3	
	KMT2F	HSET1A	H3K4me3	
	KMT2G	HSET1B	H3K4me3	
	KMT2H	ASH2	H3K4me3	
KMT3	KMT3A	SET2	H3K36me3	
	KMT3B	NSD1	H3K36me2, H4K20me2	NFKB
	KMT3C	SMYD2	H3K36me2, H3K4me	P53, RB
	KMT3D	SMYD1	H3K4me	
	KMT3E	SMYD3	H3K4me3	VEGFR
KMT4	KMT4	DOT1L	H3K79me2/3	
KMT5	KMT5A	SETD8	H4K20me1	P53, PCNA
	KMT5B	SUV420H1	H4K20me2, H4K20me3	
	KMT5C	SUV420H2	H4K20me3, H4K20me2	
KMT6	KMT6A	EZH2	H3K27me3	
	KMT6B	EZH1	H3K27me3	
KMT7	KMT7	SET7/9	H3K4me1	P53, TAF7, TAF10, ERA, AR, DNMT1, NFKB, RB, E2F1, STAT, TAT
KMT8	KMT8	PRDM2	H3K9me3	

Table 1.4 | KMT families and their substrates.

1.3.1.1 Classification of KMT5 family

The KMT5 family consists of three enzymes that methylate H4K20 **(Table 1.5)**. KMT5A monomethylates H4K20, KMT5B and KMT5C catalyze di- and tri-methylation of H4K20 (Schotta et al., 2004). KMT5B and KMT5C exhibit a preference for methylating H4K20me1 over unmethylated H4K20 (Beck et al., 2012). Furthermore, each of the methylation states exhibits unique genomic distributions and is recognized by specific binding proteins, highlighting their distinct roles (Oda et al., 2010). Regulation of H4K20 methylation is essential since knockout studies have shown that *Kmt5a* and *Kmt5b* are required for development in mice (Schotta et al., 2008). In contrast, *Kmt5c* knockout mice are viable but exhibit defects in telomere maintenance (Benetti et al., 2007; Schotta et al., 2008)

H4K20 mark	Responsible Enzyme	Transcriptional role	Cell cycle roles	References
H4K20me1	KMT5A	Activation Repression	Condensation Mitotic Progression	(Houston et al., 2008; Jorgensen et al., 2007; Karachentsev et al., 2005; Oda et al., 2010)
H4K20me2	KMT5B KMT5C	Activation	Replication Damage repair	(Houston et al., 2008; Karachentsev et al., 2005)
H4K20me3	KMT5C KMT5B	Repression	Silencing repetitive DNA transposons	(Benetti et al., 2007)

Table 1.5 | Known roles of H4K20 methylation marks in transcription and cell cycle.

1.3.2.2 Cellular functions of KMT5A

1.3.2.2.1 Histone Methylation

While both KMT5B and KMT5C catalyze di and tri methylated forms, KMT5A is the only known enzyme to monomethylate H4K20 (Milite et al., 2016). The monomethylation of H4K20 has been shown to associate with both gene repression and activation, depending on its chromatin context (Karachentsev et al., 2005). H4K20me1 is canonically thought of as a mark of transcriptional repression due to inactivation of E2F transcription (Abbas et al., 2010; Liu et al., 2010; Yu et al., 2013). The mechanism of repression by H4K20me1 has been demonstrated to be by directly promoting chromatin compaction (Lu et al., 2008). Ultimately, repression of transcription may be indirectly mediated by facilitating establishment of H4K20me2 and H4K20me3 (Schotta et al., 2008). Both the dimethylation and trimethylation of H4K20 have well-established roles in gene repression, especially in repetitive elements (Schotta et al., 2008).

H4K20me1 has been shown to act as a transcriptional activator in the context of Wnt target genes (Li et al., 2011). In HEK293 cells, KMT5A is recruited to the TCF-binding element of WNT target genes and directly binds to LEF1 upon WNT stimulation, promoting transcription of WNT target genes. The role of H4K20me1 may also be context-dependent, since H4K20me1 is observed to be enriched on highly expressed tissue-specific genes. The conflicting roles of H4K20me1 in transcriptional activation and repression may be explained by proliferation rates of different cell types given the cell cycle-dependence of KMT5A expression and levels of H4K20me1. In addition, neighboring modifications on the H4 tail may

affect H4K20me1 function. The presence of H4K20me1 at highly expressed genes may potentially be affected by the co-occurrence of neighboring H4K16 acetylation (H4K16ac), which has an established role in activating gene expression (Beck et al., 2012). H4K16 acetylation has a known role in regulating higher order chromatin structure and may override the function of a subset of H4K20me1 marks, making the repressive H4K20me1 appear as promoting activation.

1.3.3.2.2 Non-histone protein methylation

Although lysine methylation of histones has been highly studied to gain insight into epigenetic regulation of chromatin, this modification also occurs on non-histone proteins. Several KMTs have been identified as regulators of P53 via methylation, making P53 the most extensively studied non-histone protein undergoing lysine methylation (Huang et al., 2010). Fine-tuned regulation through lysine methylation of P53 may explain how P53 can participate in multiple cellular functions. Through lysine methylation, protein KMTs dynamically generate distinct populations of P53, each methylated at a specific C-terminal lysine residue (West and Gozani, 2011).

Accumulating evidence suggests that lysine methylation plays a key role in regulating protein stability, protein–protein interactions, and transactivation activity of P53. Acetylation at human P53 lysine residue 382 (K382) activates the transcriptional regulation activity of P53 via recruitment of co-activators p300 and CBP (Reed and Quelle, 2014) **(Figure 1.5)**. This acetylation is directly inhibited

by monomethylation on the same residue by KMT5A (Shi et al., 2007). KMT5A-mediated P53K382 methylation promotes the interaction between P53 and L(3)Mbt-like1 (L3MBTL1) and robustly suppresses P53-mediated transcription activation of highly responsive target genes (West et al., 2010). Depletion of KMT5A augments the proapoptotic and checkpoint activation functions of P53 upon DNA damage (Shi et al., 2007; West et al., 2010).

P53 gene is the most frequently mutated tumor suppressor gene in human cancers (Levine, 1997); however, in contrast to solid tumors, hematologic malignancies exhibit a low rate of genetic mutations in *P53* (Nahi et al., 2008*).* Nonetheless, alterations in *P53* transcript levels correlate with an inferior clinical outcome in hematologic cancers (Seifert et al., 2009), suggesting that other mechanisms besides mutations such as post-transcriptional modifications could be involved in the deregulation of the *P53* pathway.

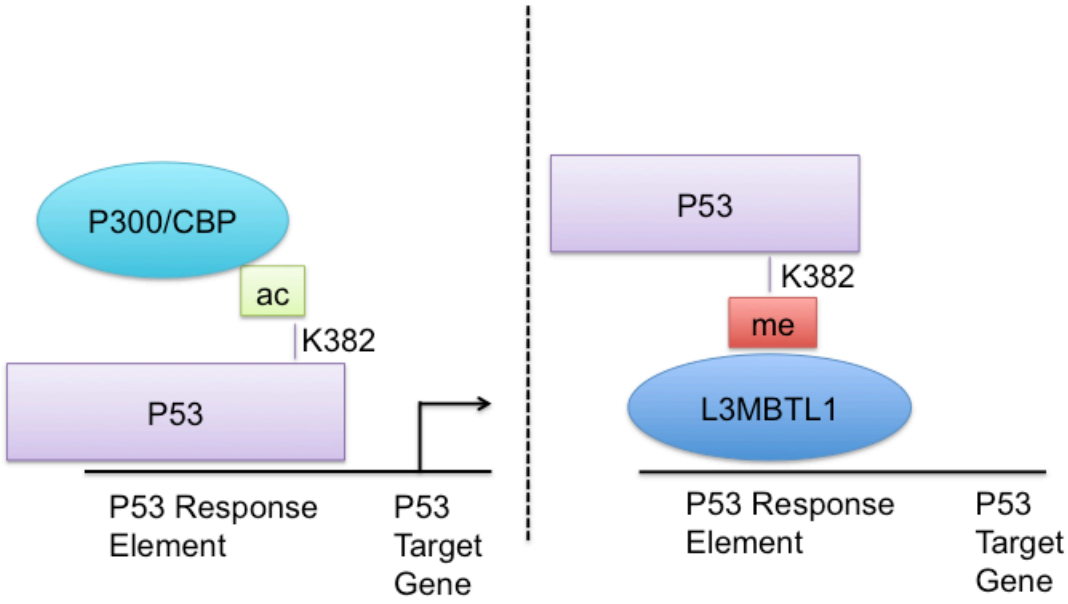

Figure 1.5 | Regulation of P53-mediated transcription at Lysine 382. The ability of P53 to access P53 response elements of target genes is either positively regulated by acetylation (left) or negatively regulated by methylation at lysine 382 by the recruitment of different binding partners. Acetylated K382 stabilizes the interaction of P53 with co-activators P300 and CBP at target gene response elements, while methylation at K382 stabilizes the interaction of P53 with L3MBTL1 that directly block access to the response element and therefore the target gene is not expressed.

1.3.2.2 Regulation of KMT5A

In proliferating cells, only very low levels of H4K20me1 and H4K20me3 are present together with a small fraction of unmodified histone H4. The majority is thus in the abundant H4K20me2 form (Pesavento et al., 2008; Schotta et al., 2008). There is highly dynamic cell cycle regulation of the various H4K20 methylation states of which H4K20me1 seems to have the highest cycle-dependent fluctuations **(Figure 1.6)**. H4K20me1 declines during G1 phase, resulting in a very low level of H4K20me1 in the beginning of S phase. It accumulates during S and G2 phases resulting in a peak in M phase (Oda et al., 2009). This cell cycle-dependent regulation is mirrored in the abundance of the KMT5A enzyme. In G1 and S phase, proteolytic degradation keeps KMT5A at a low level, whereas the enzyme is stabilized in G2 and M phase, resulting in elevated levels of H4K20me1 (Abbas et al., 2010; Centore et al., 2010; Jorgensen et al., 2007; Oda et al., 2009).

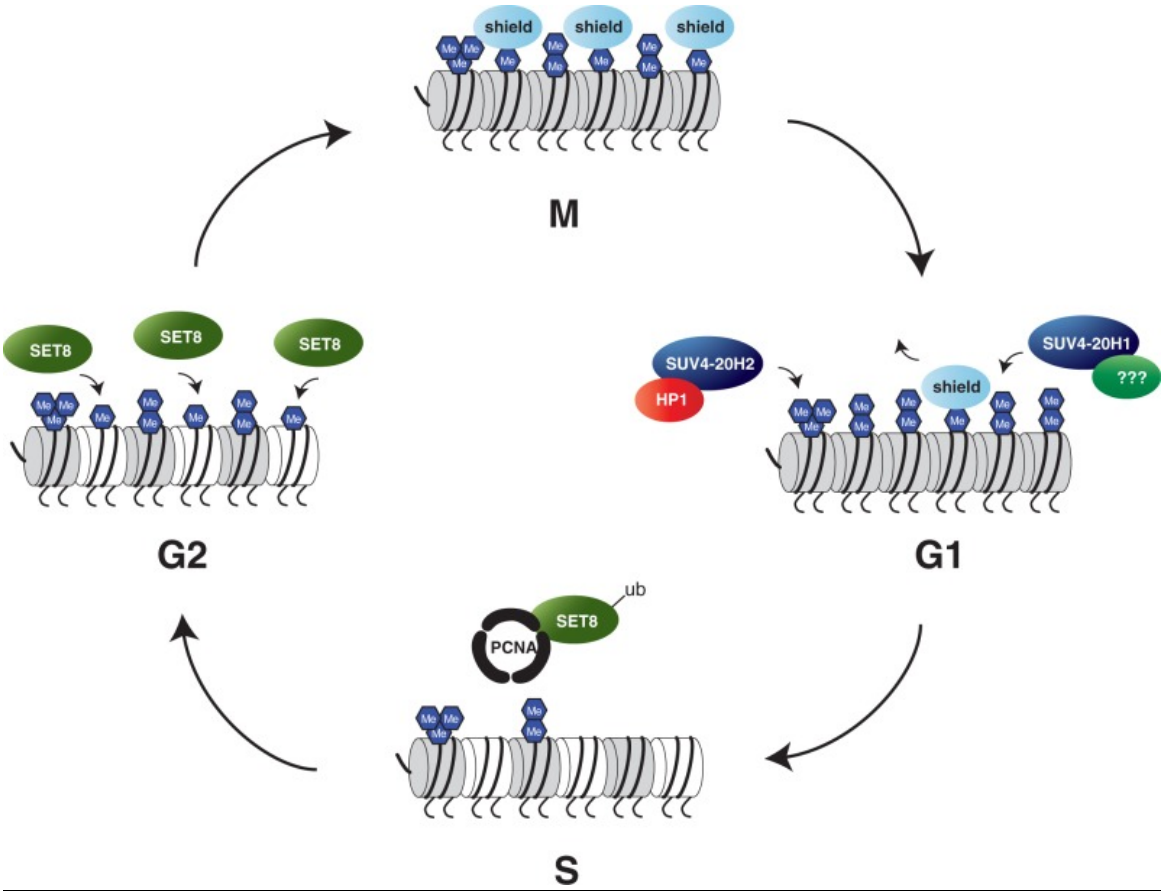

Figure 1.6 | Cell cycle dynamics of KMT5A and H4K20me1. KMT5A protein levels (shown here as SET8) peak in the G2 phase of the cell cycle and catalyzes the monomethylation of H4K20. The mark accumulates and is shielded during the M phase. H4K20me1 is then either further methylated by KMT5B (SUV420H1) or demethylated during the G1 phase (Jorgensen et al., 2013).

In addition to being regulated by cell cycle, alterations in *Kmt5a* levels also directly impact cell cycle. Knockdown of *Kmt5a* has been shown to arrest replication forks, induce double-stranded DNA breaks and a Chk1-mediated cell-cycle arrest in S and G2/M phases of the cell cycle. KMT5A controls the G1/S transition by blocking lysine acetylation through binding to the H4 N-terminal tail (Beck et al., 2012; Yin et al., 2008). However, in studies of self-renewing erythroblasts (ESREs), lentiviral knockdown of *Kmt5a* was found to have no effect on cell cycle, apoptosis, and proliferation (Malik et al., 2015).

The accumulating evidence of *Kmt5a* deregulation in hematologic and non-hematologic cancers has increased interest in understanding the molecular mechanisms of *Kmt5a*-regulated processes (Milite et al., 2016). *Kmt5a* is overexpressed in different types of cancer tissues and cancer cell lines including bladder cancer, non-small cell and small cell lung carcinoma, chronic myelogenous leukemia, hepatocellular carcinoma, and pancreatic cancer (Takawa et al., 2012). In addition to investigating the role of *Kmt5a* in genomic stability and its contribution to cancer phenotypes, it is important to understand the role of *Kmt5a* in normal hematopoiesis and its contribution to lineage fate phenotypes. With greater insight into how an epigenetic enzyme may contribute to cellular fate, we will gain a better understanding of the mechanisms by which deregulation causes aberrant hematopoietic conditions, how we might better target these pathways, and how our current therapies might impact normal cells.

1.4 Thesis Aims

Aging leads to the decline of the hematopoietic system over the life of an individual caused by an increased susceptibility to infections and a reduced functional repertoire of immune cells to regenerate the innate and adaptive immune systems after injury (Dykstra et al., 2011). Additionally, aging is associated with an increased risk of leukemia and myeloproliferative diseases. At the cellular level, aging is associated with myeloid-biased hematopoietic cell production at the expense of lymphoid cell production (Kim et al., 2003). Studies have mainly focused on the HSC population as the driver of age-associated hematopoietic decline and little is known about alterations that occur in the multipotent progenitor compartment. Recent lineage tracing experiments have suggested that these progenitor cell populations contribute to long-term, steady-state hematopoiesis to a greater extent than previously thought (Busch et al., 2015; Sun et al., 2014b).

The multipotent progenitor compartment is a heterogeneous pool of populations that can tailor their cellular output to meet the demands of the adult hematopoietic system. The compartment is comprised of functionally distinct populations that are primed towards specific mature lineages- erythroid, myeloid and lymphoid- but can produce multiple lineage cell types (Pietras et al., 2015a). Multipotent progenitor populations, therefore, are important intermediates in hematopoietic cellular differentiation that denote the final branching points between specific mature lineages and key populations to target for modulation of hematopoietic cell production.

Epigenetic regulation of cellular fate in hematopoiesis is becoming of increasing interest due to its reversible nature. Although there is evidence for many epigenetic factors involved in hematopoiesis, the role of epigenetics in regulating the output of myeloid and lymphoid cell production from lymphoid-primed multipotent progenitors remains unclear. It is the goal of this thesis to examine the phenotypic and functional alterations in the multipotent progenitor compartment that occur with aging and identify epigenetic factors involved in regulating lineage output from lymphoid-primed multipotent progenitors. Investigating the contribution of multipotent progenitors to hematopoietic cell production may provide insights into the drivers of myeloid-biased production of hematopoietic cells in aging, bone marrow regeneration, and cancer to offer possible avenues for reversing deleterious bone marrow conditions.

CHAPTER 2: MATERIALS AND METHODS

2.1 Materials

2.1.1. Flow Cytometry antibodies

Antibody	Clone	Vendor	Final Dilution
anti-CD3	17A2	ebioscience	1:200
anti-mouse CD4	RM4-5	BD Pharmingen	1:200
anti-mouse CD8	53-6.7	ebioscience	1:200
anti-mouse CD11c	N418	ebioscience	1:200
anti-mouse CD16/CD32	93	ebioscience	1:200
anti-mouse CD19	1D3	ebioscience	1:200
anti-mouse CD34	RAM34	ebioscience	1:100
anti-mouse CD45.1	A20	ebioscience	1:200
anti-mouse CD45.2	104	ebioscience	1:200
anti-mouse CD48	HM48-1	ebioscience	1:200
anti-mouse CD150	TC15-12F12.2	ebioscience	1:200
anti-mouse c-Kit	2B8	ebioscience	1:200
anti-mouse Gr-1	RB6-8C5	ebioscience	1:200
anti-mouse IL-7Ra	A7R34	ebioscience	1:200
anti-mouse Sca-1	D7	ebioscience	1:200
anti-mouse Ter-119	TER-119	ebioscience	1:200
anti-mouse B220	RA3-6B2	ebioscience	1:200
anti-mouse CD11b	M1/70	ebioscience	1:200
Anti-mouse CD135 (Flt3)	A2F10	ebioscience	1:200
Strepavidin		Life Technologies	1:400

Table 2.1 | Antibodies used for flow cytometry.

2.1.2 Bacterial Strains

One Shot Top 10 (Invitrogen) strain was used for transformation to amplify plasmids. Bacteria were grown in Luria-Bertani (LB) broth or on LB-agar plates with 100 ng/mL Carbenicillin.

XL-10 Gold Ultracompetent (Agilent) strain was used to transform bacteria only for mutagenesis of pCMV6 (2.2.12.1) Bacteria were grown in SOC medium and LB-agar plates with 10 µg/mL X-gal and 20 µg/mL IPTG.

2.1.3 Cell lines

Human cell line HEK-293 was used for lentiviral particle production. Cells were cultured in Dulbecco's Minimum Essential Medium (DMEM) supplemented with 10% Fetal Bovine Serum (FBS).

Mouse fibroblast cell line NIH-3T3 was used for titering lentiviral particles. Cells were cultured in Roswell Park Memorial Institute (RPMI) supplemented with 10% FBS.

Mouse stromal cell line OP9 was used for lymphoid differentiation assays. Cells were cultured in α-Minimum Essential Medium (α-MEM) supplemented with 10% FBS, 1% Penicillin-Strepavidin, and 55 nM β-Mercaptoethanol.

Mouse erytho-leukemia cell line MEL was used for quantitative real-time polymerase chain reaction (qRT-PCR) expression studies. Cells were cultured in RPMI supplemented with 10% FBS.

2.1.4 Mice

Female C57BL/6J mice between 2 months and 30 months of age were used for the work of this thesis. 2 month old B6.SJL-Ptprca *Pepcb/* BoyJ females were used in bone marrow transplantation as recipients. Mice were bred and housed in the Research Animal Facility at the Jackson Laboratory (Bar Harbor, ME). All mouse experiments were approved by Animal Care and Use Committee and performed according to AAALAC guidelines.

2.1.5 Plasmids

Plasmid	Source
pLKO.3G	Addgene
pLKO.mCherry	Rick Maser
pHIV-MND-iRES-GFP	Challen Laboratory (Washington University School of Medicine)
pCMV6-KMT5A	Origene
REV	Addgene
TAT	Addgene
VSVG	Addgene
pHIV-*Kmt5a*-MND-iRES-GFP	Subcloned from pHIV-MND-iRES-GFP
pHIV- *Kmt5a*K376R-MND-iRES-GFP	Subcloned from pHIV-MND-iRES-GFP
pLKO.1-sh*Atxn7l1*-GFP	Subcloned from pLKO.3G
pLKO.1-sh *Atxn7l3*-GFP	Subcloned from pLKO.3G
pLKO.1-sh*Crebbp*-GFP	Subcloned from pLKO.3G
pLKO.1-sh*Cxxc1*-GFP	Subcloned from pLKO.3G
pLKO.1-sh*Dach1*-GFP	Subcloned from pLKO.3G
pLKO.1-sh*Ezh1*-GFP	Subcloned from pLKO.3G
pLKO.1-sh*Kdm5b*-GFP	Subcloned from pLKO.3G
pLKO.1-sh*Kmt5a*-GFP (1074)	Subcloned from pLKO.3G
pLKO.1-sh*Ndn*-GFP	Subcloned from pLKO.3G
pLKO.1-sh*Ncor2*-GFP	Subcloned from pLKO.3G
pLKO.1-sh*Prdm16*-GFP	Subcloned from pLKO.3G
pLKO.1-sh*Rnf40*-GFP	Subcloned from pLKO.3G
pLKO.1-sh*Setd7*-GFP	Subcloned from pLKO.3G
pLKO.1-sh*Suv39H2*-GFP	Subcloned from pLKO.3G
pLKO.1-sh*Tblx1*-GFP	Subcloned from pLKO.3G
pLKO.1-sh*Kmt5a*-mCherry (1070)	Subcloned from pLKO.mCherry
pLKO.1-sh*Kmt5a*- mCherry (1072)	Subcloned from pLKO.mCherry
pLKO.1-sh*Kmt5a*- mCherry (1074)	Subcloned from pLKO.mCherry
pLKO.1-no-targeting-GFP	Subcloned from pLKO.3G
pLKO.1-no-targeting-mCherry	Subcloned from pLKO.mCherry

Table 2.2 | Plasmids used in this thesis

2.2 Methods

2.2.1 Agarose gel electrophoresis

1% Agarose gel solution was made by dissolving 1 g of agarose (Fisher Scientific) powder in 100 mL Tris-acetate-EDTA (TAE) buffer containing 40 mM Tris-acetate and 1 mM EDTA, via microwave heating. 1x TAE buffer also served as the electrophoresis buffer. Samples were mixed with 6x gel loading dye before loading on agarose gel. Electrophoresis was run at 100 volts at room temperature. The electrophoresis was stopped when tracking dye migrated at three quarters of the gel. Nucleic acids were visualized by staining with ethidium bromide (Sigma).

2.2.2 Bacterial transformation

Competent One Shot Top10 cells were thawed on ice for 5 minutes. 50-100 ng of plasmid DNA was added into 50 µL of competent cells and incubated on ice for 20 minutes. The cells were heat shocked at 42°C for 90 seconds and placed on ice for 90 seconds. 500 µL of SOC medium (LB broth containing 2.5 mM KCl, 10 mM MgCl2 and 20 mM glucose) was added and the cells were incubated in a shaker at 37°C for 1 hour. For each transformation, 50 µL and 100 µL of cells were plated on two carbenicillin-supplemented LB plates. The plates were checked the next morning for the presence of colonies.

2.2.3 Bone marrow transduction and transplantation

2.2.3.1 Production of lentiviral supernatants

4 x 10^6 of HEK-293T cells were seeded in a cell culture dish (100 mm x 20 mm) the day before transfection in full culture medium. On day of transfection, 12 µL of Trans-IT transfection reagent (Mirus Bio) is added to 400 µL serum-free DMEM. Plasmids Rev, Tat, PM2, VSVG are incubated with the plasmid of interest (Table 2.2) in a ratio of 1:2:2:2:10 for 20 minutes in 400 µL serum-free DMEM. The transfection mix was combined and added dropwise to cells. After 48 hours of culture, the supernatant of transfected cells was collected and syringe-filtered (0.45 µm pore size), aliquoted into 2.0 mL cryovials, and stored at -80°C.

2.2.3.2 Determination of lentiviral titer

2 x 10^5 3T3 cells in 2 mL of culture medium were seeded per well of a 6-well plate the day before transduction. On the transduction day, the existing culture medium was replaced with 1 mL of fresh pre-warmed medium containing 5 ng of polybrene. Lentiviral supernantant amounts of 1.6 µL, 8 µL, 40 µL, 200 µL, and 1000 µL were diluted to 1000 uL using culture medium and then added to single wells. After 24 hours of culture, media was replaced and cultured for another 24 hours before harvest. At harvest cells washed once with phosphate buffered saline (PBS) and trypsinized to detach the cells. Trypsin was quenched with culture medium and cells were centrifuged at 1250 RPM at 4°C for 5 minutes. The cell pellet was resuspended in 500 mL of 3% FBS-supplemented PBS and was analyzed by FACS analysis. Titer (Transfection units/mL) was calculated

based of the volume of supernatant that produced between 5-10% green fluorescent protein (GFP) positive 3T3 cells. Lentiviral transductions were then performed using this calculation at a Multiplicity of Infection (MOI) of 100.

2.2.3.3 Ex vivo culture and LMPP/MPP4 transduction

Bone marrow was collected and isolated as described in section 2.2.10.1 and 2.2.8.1. LMPP or MPP4 cells were resuspended in Iscoves Minimum Dulbecco's Medium (IMDM) supplemented with 10% FBS and supplemented with rmIL-3 (10 ng/mL), rmIL-6 (10 ng/mL), rmIL-7 (20 ng/mL), SCF (100 ng/mL), LIF (20 ng/mL) and polybrene (5 ng/mL). Lentiviral supernatant was added at an MOI of 100 and plates were incubated for 48 hours and then sorted via FACS for fluorescent positive cells.

2.2.4 Transplantation and monitoring

On day of transplant, recipient B6.SJL mice were sub-lethally irradiated with one dose of irradiation at 600 rads given 30 minutes prior to injections. 200 µL of donor cells (5000 LMPPs resuspended in serum-free DMEM) were then injected via retro-orbital injection into each recipient. The recipients were monitored by weekly retro-orbital blood collection and FACS analysis for up to 7 weeks post transplantation. Mice were euthanized when they showed any of the following symptoms of disease: severe cachexia, lethargy, or hunching.

2.2.5 Cell counting by trypan blue exclusion

10 µL of 0.4% trypan blue solution was added to 10 µL of cell suspension and was mixed by pipetting up and down. 10 µL of cell mixture was loaded onto a

hemocytometer and examined immediately under an inverted microscope at low magnification. Only unstained live cells were counted in four of the large nine squares. The concentration of cells per mL in suspension was calculated as:

Mean number of live cells per square x Dilution factor x 10^4

2.2.6 Colony Forming Assays

After the 48 hour the culture period described in 2.2.3.3, the clonogenic growth of isolated cells was evaluated by *in vitro* colony formation assays. CFU- G/M/E colonies were evaluated with methylcellulose media with IL-6 (20 ng/mL) + IL-3 (20 ng/mL) + SCF (10 ng/mL) (Stem Cell Technologies, M3434). CFU-PreB colonies were evaluated with methylcellulose media with IL-7 (20 ng/mL) (Stem Cell Technologies, M3630) supplemented additionally with Flt3L (25 ng/mL) and SCF (50 ng/mL). Colonies were scored with an inverted microscope on day 7.

For bulk assays, 100 sorted LMPP or MPP4 cells were cultured for 48 hours as described above, resuspended in 100 µL IMDM supplemented with 2% FCS, then added to 1mL of either CFU-G/M/E (M3434) assay or CFU-PreB (M3630). For Single Cell Assays, single LMPP or MPP4 cells were directly sorted into wells of a 96-well plate with 50 µL of cytokine-supplemented culture medium. After 48 hours of culture, cells were washed with PBS and resuspended in 50 µL of 2% FBS/IMDM. 25 µL of each well is added to 200 µL of either CFU-G/M/E assay or CFU-PreB. Colony readout occurs after 7 day incubation at 37°C. Colonies are scored by microscopy under 4x and 10x magnification using a Nikon Eclipse TS100 microscope. Colonies were scored with respect to colony and cell morphology (STEMCELL M3434 Technical Manual, v3.3.0).

CFU-G: Granulocytes- round, bright, and are much smaller and more uniform in size than macrophage cells.

CFU-M: Monocyte- macrophages are large cells with an oval to round shape and appear to have a grainy or grey center.

CFU-GM: Mixed Granulocyte and Monocyte- colonies contain 30 to thousands of cells from both granulocyte and macrophage lineage. Individual cells are easy to distinguish.

BFU-E: Burst Forming Erythoid- A colony is made up of erythroid clusters. Each cluster contains tiny, irregular cells that are hard to distinguish from each other.

CFU-GEMM: Mixed Granulocyte, Monocyte, and Erythroid- Large colonies containing all three type of lineages.

2.2.7 Cytospin preparation and staining

Single colonies were harvested from CFU methylcellulose medium and washed in PBS. Cells were resuspended in 100 µL of PBS and deposited onto a glass slide using ShandonTM CytospinTM 4 Cytocentrifuge. The cells were centrifuged at 500 rpm and at room temperature for 5 minutes with medium acceleration rate. Slides were fixed in methanol for 10 minutes, washed in PBS, and submitted to histology core services for Giemsa staining.

2.2.8 Flow cytometry

2.2.8.1 Surface staining

Cell suspensions from bone marrow were prepared according to 2.2.10.1 and were stained for biotin labeled antibodies against lineage markers (B220, CD11b, CD11c, Gr-1, CD3, CD4, CD8, Ter-119), CD-150, CD48, c-Kit, Sca-1, CD135

(Flt3), and CD34 at concentrations marked in Table 2.1 for 45 minutes at 4°C. Cells were washed with 3% FBS/PBS and then resuspended at the same concentration and stained with flurochrome-conjugated streptavidin secondary antibody for 15 minutes at 4°C. Cells were centrifuged at 1250 RPM and at 4°C for 5 minutes and resuspended at 25 x 10^6 cells/mL in 3% FBS/PBS for FACS.

Cell suspensions from peripheral blood analysis were prepared according to 2.2.10.2 at were stained for B220, CD11b, Gr-1, and CD3 at concentrations marked in Table 2.1 for 15 minutes at 4°C. Cells were washed with 3% FBS/PBS, centrifuged at 1250 RPM at 4°C for 5 minutes, and then resuspended in 300 µL 3% FBS/PBS for FACS analysis.

2.2.8.3 DNA staining for viability

Live/Dead cell discrimination during FACS was determined by staining with Propidium Iodide (PI) at 1 µg/mL or 4',6-Diamidino-2-Phenylindole, Dilactate (DAPI) at 500 ng/mL.

2.2.9 GSEA analysis

Gene expression profiles of 4 month old and 14 month old LMPP samples were used in GSEA (Subramanian et al., 2005) and performed using the default settings. Gene sets from the Molecular Signatures Database v5.0 of GSEA (Broad Institute of MIT and Harvard, Cambridge, MA, USA) were used.

2.2.10 Primary cell isolation

2.2.10.1 Hematopoietic stem and progenitor cell isolation from bone marrow

Pelvises, femurs and tibias collected from euthanized mice were dissected free of muscle tissues and tendons. The bones were crushed in 3% FBS/PBS using a mortar and pestle. The resulting bone marrow cell suspension was filtered through a 40μM cell strainer. The cell pellets were resuspended in 6mL 3% FBS/PBS and were counted by trypan blue exclusion at dilution factor of 20. Cell suspension was gently layered on top of 6mL Ficoll-Paque Premium (GE) gradient and centrifuged for 18 minutes at a speed of 1440 RPM at room temperature with 0 deceleration. Lymphocyte layer was extracted using manual aspiration with a glass Pasteur pipet and centrifuged at 1250 RPM for 5 minutes at 4°C. Cells were resuspended in 1mL of 3%FBS/PBS and counted via trypan blue exclusion at a dilution factor of 20. Cells were then resuspended to a concentration of 1 x 10^7 cells/mL and stained for stem and progenitor populations according to 2.2.8.1.

2.2.10.2 Hematopoietic mature lineage cell isolation from peripheral blood

Approximately 50 uL of peripheral blood was collected via retro-orbital blood collection into a K2-EDTA lined vial (BD Biosciences). Blood was placed on ice and 1mL of Lysis Buffer (155mM NH_4Cl, 10mM $KHCO_3$, 0.1mM EDTA, pH7.3) was added an incubated for 10 minutes. Cells were pelleted by centrifugation for 10 minutes at 10,000RPM at 4°C and then resuspended in 50 μL of 3% FBS/PBS.

2.2.11 Plasmid Construction

2.2.11.1 Mutagenesis to derive pCMV6-p53K376R

Site directed mutagenesis was performed on pCMV6-*p53* plasmid (Origene) using the QuickChange Lightning mutagenesis kit (Agilent technologies). Primers designed by QuickChange Primer Design Program (Agilent Technologies) were used to amplify the pCMV6-*p53* with an A to G base pair modification to produce the plasmid pCMV6-*p53*K376R. The plasmid was transformed in bacteria and DNA was extracted from single colonies grown in 5 mL LB broth for 8 hours using the QIAGEN miniprep kit. Plasmid was verified by Sanger sequencing across the P53 cassette.

2.2.11.2 Sub-cloning to derive pHIV-p53$^{+/+}$-MND-IRES-GFP

pHIV-MND-GFP and pCMV6-*p53* was double-digested using XhoI and AscI restriction enzymes (New England Biolabs) and subsequently fractionated by agarose gel electrophoresis. The *p53* cassette (1267bp band) from pCMV6-*p53* and pHIV-MND-GFP backbone (7.8kb band from pHIV-MND-GFP) were extracted using QIAquick Gel Extraction Kit. The GFP cassette and pHIV backbone were ligated using Quick Ligase (New England Biolabs) at a 3:1 molar ratio, respectively. The plasmid was transformed in bacteria and DNA was extracted from single colonies grown in 5 mL LB broth for 8 hours using the QIAGEN miniprep kit. Plasmid was verified by Sanger sequencing across the MND promoter.

2.2.11.3 Sub-cloning to derive pHIV-p53^{K376R}-MND-IRES-GFP

pLKO.HIV-MND-GFP and pCMV6-*p53*K376R was double-digested using XhoI

and AscI restriction enzymes (New England Biolabs) and subsequently fractionated by agarose gel electrophoresis. The *p53* cassette (1267bp band) from pCMV6-*p53*K376R and backbone of pHIV-MND-GFP (7.8kb band from pHIV-MND-GFP) were extracted using QIAquick Gel Extraction Kit. The GFP cassette and pHIV backbone were ligated using Quick Ligase (New England Biolabs) at a 3:1 molar ratio, respectively. The plasmid was transformed in bacteria and DNA was extracted from single colonies grown in 5 mL LB broth for 8 hours using the QIAGEN miniprep kit. Plasmid was verified by Sanger sequencing across the MND promoter.

2.2.11.4 Sub-cloning to derive pHIV-Kmt5a-MND-IRES-GFP

pLKO.HIV-MND-GFP and pCMV6-*Kmt5a* was double-digested using KpnI and StuI restriction enzymes (New England Biolabs) and subsequently fractionated by agarose gel electrophoresis. The *Kmt5a* cassette (1193bp band) from pCMV6-*Kmt5a* and pHIV-MND-GFP (7.8kb band from pLKO.1-shRNA) were extracted using QIAquick Gel Extraction Kit. The GFP cassette and shRNA backbone were ligated using Quick Ligase (New England Biolabs) at a 3:1 molar ratio, respectively. The plasmid was transformed in bacteria and DNA was extracted from single colonies grown in 5 mL LB broth for 8 hours using the QIAGEN miniprep kit. Plasmid was verified by Sanger sequencing across the MND promoter.

2.2.11.5 Sub-cloning GFP into pLKO.1-shRNA

pLKO.3G (Addgene) and pLKO.1-shRNA (Sigma) was double-digested using Bam-HI and KpnI restriction enzymes (New England Biolabs) and subsequently

fractionated by agarose gel electrophoresis. The GFP reporter cassette (700bp band) from pLKO.3G and shRNA backbone (6.7kb band from pLKO.1-shRNA) were extracted using QIAquick Gel Extraction Kit. The GFP cassette and shRNA backbone were ligated using Quick Ligase (New England Biolabs) with 3:1 molar ratio, respectively. Bacterial transformation was performed as described in section 2.2.3. Colonies were picked and screened by colony PCR for GFP.

2.2.12 Quantitative RT-PCR

Gene expression levels were measured using SYBR Green Master Mix (QIAGEN). Primer sequences are listed in Table 2.25. Each target was measured in triplicate reactions. 2 µL of cDNA was added into each reaction. The plate was sealed and centrifuged briefly before loaded onto the Applied Biosystems 7500 Real-Time PCR system. Expression of target genes was normalized relative to *HPRT.* Relative mRNA levels were calculated using the 2-ΔΔCT method.

Gene	Forward Primer	Reverse Primer
Atxn7l1	CAAGCCCTAGAACAGCGTCA	AGCAAGTTTCTGCCCTCACA
Atxn7l3	AAGGAGTGTGTTTGCCCCAA	AGACTTGGATCTTCGAGGGGA
Crebbp	CCAAACGAGCCAAACTCAGC	TTTGGACGCAGCATCTGGAA
Cxxc1	CCAAACGAGCCAAACTCAGC	TTTGGACGCAGCATCTGGAA
Dach1	GGCTTTCGACCTGTTCCTGA	AGGAAGTTCCAGTCCAACACT
Ezh1	CAACACTTCCCGCTGCATTC	GGCGCTTCCGTTTTCTTGTT
Hprt	GGTTAAGCAGTACAGCCCCA	TCCACCACTTCGAGAGGTCC
Kdm5b	CGAGCTGGGAAGAGTTCGC	ATCACAAGCGAATGGTGGCT
Kmt5a	CAGACCAAACTGCACGACATC	CTTGCTTCGGTCCCCATAGT
Ndn	CCAGAGGAGCTAGACAGGGT	ACGCCTGGGGATCTTTCTTG
Ncor2	CCTGGTGGAAGTTCGTGGAC	ATGGTACTGGCGCTGTGTCAG
Prdm16	ATGGATCCCATCTACAGGGTA	CATTGCATATGCCTCCGGGT
Rnf40	GACCCTACGGTGACGGAAGT	CCAGTAGCGGTTGACGATGT
Setd7	GCCATGGATAGCGACGATGA	TCTGTCCGTGGAGGAGTAGG
Suv39H2	GACCGCGCCAGTTTGAATG	CTAAAGGTGGGCCCTCCAAG
Tbl1x	CACAAGTTGCACGGCTCG	ACTGTGGCTTTACTCGGTGG

Table 2.3 | Primers used for quantitative RT-PCR

2.2.13 RNA sequencing

2.2.13.1 Bulk sequencing

Four independent biological replicates of bulk LMPPs (20,000–32,000 cells), GMPs (30,000–61,000 cells), or CLPs (8,500–28,142 cells) isolated from 4-mo C57BL/6J female mice were sorted directly into 350 µl RLT buffer (QIAGEN) and flash frozen. Total RNA was isolated (QIAGEN), including DNase treatment. RNA was processed using an Ovation RNA-Seq kit (V2; NuGen). After shearing, a

TruSeq DNA sample prep kit (v2; Illumina) was used to prepare libraries. Libraries were sequenced on the HiSeq 2000 platform (Illumina) at a sequencing depth of >35 million reads per sample. Transcript abundances were estimated for each RNA-seq sample using RSEM. Read counts estimated for each gene by RSEM were given as input to the R package edgeR for differential expression analysis (Robinson et al., 2010). Genes were considered differentially expressed among LMPPs, GMPs, and CLPs based on log fold change >2 and FDR <0.05 criteria.

2.2.13.2 Single Cell RNA sequencing

Isolated LMPPs were resuspended at a concentration of 200 cells/µl. This cell suspension was mixed with C_1 Cell Suspension Reagent (Fluidigm, 634833) at the recommended ratio of 3:2 immediately before loading 5 µl of this final mix on the C_1 IFC along with 20 µl of freshly prepared staining buffer (2.5 µl ethidium homodimer-1 and 0.625 µl calcein AM from Life Technology's LIVE/DEAD Viability/Cytotoxicity Kit added to 1.25 ml C_1 Cell Wash Buffer) in their respective input wells. Images of captured cells were collected with a Leica DMI 4000B microscope in the brightfield, GFP and CY3 channels using ZenPro software.

Single-cell RNA extraction and mRNA amplification were performed on the C_1 Single-Cell Auto Prep Integrated Fluidic Circuit (IFC) following the methods described in the protocol (PN 100-7168, http://www.fluidigm.com/). Exogenous spike-in controls were added to the lysis mix at a 20,000-fold dilution.

The cDNA reaction products were quantified using the Quant-iT PicoGreen dsDNA (double-stranded DNA) Assay Kit (Life Technologies) and high-sensitivity DNA chips (Agilent) and were then diluted to a final concentration of 0.15–0.30 ng/μl using C_1 Harvest Reagent. The diluted cDNA reaction products were then converted into mRNA-seq libraries using the Nextera XT DNA Sample Preparation Kit (Illumina, FC-131-1096 and FC-131-1002, 1 kit used for 4 C_1 IFCs and 384 samples) following the manufacturer's instructions. After the PCR step, samples were pooled, cleaned twice with 0.9× Agencourt AMPure XP SPRI beads (Beckman Coulter), eluted in Tris + EDTA buffer and quantified using a high-sensitivity DNA chip (Agilent). For high-coverage sequencing, libraries from a subset of captured cells from each source were pooled to reach a target of 1 million aligned reads per cell.

An index for RNA-Seq by expectation maximization (RSEM) was generated on the basis of the mmR19 RefSeq transcriptome downloaded from the UCSC Genome Browser database (23,637 total genes). Read data were aligned directly to this index using RSEM/bowtie. Quantification of gene expression levels in TPM for all genes in all samples was performed using RSEM v1.2.4. Quantification of gene expression levels in transcripts per million (TPM) for all genes in all samples was performed using RSEM v1.2.8. Before all subsequent analyses, we filtered the data as previously described (Kowalczyk et al., 2015). First, we filtered out cells with < 2500 genes with $\log_2(TPM + 1) > 2$. Second, we excluded genes whose $\log_2(TPM + 1) < 4$ in aggregated data. Third, we centered the data by subtracting from each gene its average expression ($\log_2(TPM + 1)$)

across all cells. After filtering, our dataset included 94 single cell transcriptomes, 54 representing 4mo LMPP and 40 representing 14mo LMPP, and 1,467 genes. These libraries had < 20% of counts mapping to mitochondrial genes (4.64 ± 3.13%; mean ± SD). Principal component analysis was performed using the R stats prcomp() function with variables scaled for unit variance and a 0.05 tolerance. GSEA was performed with the javaGSEA application (version 2.0.14) with default settings (Subramanian et al., 2005). Enrichment was considered significant if FDR < 25% and $p < 0.05$. Cell cycle genes were defined as those cycling (G1/S, S, G2/M) in synchronized HeLa cells (Kowalczyk et al., 2015; Whitfield et al., 2002). We refined this list by only including genes present in our filtered dataset. We plotted the average of the G1/S transition signature versus the average of the S + G2/M signatures for each cell. Lineage-specific gene sets (CLP, PreGM, MkP, preCFU-E) were previously published (Sanjuan-Pla et al., 2013). Comparison to bulk RNA-seq libraries was performed by calculating geometric mean of all 4mo or 14mo LMPP scRNA-seq data ($\log_2$(TPM + 1)) and comparing to bulk RNA-seq $\log_2$(TPM + 1). Pearson correlation coefficients were calculated based on linear fit.

2.2.14 RNA extraction and cDNA synthesis

Total ribonucleic acid (RNA) was extracted from cells using RNeasy Mini Kit (Qiagen). Cells were washed once in ice-cold PBS and centrifuged at 350 x g and at 4°C for 5 minutes. Cells were resuspended in 100 µL of Buffer RLT containing 1% β-mercaptoethanol was added to the cell pellet. Cell lysis was performed by transferring lysate to a QIAshredder spin column placed in a 2 mL

collection tube and centrifuged for 2 minutes at full speed and at room temperature. Sample was transferred to an RNeasy spin column and RNeasy manufacturer protocol was followed for extraction. The RNA concentration was determined using NanoDrop ND-1000 Spectrophotometer. All RNA samples were stored at -80°C.

cDNA was synthesized using First Strand cDNA Synthesis Kit. Reactions were prepared containing up to 6 µL of RNA was added into each reaction. All cDNA samples were stored at -20°C.

2.2.15 Statistics

GraphPad Prism (version 5.03; LA Jolla, CA, USA) was used for statistical analysis and graphing. An unpaired, two tailed, Student's t-test was applied for comparison of two groups. For analysis of multiple groups, two-way analysis of variance (ANOVA) with Bonferroni post-tests was applied. Pearson correlation test was applied to examine association between single cell LMPP samples to GSE33315 data set (Zhang et al., 2012c). This data set was downloaded from Gene Expression Omnibus and Robust Multichip Average method was used for data normalization. Statistical significance of differences was attained when P value < 0.05 and was indicated in the related graphs. Statistical analyses where P value ≥ 0.05 are not indicated in the graphs and deemed not significant.

2.2.16 Tissue culture

Cell lines from 2.1.3 were cultured in specified medium. To maintain the HEK-293T cell lines, cells were sub-cultured at 1:5 or 1:10 ratio in fresh medium every 2-3 days. Trypsin-EDTA solution was used to detach the cells from growth surface. To maintain the NIH-3T3 cell line, cells were sub-cultured at 3 x 10^5 cells in fresh medium every 2-3 days. Trypsin-EDTA solution was used to detach the cells from growth surface. MEL cell line was subcultured at 1:10 ratio every 2-3 days. OP9 cell line was subcultured at 1:4 ratio every 2 days.

To cryopreserve cells, cells were centrifuged at 1250 RPM and at room temperature for 5 minutes. Cells were resuspended in ice-cold 10% DMSO-supplemented FBS with gentle pipetting. 1 mL of cell suspension was aliquoted into each cryotube, and stored at -80°C for short term and in liquid nitrogen tank for long term. To return frozen cells to culture, cryopreserved cells were thawed at 37°C by drop-wise addition to the pre-warmed culture medium. The cells were centrifuged at 1250RPM at room temperature for 5 minutes. The cell pellet was resuspended in complete culture medium and transferred to a culture flask and cultured at 37°C.

CHAPTER 3: RESULTS

3.1: *In vitro* and *in vivo* assay development for quantification of myeloid and lymphoid differentiation from LMPPs.

Multiple *in vitro* methods have been developed for the identification and quantification of immature hematopoietic cells, each with unique strengths and weaknesses **(Figure 3.1)**. Fluorescence-activated cell sorting (FACS), the only method that can prospectively identify and isolate HSCs and progenitors, provides no direct functional data. *In vitro* colony forming assays can be used to assess functional potential of hematopoietic progenitor cells, but these are best utilized to assess myeloid and erythroid cell potential rather than lymphoid cell potential. Long-term stromal co-culture assays have been developed to assay functional potential of HSC cells; however, unlike *in vivo* transplantation assays they do not assess some of the functional properties of HSCs such as homing and self-renewal (Aggarwal et al., 2012).

Currently, a combination of stromal co-culture and CFU assays are used separately or in parallel to assay the full lineage potential of multipotent progenitor populations. However, the need for two separate assays creates a barrier to assessing the full potential of a single multipotent progenitor cell. In order to assess functional properties of LMPPs and interrogate whether these functional properties are altered in aging or other conditions, I developed and optimized *in vitro* and *in vivo* assays to allow interrogation of the full lineage potential of LMPP cells.

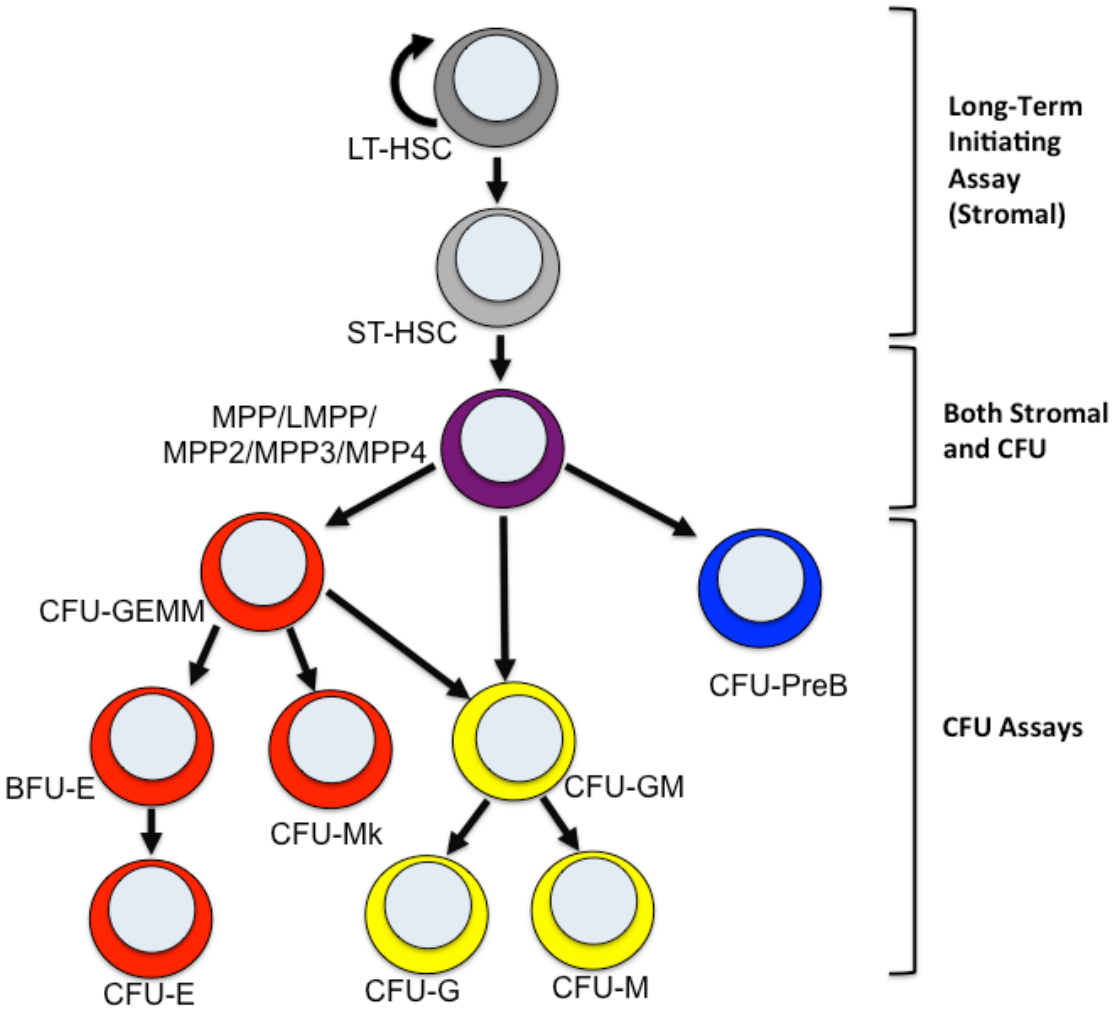

Figure 3.1 | Commonly used *in vitro* assays to determine the functional output of hematopoietic stem and progenitor cells. Stromal assays are used for more primitive cell types, while Colony Forming Unit (CFU) assays can be used to assess lineage-committed progenitor types. A combination of both assays must to used for multipotential progenitors. GEMM, Granulocyte Erythroid Monocyte Megakaryocyte; Pre-B, Pre-B lymphoid; Mk, Megakaryocyte; GM, Granulocyte Monocyte; G, Granulocyte; M, Monocyte; E, Erythroid; BFU-E, Burst Forming-Unit Erythoid

3.1.1 OP9 co-culture identifies relative production of mature B lymphoid and myeloid cells from multipotent progenitor cells

The OP9 mouse bone marrow stromal cell line (Kodama et al., 1994; Nishikawa et al., 1994) has been shown to stimulate the differentiation of hematopoietic progenitor cells into multiple lineages, including B cells (Carlyle et al., 1997). Despite being a commonly used protocol for lymphoid differentiation of hematopoietic progenitor cells, the OP9 assay needs to be optimized in each lab due to variations in the clone of the OP9 cell line used and cell culture reagents including serum. To optimize this assay in our laboratory, I sorted 500 hematopoietic stem and progenitor cells (defined as Lineage-/Sca-1+/c-Kit+, LSK) and placed them in pre-seeded wells of either 1000, 2000, or 5000 OP9 stromal cells supplemented with one of three different lot-defined serums. To compare the lymphoid differentiation phenotype to previous studies using OP9 cells, the wells were analyzed by FACS analysis using pan-hematopoietic (CD45), mature B-lymphoid (CD19), and myeloid (CD11b) markers every 3 days for 20 days **(Figure 3.2A)** (Pietras et al., 2015a; Reynaud et al., 2008)**.** FACS analysis at day 11 shows a predominance of myeloid cell production, while emergence of lymphoid cells is not seen until day 14 **(Figures 3.2B and 3.2C)**. By day 20, in all conditions, hematopoietic cell production is mainly B-lymphoid cells. In order to identify the conditions generating the most robust and reproducible lymphoid differentiation, the total numbers of cells for each lineage type was calculated. 500 LSK cells seeded on 1000 OP9 cells and supplemented with defined serum from Hyclone (Lot #1- AYM175301) yielded the greatest number of CD19 cells at day 20 and the dynamics of myeloid and lymphoid cell

production were consistent with previous studies **(Figure 3.2D)** (Pietras et al., 2015a; Reynaud et al., 2008).

Despite being a defined serum with minor lot-to-lot variation, the two Hyclone serum lots did exhibit differences in lymphoid cell production. Although the OP9 assay is able to assess lymphoid differentiation, there are a number of limitations in downstream analysis including the challenge of reisolating purified hematopoietic cells after OP9 co-culture. OP9 cells are extremely adherent, even with stringent FACS sorting there remains a possibility of including OP9 cells with sorted hematopoietic cells. The OP9 assay as optimized can provide insights into the dynamics of *in vitro* myeloid and lymphoid differentiation from multipotent progenitor cells; myeloid *in vitro* differentiation can be assessed as early as 5 days post-seeding and continues through day 17, while lymphoid differentiation can be assessed as early as day 11 and continues through 20 days of culture.

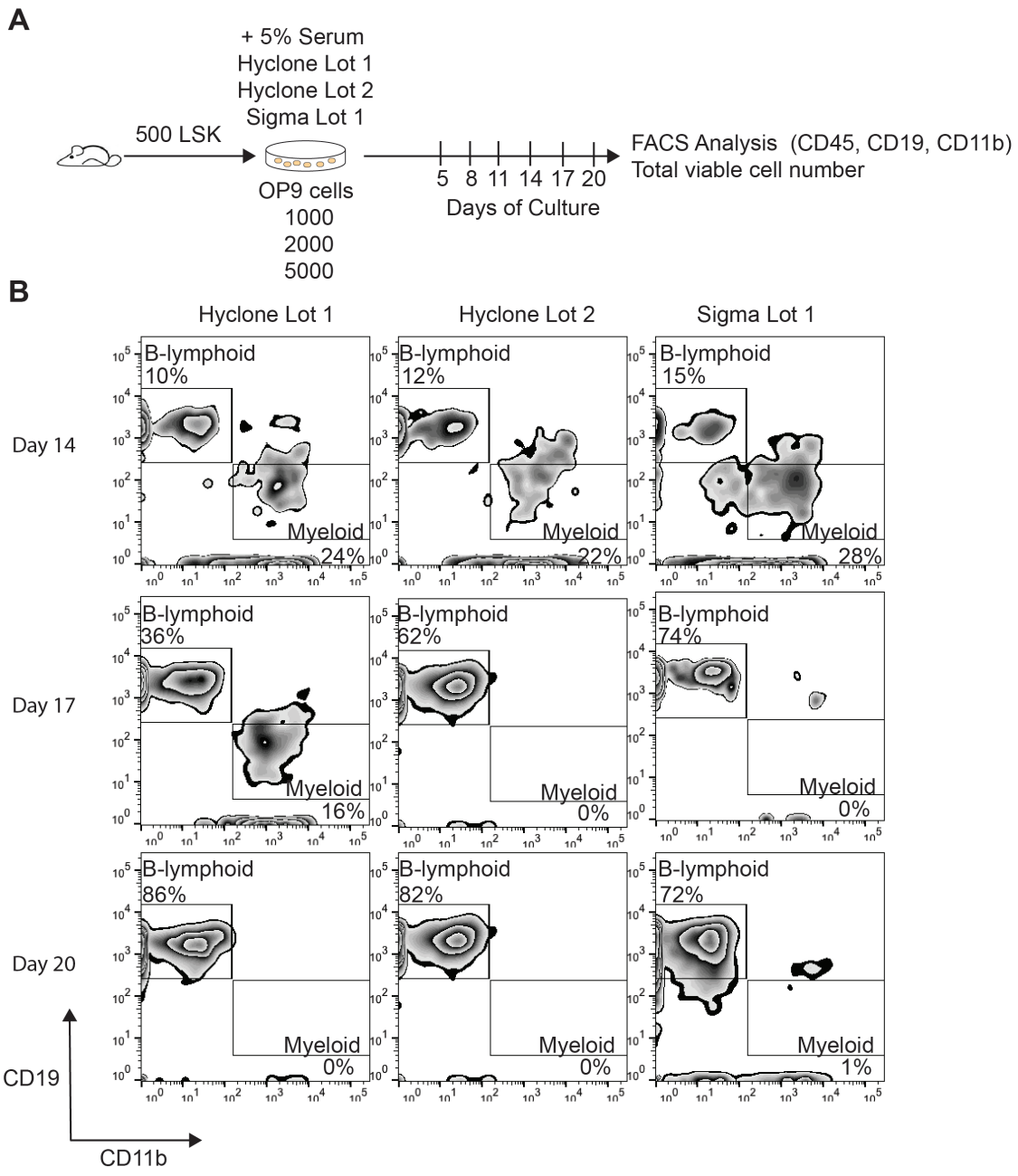
A
+ 5% Serum
Hyclone Lot 1
Hyclone Lot 2
Sigma Lot 1
500 LSK
OP9 cells
1000
2000
5000
5 8 11 14 17 20
Days of Culture
FACS Analysis (CD45, CD19, CD11b)
Total viable cell number
B
Hyclone Lot 1
Hyclone Lot 2
Sigma Lot 1
Day 14
Day 17
Day 20
B-lymphoid
10%
Myeloid
24%
B-lymphoid
12%
Myeloid
22%
B-lymphoid
15%
Myeloid
28%
B-lymphoid
36%
Myeloid
16%
B-lymphoid
62%
Myeloid
0%
B-lymphoid
74%
Myeloid
0%
B-lymphoid
86%
Myeloid
0%
B-lymphoid
82%
Myeloid
0%
B-lymphoid
72%
Myeloid
1%
CD19
CD11b

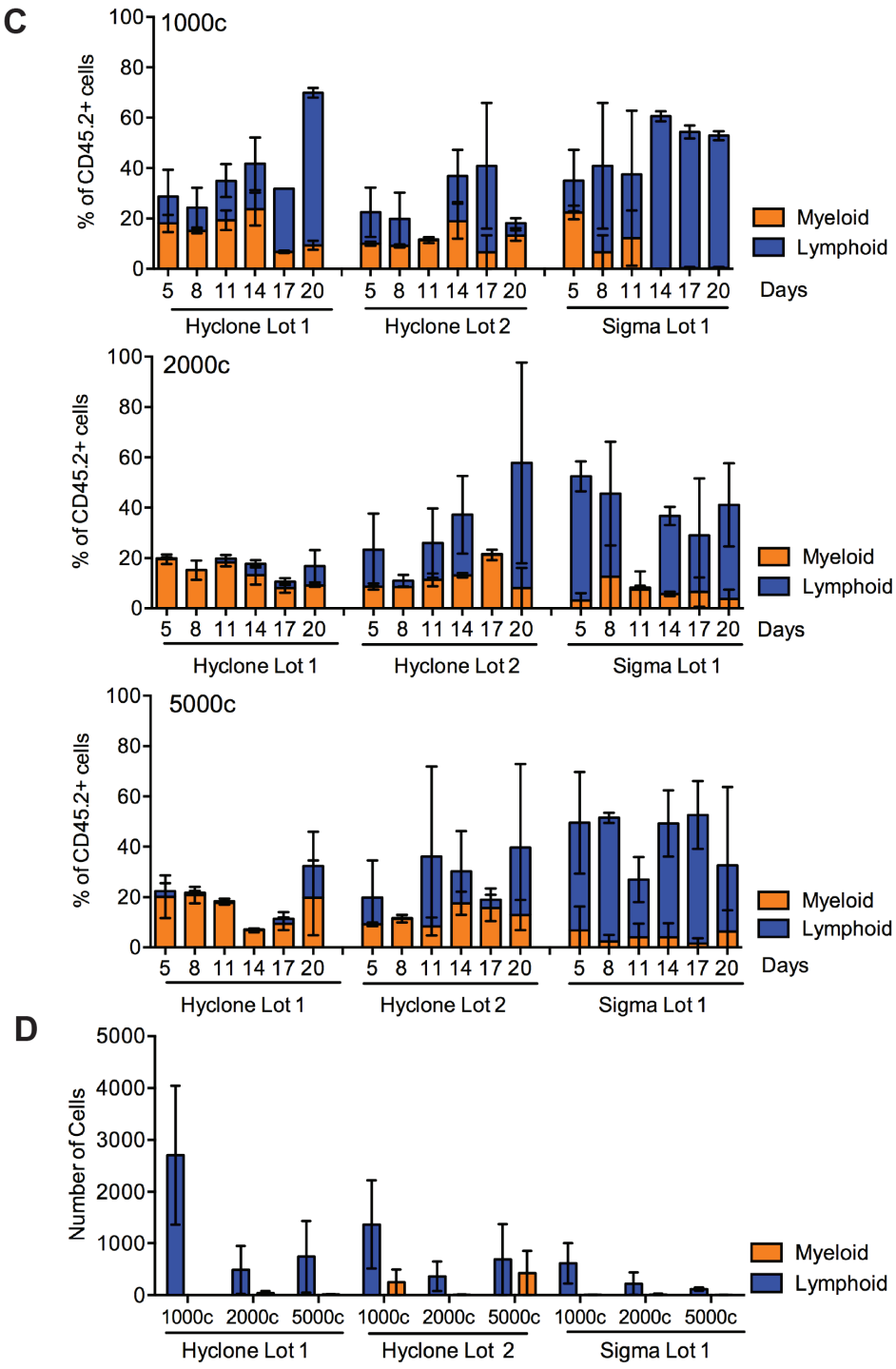

Figure 3.2 | OP9 co-culture supports myeloid and lymphoid differentiation of hematopoietic stem and progenitor cells. (A) Experimental outline to optimize conditions for the stromal OP9 co-culture with hematopoietic stem and progenitor cells (HSPCs) **(B)** Representative FACS analysis at day 14, day 17, and day 20 of culture for the lymphoid (CD19) and myeloid (CD11b) output of LSK cells seeded on 1000 OP9 cells, pre-gated on CD45.2. **(C)** Relative percentages of myeloid and lymphoid cells generated from LSK cells seeded on (top) 1000 OP9 cells, (middle) 2000 OP9 cells, and (bottom) 5000 OP9 cells. Results are shown as mean ± SEM of n=2. **(D)** Total numbers of myeloid and lymphoid cells generated at day 20. Results are shown as mean ± SEM (n=2).

3.1.2 Cytokine screening approach identifies five cytokines that are sufficient to support myeloid and B-lymphoid differentiation from lymphoid-primed multipotent progenitors in stroma-free culture

The CFU assay has been used to quantify clonal alterations in progenitor populations (Randall and Weissman, 1997). Directly seeding multipotential progenitor cell types into methylcellulose-based media containing defined growth factors supporting differentiation of myeloid cells (M3434; STEMCELL Technologies) robustly quantifies clonal myeloid colony-forming units (CFU) **(Figure 3.3A)**. Limited erythroid output is seen from LMPP and MPP4 cells consistent with known functional output from these cells (Adolfsson et al., 2005). However, direct seeding of multipotent progenitor cell types into a B-lymphoid CFU assay (M3630; STEMCELL Technologies) does not support B cell differentiation from these populations **(Figure 3.3B)**.

As the addition of Fms-related tyrosine kinase 3 ligand (Flt3L) and stem cell factor (SCF), has been shown to promote increased B-lymphoid colony readout from lymphoid progenitors (Nemeth et al., 2006), I supplemented our methylcellulose media with these growth factors. Although there was an increase in total colony output in the supplemented M3630, there was still very little pre-B lymphoid output from MPP4 and LMPP cells **(Figure 3.3C)**. The addition SCF has been shown to promote CFU-M, a myeloid colony type, in M3630 media (STEMCELL Technologies, 2016), consistent with my observation. The lack of robust lymphoid cell production in these conditions may be explained by the dynamics of *in vitro* lymphoid differentiation being much slower compared to

myeloid differentiation, but more likely that multipotent progenitors do not express *Il-7r* which is crucial for readout in the M3630 methylcellulose media that is supplemented with IL-7.

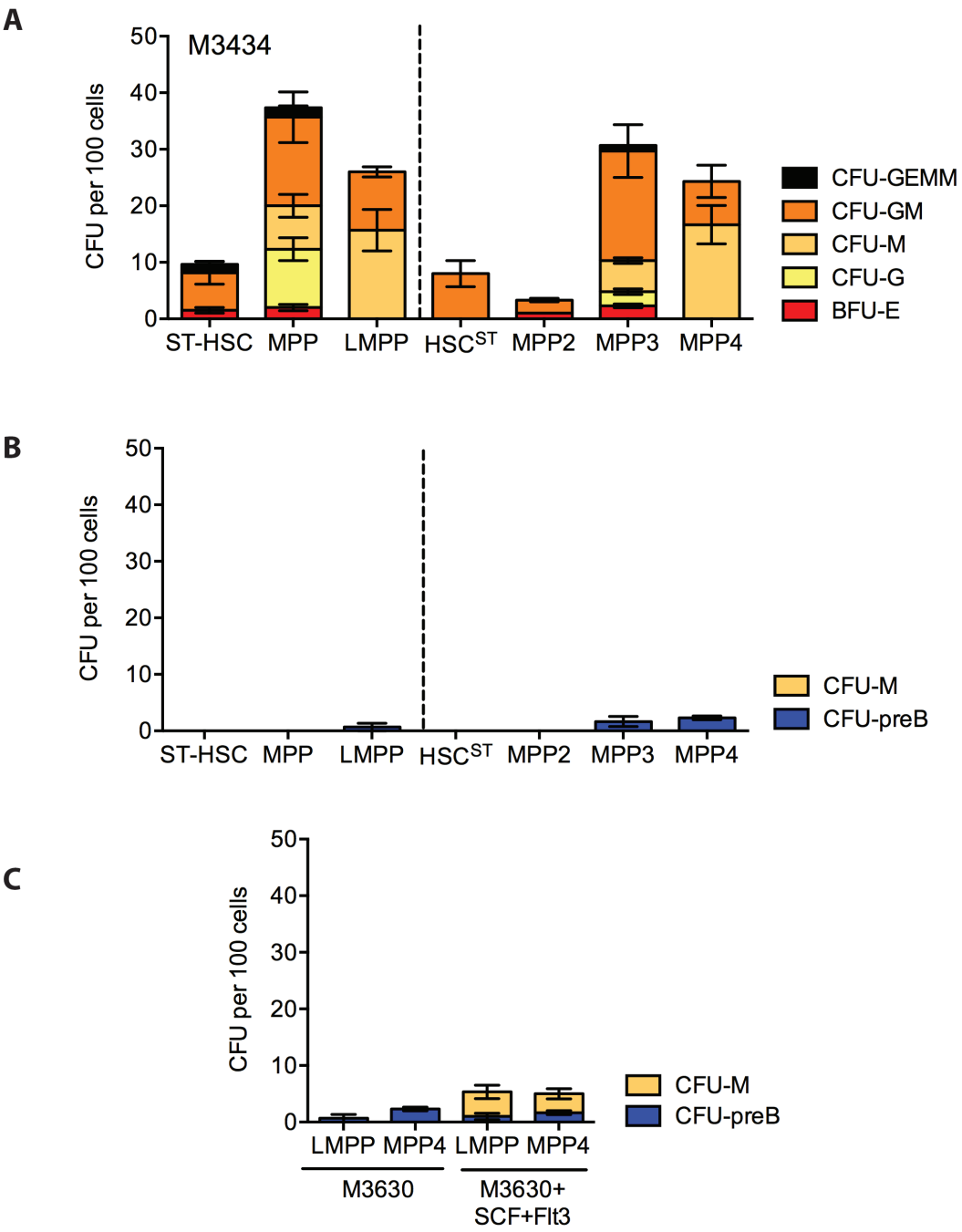

Figure 3.3 | *De novo* isolated HSC and multipotent progenitor cells are unable to form pre-B colonies in B-lymphoid-promoting M3630 methylcellulose media. CFUs per 100 *de novo* isolated HSC and multipotent progenitor cell subsets (gating strategies separated by dotted line) plated into **(A)** myeloerythroid-promoting M3434 or **(B)** preB-promoting M3630 methylcellulose media. Results are shown as mean ± SEM (n=3) **(C)** CFUs per 100 *de novo* isolated LMPP and MPP4 cells in preB-promoting M3630 methylcellulose with and without supplement of SCF (50ng/mL) and Flt3L (20 ng/mL). Results are shown as mean ± SEM (n=3). GEMM, Granulocyte Erythroid Monocyte Megakaryocyte; Pre-B, Pre-B lymphoid; Mk, Megakaryocyte; GM, Granulocyte Monocyte; G, Granulocyte; M, Monocyte; E, Erythroid; BFU-E, Burst Forming-Unit Erythoid

Lack of a robust, feeder-free assay to evaluate clonal lymphoid differentiation potential of multipotential progenitor cells has impeded the ability to directly compare factors controlling lymphoid versus myeloid cell fate commitment. To address this gap, I developed a novel, feeder-free *in vitro* system to examine myeloid and B-lymphoid differentiation of multipotent progenitor cells. I began by selecting cytokines and growth factors to be used in a pre-culture to stimulate both lymphoid and myeloid development from multipotent progenitors **(Table 3.1)**. To identify growth factors that could stimulate B-lymphoid differentiation, I examined existing gene expression data from *Lyl1*-deficient mice that exhibit profound defects in the generation of LMPPs, CLPs and ETPs, to identify growth factors that could stimulate B-lymphoid differentiation (Zohren et al., 2012). The authors performed differential expression analysis from microarray data between wild-type and *Lyl1*-deficent LMPP cells using DNASTAR Arraystar software (fold change >1.6 and P-value <0.05) and found 56 genes significantly downregulated in the *Lyl1*-deficent LMPP cells. From this data, I selected the growth factors TSLP, SDF-1, and LIF that were significantly downregulated in *Lyl1*-deficient LMPP cells and could play a role in LMPP development and progression towards lymphopoiesis. In addition, I selected the commonly used cytokines IL-7 and Flt3L used in the OP9 assay to promote lymphoid development. In order to maintain myeloid potential from these progenitor cells, I included IL-3, IL-6, and SCF, cytokines used in the myeloid-promoting methylcellulose assay.

Cytokine	Known roles in hematopoiesis	References
Interleukin 3 (IL-3)	Multi-lineage Differentiation of HSCs	(Dorssers et al., 1987)
Interleukin 6 (IL-6)	Myeloid/Granulocyte Stimulation	(Ferguson-Smith et al., 1988)
Stem Cell Factor (SCF)	Stem Cell Self-renewal and Maintenance	(Kent et al., 2008)
Interleukin 7 (IL-7)	Lymphoid Differentiation	(Or et al., 1998)
Fms-related Tyrosine Kinase Ligand (Flt3L)	Progenitor Proliferation and Differentiation	(Lyman et al., 1994)
Thymic Stromal Lymphopoietin (TSLP)	T-Lymphoid Maturation	(Quentmeier et al., 2001)
Stromal Cell Derived Factor (SDF-1)	Chemotactic for lymphocytes	(Bleul et al., 1996)
Leukemia Inhibitory Factor (LIF)	Stem Cell Self-renewal	(Bender et al., 1992)

Table 3.1 | Candidate cytokines and factors to supplement media to promote myeloid and lymphoid differentiation of lymphoid-primed multipotent progenitors

I seeded LMPPs into an initial 48 hour liquid culture and performed a screen with the selected cytokines to test the ability of defined growth factor combinations to stimulate B-lymphoid lineage development. After 48 hours, cells were plated into both the myeloid CFU (M3434) and lymphoid CFU (M3630) assays. Results of this screen identified the combination of IL-3/IL-6/SCF/IL-7/LIF that stimulated LMPPs to differentiate in the B-lymphoid CFU assay while also supporting differentiation of myeloid cells **(Figure 3.4A)**. However, to promote stimulation of specifically preB colonies in this media, I incrementally added SCF and Flt3L to the M3630 to find lymphoid promoting conditions for LMPP cells. Prior to plating in the different M3630 conditions, I stimulated LMPPs for 48 hours using the combination of IL-3/IL-6/SCF/IL-7/LIF and the lymphoid promoting combination of SCF/IL-7/Flt3L, previously used in the OP9 assay, with and without IL-3 and IL-6 **(Figure 3.4B)**. Although the total number of formed colonies between the combinations of IL-3/IL-6/IL-7/SCF/LIF and IL-3/IL-6/IL-7/SCF/Flt3L are similar,

the addition of LIF promotes more CFU-preB only colonies while the addition of Flt3L promotes a more mixed colony phenotype in the M3630 media**.** Additionally, with the supplement of 50ng/mL of SCF and 20 ng/mL of Flt3L, the highest proportion of preB-only colonies is seen in combination with the pre-culture cytokines containing LIF. Importantly, 48 hour culture with these 5 growth factors- IL-3/IL-6/SCF/IL-7/LIF increased the total colony number but did not alter the known cell fate of LMPP or other hematopoietic stem and progenitor cell types **(Figure 3.4C and D)**.

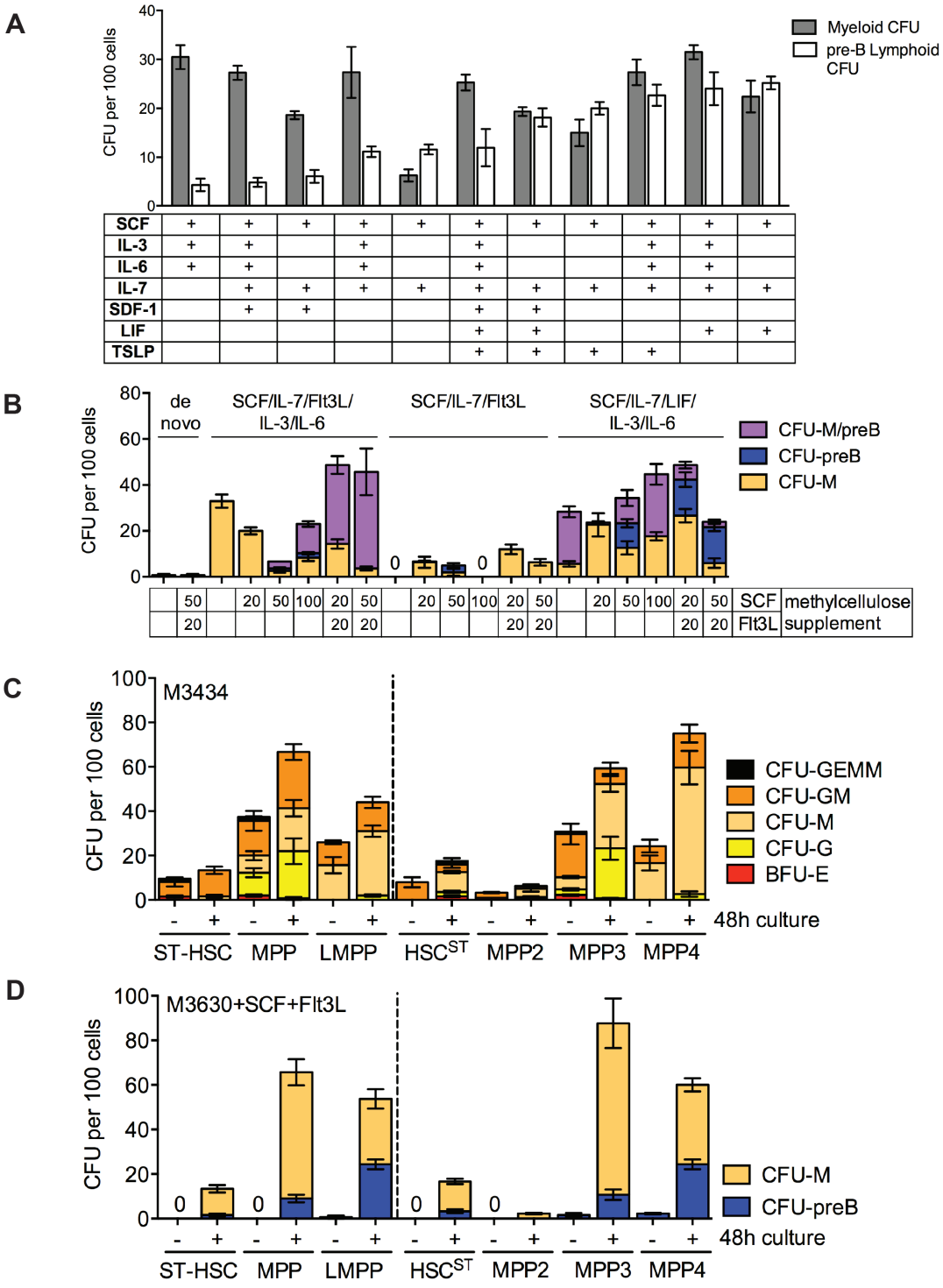

Figure 3.4 | Pre-culture of lymphoid-primed multipotent progenitors with the novel combination of SCF, LIF, IL-7, IL-3, and IL-6 promotes pre-B colony formation in B-lymphoid-promoting M3630 methylcellulose media. (A) CFUs per 100 LMPPs after 48 hour culture with cytokine combinations and **(B)** additional combination of methylcellulose supplements of SCF and Flt3L with selected cytokine combinations. Bars represent mean ± SEM (n=3) **(C)** CFUs per 100 input HSC and progenitor cell subsets (gating strategies separated by dotted line) after 48 hour culture with final combination followed by plating in M3434 or **(D)** M3630 supplemented with SCF and Flt3L. Bars represent mean ± SEM (n=3).

3.1.3 Development of single-cell assay for assessing myeloid and lymphoid potential of single LMPPs

The ability to define cell-to-cell functional heterogeneity and variation within the multipotential progenitor cell compartment has been impeded by lack of a robust assay to read out cell fate from single multipotential progenitor cells, in the absence of transplantation. To address this, I designed a single cell, *in vitro* functional assay to interrogate myeloid and B-lymphoid differentiation based on our 48h pre-culture system with defined factors **(Figure 3.5A)**. LMPP and MPP4 cells were sorted into 96-well plates at 1 cell per well. After 48h pre-culture, plating efficiency was measured by calculating the frequency of wells that contained greater than one cell, indicating that cell division had occurred. There were no significant differences in the plating efficiency or the average number of cells per well between LMPP and MPP4 cells **(Figures 3.5B,C)**. To assess lineage differentiation potential of single LMPP and MPP4 cells, the contents of each well after 48h pre-culture were harvested and split in equal volume into the myeloid CFU assay and the B-lymphoid CFU assay **(Figure 3.5D)**. With respect to lineage differentiation, I defined 3 classes of cells; myeloid (only gave rise to CFU-GM or CFU-M), B-lymphoid (only CFU-preB), or bipotential (generated both CFU-GM/CFU-M and CFU-preB). The majority of colony-forming single LMPP and MPP4 cells were bipotential, giving rise to CFU-M and CFU-preB **(Figure 3.5E).** Colony identification was verified using FACS analysis of cell surface markers B220 (lymphoid), CD11b (macrophage), and Gr-1 (granulocyte), and Giemsa-Wright staining to assess cell morphology **(Figure 3.5F)**.

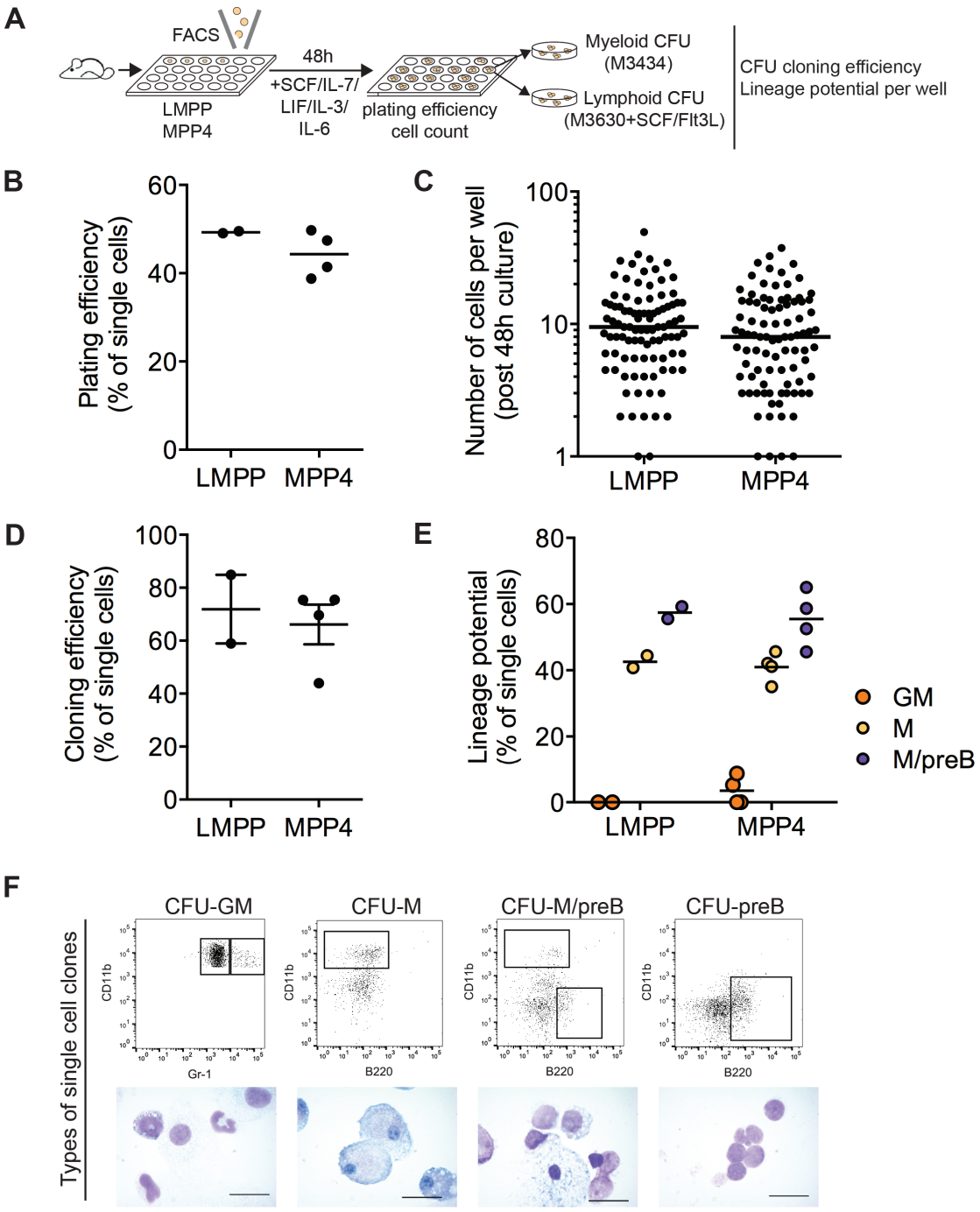

Figure 3.5 | Novel *in vitro* assay allows assessment of clonal myeloid and lymphoid differentiation from single multipotent progenitor cells. (A) Experimental design to assess lineage differentiation of single multipotent progenitor cells **(B)** Average percentage of single LMPPs and MPP4s that gave rise to >1 cell following 48h stimulation, out of 96 wells **(C)** Average number of cells per well post-48h stimulation. Results are shown as mean ± SEM of n=70. **(D)** Percentage of single LMPP and MPP4 cells that gave rise to CFU following 48h stimulation. Results are shown as mean ± SEM of n=2. **(E)** Percentage of single LMPP and MPP4 cells that gave rise to only CFU-GM, only CFU-M or CFU-M and CFU-preB post-48h stimulation. Results are shown as mean ± SEM of n=2 **(F)** Representative FACS analysis and Wright-Giemsa staining of cells isolated from single colonies.

3.1.4 *In vivo* transplantation of lymphoid-primed multipotent progenitor cells reveals dynamics of mature B-lymphoid and myeloid differentiation

In order to assess the ability of LMPP cells to produce myeloid and lymphoid lineage cell types *in vivo*, I used an irradiation transplant model to quantify LMPP multilineage output. Congenic strains C57BL/6J (expressing the CD45.2 isoform of the pan-hematopoietic marker CD45) and B6.SJL (expressing CD45.1) were used to discriminate donor and recipient contribution. 5000 donor LMPPs were transplanted into sub-lethally irradiated (600 rads) recipients and monitored weekly by peripheral blood analysis of multilineage engraftment by FACS using the cell surface markers CD45.2 and CD45.1 (donor/recipient discrimination), B220 (B-lymphoid), CD11b (myeloid), and CD3 (T-lymphoid). **(Figure 3.6A).** Since LMPPs have very limited self-renewal capacity, exhaustion of donor chimerism is seen by 7 weeks post-transplant **(Figure 3.6B)**. Engraftment peaks between 3 and 4 weeks at nearly 20% chimerism in recipient mice and multi-lineage engraftment is observed **(Figure 3.6C)**. Consistent with the dynamics of lineage differentiation observed in the OP9 assay, differentiation is predominantly myeloid at 1-2 weeks post transplant, but steadily declines over the 7 week period. B cell engraftment peaks at 4 weeks post-transplant, similar to the total engraftment, confirming B-lymphoid as the predominant cell type produced from LMPP cells. Emergence of T-lymphoid potential is not seen until after 4 week post-transplant, at which time total engraftment significantly declines, suggesting that LMPPs do not robustly contribute to the peripheral blood T-cell compartment.

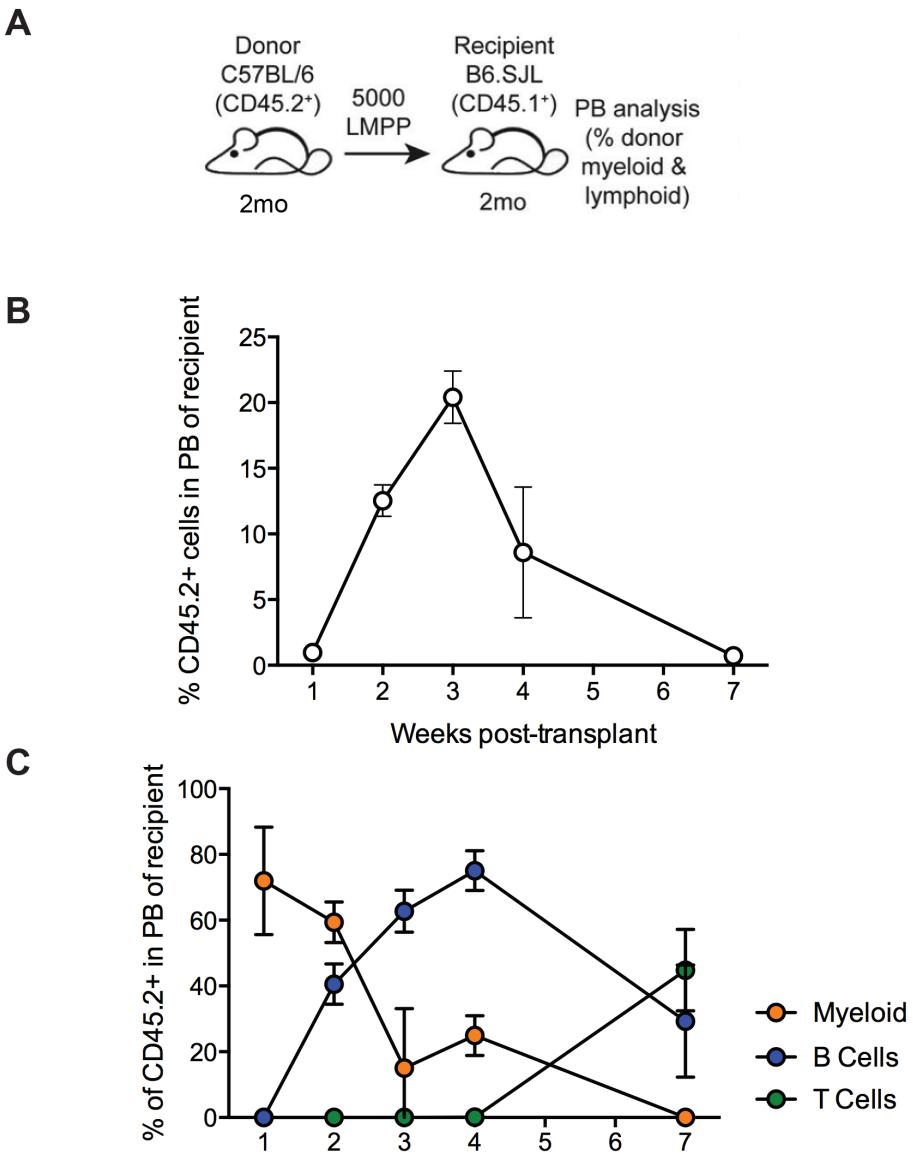

Figure 3.6 | *In vivo* transplantation assay allows assessment of multilineage engraftment dynamics of lymphoid-primed multipotent progenitors. (A) Schematic of experimental transplant design **(B)** Percent chimerism of recipient animals. Results are shown as mean ± SD (n=7). **(C)** Multilineage engraftment of LMPPs using cell surface markers CD45.2 (donor), CD45.1 (recipient), B220 (B-lymphoid), CD11b (myeloid), and CD3 (T-lymphoid). Results are shown as mean ± SD (n=7).

With the development and optimization of these *in vitro* and *in vivo* assays, the multilineage cell fate potential of lymphoid-primed multipotent progenitor cells can be effectively assayed at both the bulk and single cell level. The OP9 co-culture and *in vivo* transplantation assay can be used to assess the dynamics of lineage production of LMPP and MPP4 cells. This is particularly useful in assessing alterations in the differentiation potential of a particular population with respect to time. The bulk CFU assay is a high-throughput screening tool that can assess alterations in lineage differentiation at the population level. The development of a stroma-free, *in vitro* system to interrogate both lymphoid and myeloid differentiation potential of single cells now provides a high-throughput system to characterize multilineage output of individual lymphoid-primed multipotent progenitor cells.

3.2 Examination of the contribution of lymphoid-primed multipotent progenitor cells to age-associated hematopoietic decline

3.2.1 Lymphoid-primed multipotent progenitor cells are specifically reduced in early aging

Although much is known about aging hematopoiesis, studies have mainly focused on the primitive HSC and mature hematopoietic compartments (Morrison et al., 1996; Rossi et al., 2005). Little is known about how the multipotent progenitor compartment changes with age and contributes to aging-associated hematopoietic decline. To investigate how this heterogeneous compartment is altered with aging, I began by examining alterations in bone marrow frequency of long-term LT-HSCs (Lin-/c-Kit+/Sca-1+/CD-150+/CD34-), ST-HSCs (Lin-/c-Kit+/Sca-1+/CD-150+/CD34+), MPP2 (Lin-/c-Kit+/Sca-1+/CD-150+/CD48+), MPP3 (Lin-/c-Kit+/Sca-1+/CD-150-/CD48+), MPP4 (Lin-/c-Kit+/Flk2+/CD-150-), and the more general MPP (Lin-/c-Kit+/Sca-1+/CD-150-/CD34+/Flk2-) and LMPP (Lin-/c-Kit+/Sca-1+/CD-150-/CD34+/Flk2^{hi}) cells types across several ages using defined markers **(Figure 3.7A).** Analysis of C57BL/6J female mice between 2 and 28 months old (mo) revealed a significant increase in bone marrow frequency of LT-HSCs as early as 19-mo **(Figure 3.7B)**, consistent with known phenotypic HSC expansion with aging (Rossi et al., 2005). In contrast, a significant, progressive decline in bone marrow frequencies and total numbers of MPP4 and LMPP cells was observed by 14 months **(Figure 3.7C)**.

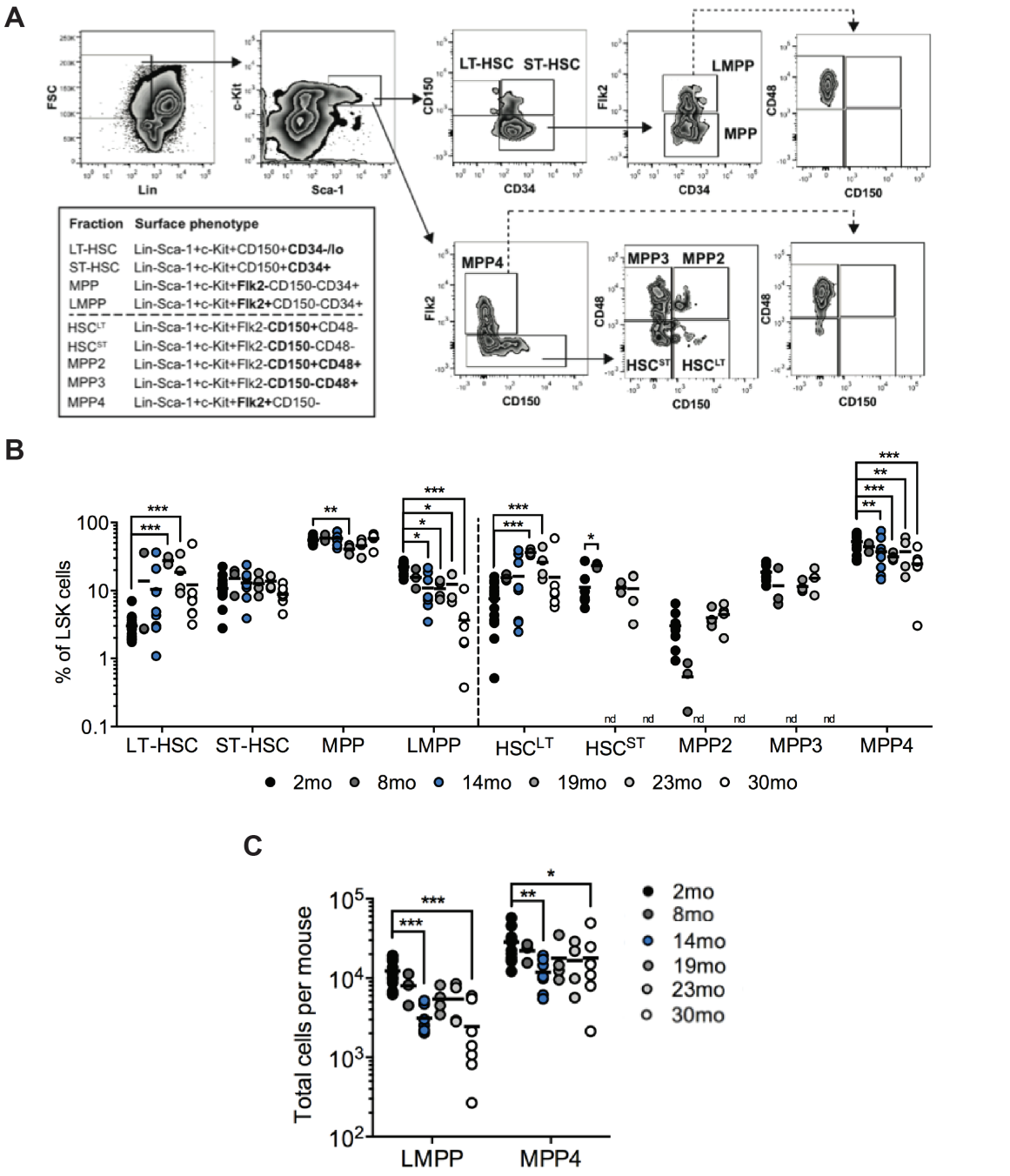

Figure 3.7 | Frequency of lymphoid-primed multipotent progenitors are specifically reduced in aging. (**A)** Phenotypic FACS gating showing isolation strategy for HSC and MPP subsets in representative 2 month old C57BL/6J female mouse. **(B)** Frequency of hematopoietic stem/progenitor cell populations within Lin- Sca-1+ c-Kit+ (LSK) cells (gating strategies separated by dotted line). Bars denote mean of replicates (circles) 2mo (n = 8-16), 8mo (n = 3), 14mo (n = 7), 19mo (n = 4), 23mo (n = 4) and 30mo (n = 7). (**P*<0.05, ***P*< 0.01, ****P*<0.001, two-way ANOVA with Bonferroni adjusted post-hoc t-test) **(C)** Total number of LMPP and MPP4 cells per mouse. Bars denote mean of replicates (circles) 2mo (n = 8-16), 8mo (n = 3), 14mo (n = 7), 19mo (n = 4), 23mo (n = 4) and 30mo (n = 7). (**P*< 0.05, **,*P*< 0.01, ****P*<0.001, two-way ANOVA with Bonferroni correction).

To compare this phenotype with previous studies of an aging-induced shift in lineage-biased HSC composition (Beerman et al., 2010; Challen et al., 2010; Dykstra et al., 2011; Morita et al., 2010), I examined $CD150^{hi}$ (myeloid biased), $CD150^{int}$ (balanced), and $CD150^{lo}$ (lymphoid biased) HSCs **(Figure 3.8A)**. I observed significant increase in frequency of $CD150^{hi}$ HSCs, concomitant with decrease in frequency of balanced $CD150^{int}$ HSCs **(Figure 3.8B)**. The increase in total numbers of $CD150^{hi}$ HSC is seen reaching significance at 14 months while no significant changes in total numbers are seen in the $CD150^{int}$ and $CD150^{lo}$ fractions **(Figure 3.8C).** Although this defines an overall myeloid skewing of the HSC compartment mediated by expansion of $CD150^{hi}$ HSCs, I find that lymphoid-biased HSCs ($CD150^{lo}$) are not specifically depleted with aging. These data suggest that the loss of MPP4/LMPP cells with aging may be independent of alterations in the lymphoid-biased $CD150^{lo}$ HSC compartment.

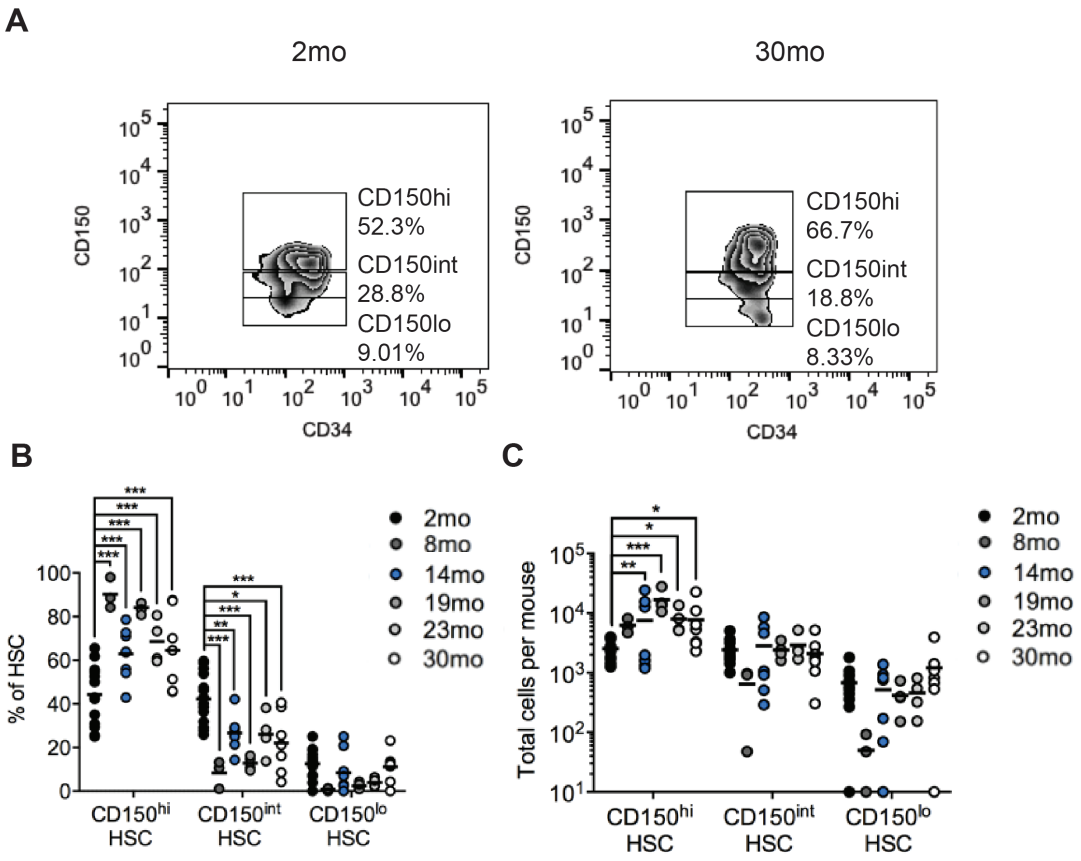

Figure 3.8 | Reduction of lymphoid-primed multipotent progenitors occurs independent of reduction of lymphoid-biased HSCs. (A) Representative FACS gating showing frequency of CD150^{hi}, CD150^{int}, and CD150^{lo} HSCs pregated on Lin, c-Kit, Sca-1, and CD34 in representative 2-mo and 30-mo mice. **(B)** Frequency of CD150^{hi}, CD150^{int} and CD150^{lo} cells within HSCs. Bars denote mean of replicates (circles) 2mo (n = 16), 8mo (n = 3), 14mo (n = 7), 19mo (n = 4), 23mo (n = 4) and 30mo (n = 7) (*P< 0.05, **P< 0.01, ***P<0.001, two-way ANOVA with Bonferroni correction). **(C)** Total number of CD150^{hi}, CD150^{int} and CD150^{lo} HSCs per mouse. Bars denote mean of replicates (circles) 2mo (n = 8), 8mo (n = 3), 14mo (n = 7), 19mo (n = 4), 23mo (n = 4) and 30mo (n = 7) (*P< 0.05, ** P< 0.01, ***P<0.001, two-way ANOVA with Bonferroni correction).

3.2.2 Aged lymphoid-primed multipotent progenitors exhibit increased cycling

I performed single cell RNA-seq using the C1 system (Fluidigm) on LMPPs isolated from 4mo and 14mo mice, the first age at which I observed a significant decrease in the frequency of the LMPP population. Following stringent filtering, I retained 54 and 40 libraries from 4mo and 14mo LMPP, respectively. Average gene expression in 4mo single cells was well correlated with expression in bulk 4mo cells (Pearson; $r = 0.701 \pm 0.026$; $n = 4$) **(Figure 3.9A)**. Principal component analysis revealed separation between 4mo and 14mo LMPP **(Figure 3.9B)**. Gene set enrichment analysis (GSEA) focusing on hallmark gene sets (Subramanian et al., 2007) identified significant enrichment ($P < 0.05$, FDR < 0.25) in 14mo LMPP restricted to cell cycle-related gene signatures and *Myc* targets **(Figure 3.9C)**.

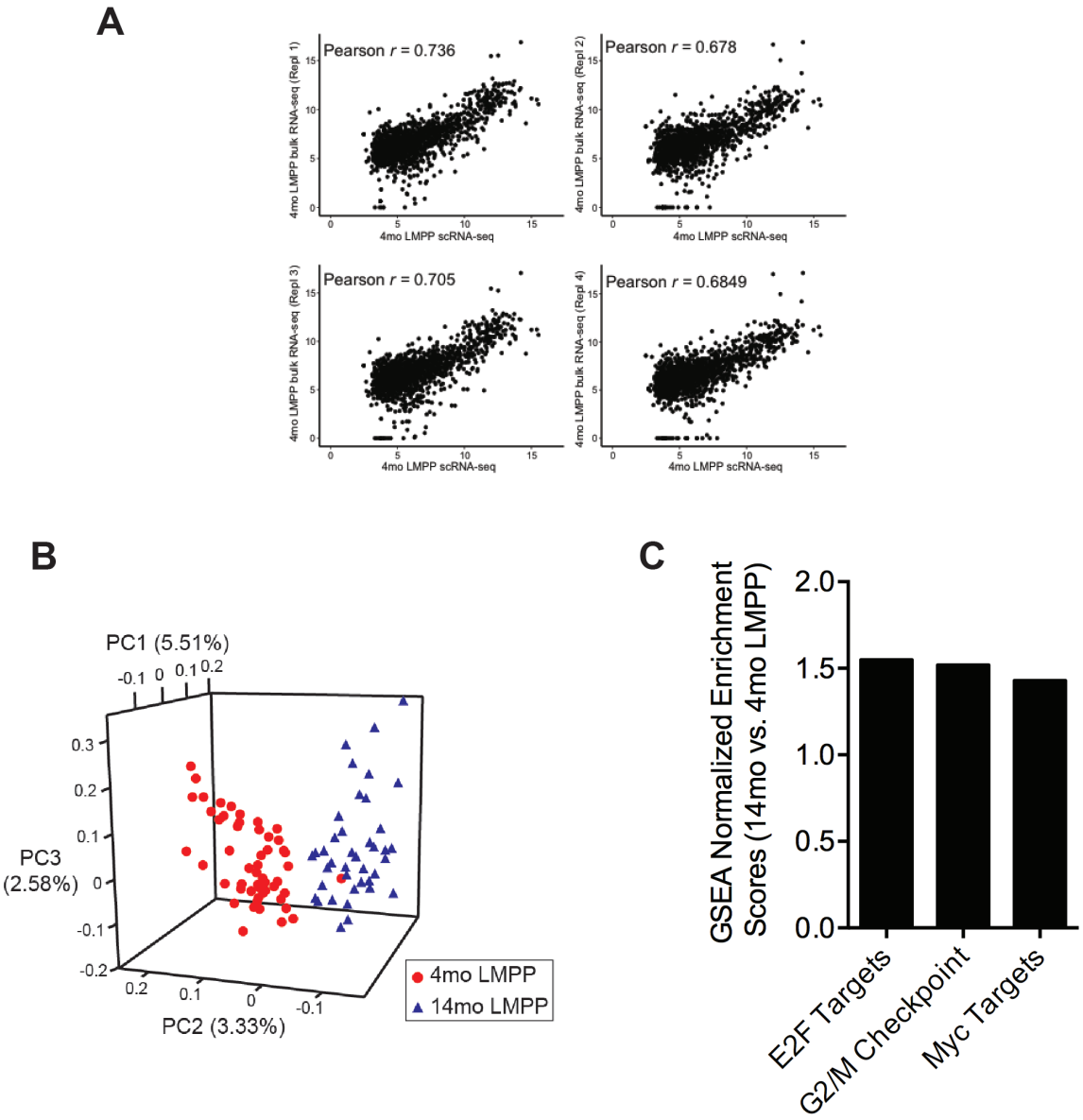

Figure 3.9 | LMPPs are transcriptionally altered with aging. (A) Scatter plots of the average gene expression of single cells (*n* = 54) and compared with those of bulk 4mo LMPP samples (n = 4). Pearson correlation coefficients for linear fit are shown. **(B)** Loading plot of the top three principal components in 4mo (n=54) and 14mo (n=40) LMPPs. Percent contribution of each principal component to total variation is shown. **(C)** GSEA normalized enrichment scores of significantly enriched gene sets ($P < 0.05$, FDR < 25%) in 14mo versus 4mo LMPPs.

To further dissect cell cycle state, I scored cells via average expression of G1/S transition, S and G2/M phase-specific signatures, based on previous annotation (Kowalczyk et al., 2015); (Tsang et al., 2015). Plotting each cell's phase-specific signature score defines three groups of cells: G0 (quiescent), G1 and S/G2/M **(Figure 3.10A).** By these estimates, ~9% of 4mo LMPP are quiescent and ~43% are in S/G2/M, consistent with known cell cycle status of MPP4 cells (Wilson et al., 2008). The frequency of cells in the S/G2/M cluster was significantly increased in 14mo versus 4mo LMPP (67.5% vs. 42.5%; p = 0.0097, hypergeometric test) **(Figure 3.10B)**, suggesting increased cycling of LMPPs with aging.

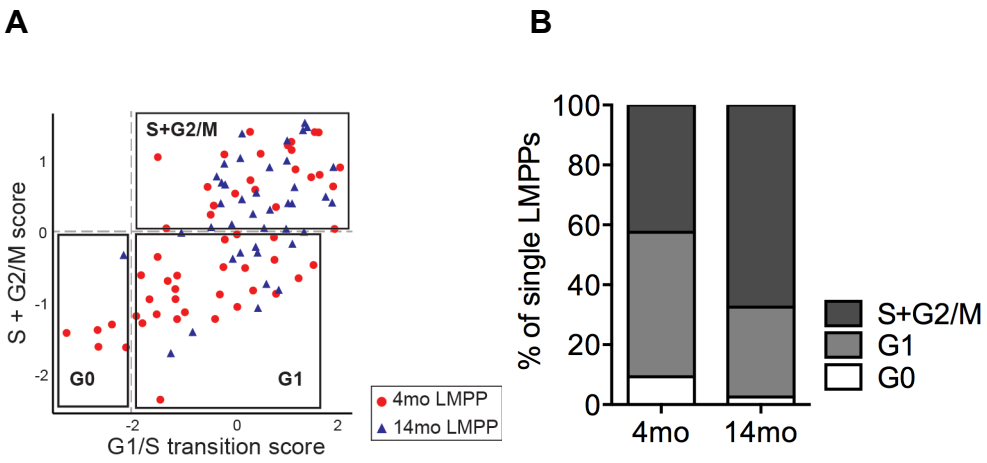

Figure 3.10 | Single cell RNA-seq identifies altered cycling of aged lymphoid-primed multipotent progenitors. (A) Average expression of G1/S transition genes (x-axis) and S + G2/M genes (y-axis) in each sample. The cells are partitioned into three groups representing G0, G1, and S + G2/M. **(B)** Frequency of 4mo and 14mo LMPPs annotated as being in G0, G1, and S + G2/M cell cycle phases.

3.2.3 Lymphoid-primed multipotent progenitor cells exhibit downregulation of lymphoid gene signatures with aging

To examine whether transcriptional differences between 4mo and 14mo LMPP involve hematopoietic lineage priming or differentiation, we used bulk RNA-seq data to define transcriptional signatures of LMPP, CLP, and GMP cells. Differential expression analysis between these cell types defined a “lymphoid priming” signature; genes upregulated in CLP or LMPP versus GMP (log fold change (logFC) > 2, FDR < 0.05) and a “myeloid priming” signature; genes upregulated in GMP versus CLP or LMPP (logFC > 2, FDR < 0.05). GSEA revealed significant enrichment (*P* = 0.028, FDR = 0.080) of the lymphoid priming signature in 4mo versus 14mo LMPP **(Figure 3.11 A)**. To independently validate these findings, I examined enrichment using GSEA of previously published lymphoid (CLP), granulocyte-macrophage (preGM), megakaryocyte (MkP) and erythroid (preCFU-E) gene signatures (Sanjuan-Pla et al., 2013) in my data. These gene sets included genes unique to each lineage committed progenitor, representative of lineage specific priming. I observed enrichment of the CLP signature only (*P* = 0.077, FDR = 0.149) in 4mo versus 14mo LMPP while no significant enrichment was seen in the other lineage priming sets. This suggest a reduction in lymphoid priming at the population level of LMPP cells at 14mo that is independent of alterations in other transcriptional lineage priming.

To compare relative lymphoid priming between single cells, I quantitated the mean expression of lymphoid driver genes identified by GSEA in each cell,

including genes upregulated during B lymphocyte differentiation from LMPP cells (*Fos*, *Jun*, *Gm2a*, *Tmem173*, and *Pde4b*) (Mercer et al., 2011; Ng et al., 2009) and the Ebf1-activated gene *Dusp2* (Vilagos et al., 2012). I observed that the lymphoid-priming driver gene score was significantly decreased in 14mo LMPP **(Figure 3.11B)**. On a per-cell basis, 14 out of 40 (35%) sampled 14mo LMPP had a lymphoid priming driver gene score below the range observed in 4mo LMPP. These results suggest a deficiency in expression of lymphoid-priming genes as a consequence of aging in the LMPP compartment.

A

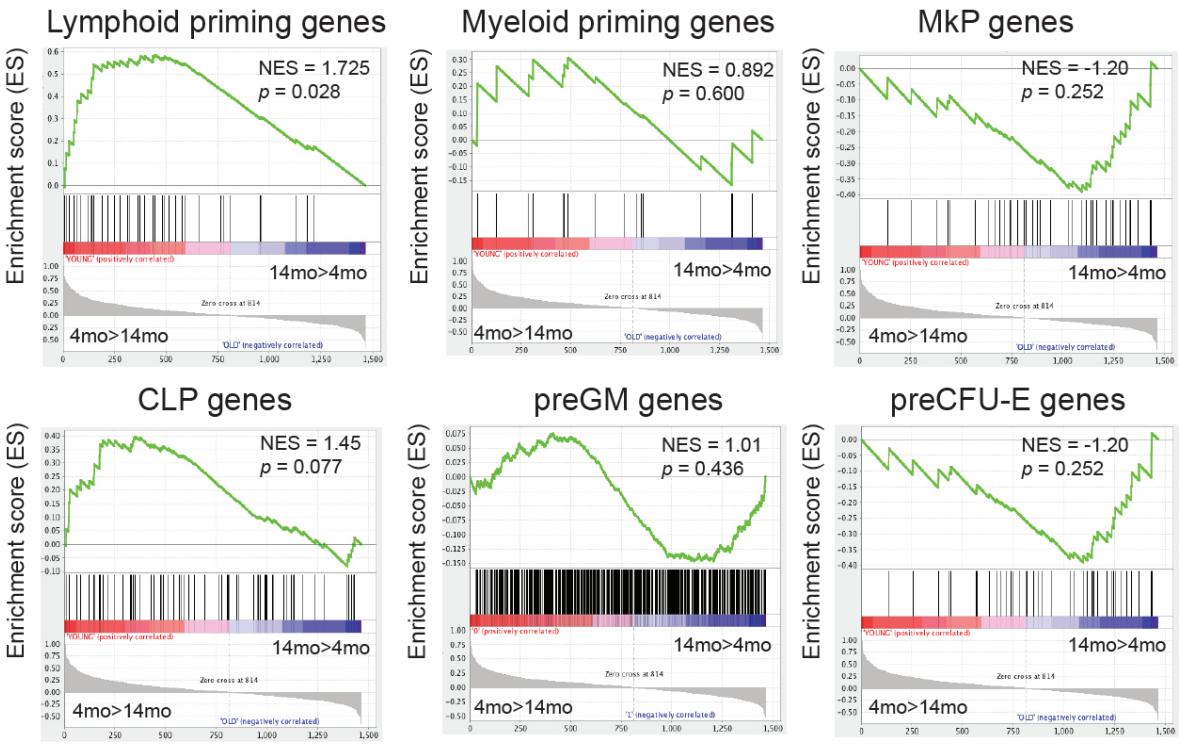

B

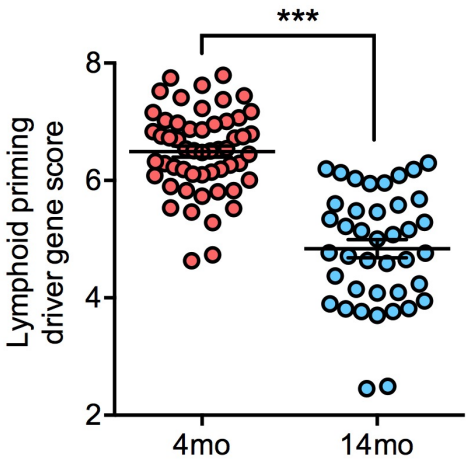

Figure 3.11 | Single cell RNA seq identifies downregulation of lymphoid priming in 14mo versus 4mo LMPPs. (A) Enrichment of lymphoid priming, myeloid priming, MkP, CLP, preGM, and preCFU-E gene signatures in 4mo versus 14mo LMPP scRNA-seq data. **(B)** Average expression of lymphoid priming driver genes in each sample of 4mo (n = 54) and 14mo (n = 40) LMPP (***P < 0.001, one-way ANOVA with Bonferroni adjusted post-hoc t-test).

3.2.4 Aged lymphoid-primed multipotent progenitor cells exhibit reduced B-lymphopoiesis *in vitro*

To assess clonal alterations in lymphoid-primed multipotent progenitor cells with aging, I utilized our defined-growth factor, single-cell assay. I observed no significant differences in the plating efficiency of LMPP and MPP4 cells isolated from 2mo, 8mo, and 23mo mice **(Figure 3.12A)**. I also did not observe significant differences in the median number of cells generated from single cells in 48 hours based on age **(Figure 3.12B)**. However, I did observe an absence of quiescent/slow cycling (0-1 cell divisions in 48h) LMPP and MPP4 in 23mo mice. Interrogating single cell lineage potential revealed several alterations in population composition of LMPP and MPP4 cells with aging **(Figure 3.12C).** First, LMPP cells with granulocyte-restricted potential (G) were significantly increased in frequency in 23mo versus 2mo mice. Second, LMPP and MPP4 cells with both macrophage and B lymphoid differentiation potential (M/preB) were significantly decreased in frequency with age.

Given my observation of age-associated loss in total numbers of LMPP and MPP4 cells **(Figure 3.7B)**, I used population frequency to calculate estimated total numbers of cells with given lineage potentials in whole bone marrow. This analysis revealed a significant loss in total numbers of macrophage- and B lymphoid-potent (M, M/preB, preB) LMPP and MPP4, progressively with aging **(Figure 3.12D)**. Furthermore, I did not observe significant differences in total numbers of cells with multilineage potential (G/M/preB, G/preB, GM) with aging. These data suggest a shift in composition of the LMPP and MPP4 population

with aging, with specific depletion of cells as they commit to the macrophage and/or preB lineages as early as 8mo of age, suggesting that loss of macrophage and B cell-restricted progenitors is initiated early in the process of aging.

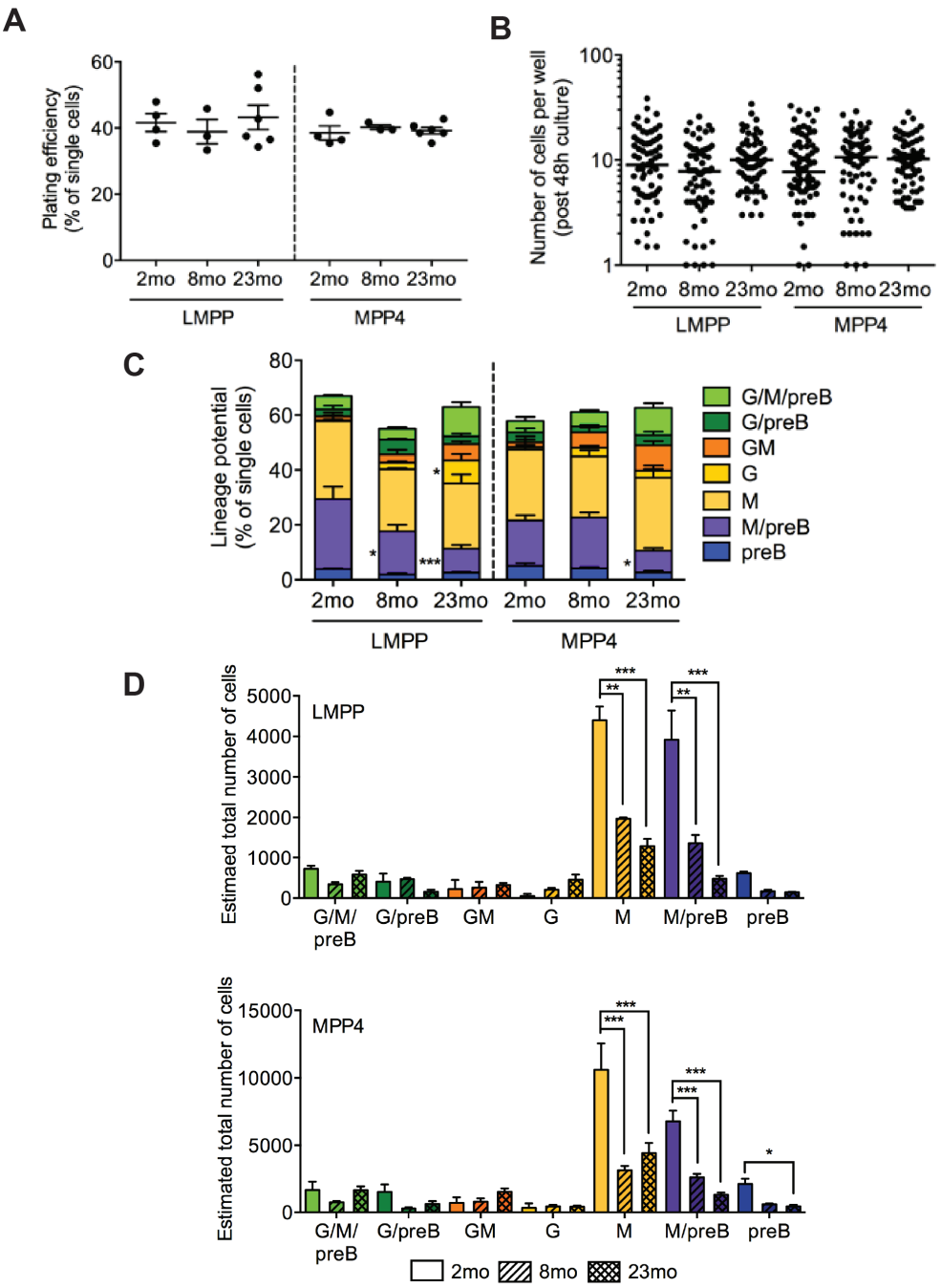

Figure 3.12 | Single cell functional assays reveal impaired lymphoid differentiation of aged lymphoid-primed multipotent progenitors *in vitro*. **(A)** Frequency of single LMPP and MPP4 isolated from 2mo, 8mo and 23mo mice that gave rise to ≥1 cell following 48h culture. Each dot represents the number of cells in a single 96-well. Results are shown as mean ± SEM of *n* = 4 (2mo), *n* = 3 (8mo) or *n* = 6 (23mo). **(B)** Number of cells per well post-48h culture. Bars denote median of *n* = 4 (2mo), *n* = 3 (8mo) or *n* = 6 (23mo). **(C)** Frequency of single LMPP or MPP4 isolated from 2mo, 8mo and 23mo mice that gave rise to G/M/preB, G/preB, GM, G, M, M/preB, or preB colonies. **(D)** Estimated total number of LMPP (top panel) or MPP4 (bottom panel) per mouse with each of the lineage potentials as defined in **(C)**. **(C, D)** Results are shown as mean ± SEM of *n* = 4 (2mo), *n* = 3 (8mo) or *n* = 6 (23mo). (**P* < 0.05; ***P* < 0.01; ****P* < 0.001, two-way ANOVA with Bonferroni adjusted post-hoc t-test)

3.2.5 Aged lymphoid-primed multipotent progenitor cells exhibit reduced B-lymphopoiesis *in vivo*

To interrogate functional changes in LMPPs *in vivo*, I transplanted 2,000 LMPP cells isolated from 4mo or 14mo CD45.2+ C57BL/6J mice into sublethally irradiated 4mo CD45.1+ B6.SJL recipient mice **(Figure 3.13A)**. While I did not observe a significant difference in peripheral blood reconstitution of 14mo LMPPs versus 4mo LMPPs **(Figure 3.13B)**, I observed that myeloid production was significantly increased from the 14mo donor cells at 2 weeks post transplant **(Figure 3.13C)**, whereas B cell production was significantly decreased at the peak of lymphoid engraftment, approximately 3 weeks post transplant **(Figure 3.13D)** suggesting a reduced B lymphoid differentiation potential of 14mo LMPPs. Together this data supports cell-intrinsic lineage skewing of aging LMPPs toward myeloid cell production at the expense of B cell production.

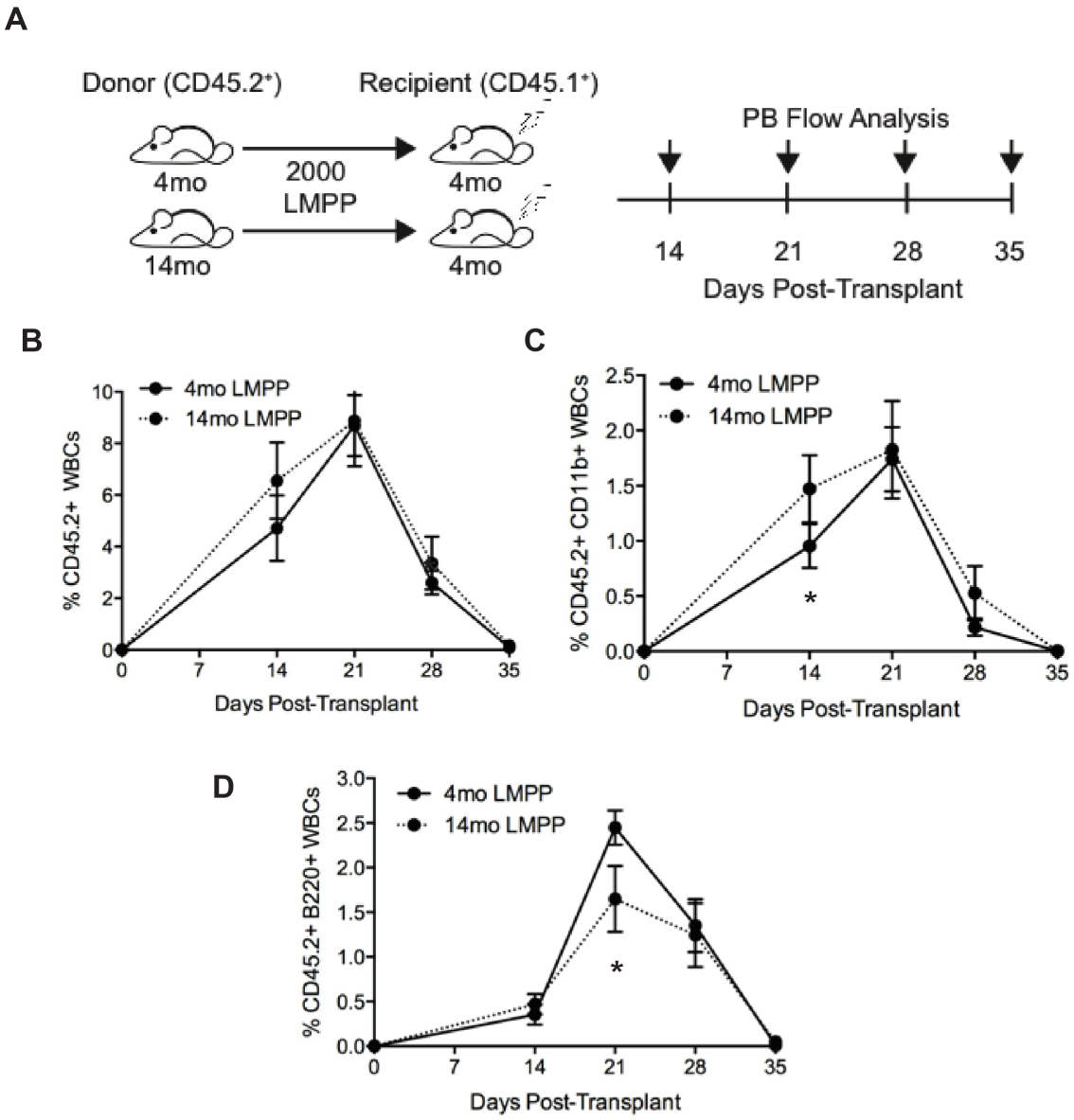

Figure 3.13 | *In vivo* transplant reveals cell-autonomous lineage skewing of aged lymphoid-primed multipotent progenitor cells (A) Experimental design to assess engraftment and lineage differentiation of LMPPs isolated from 4mo and 14mo mice. **(B**) Percentage of peripheral blood (PB) engraftment of LMPPs from 4mo or 14mo mice in sublethally irradiated recipient mice up to 5 weeks post-transplant. Results are shown as mean ± SEM (n=5). **(C)** Percentage of myeloid ($CD11b^+$) PB engraftment up to 5 weeks post-transplant. Results are shown as mean ± SEM (n=5)**.** (**P*<0.05, student's t-test) **D)** Percentage of B-lymphoid (B220+) PB engraftment up to 5 weeks post-transplant. Results are shown as mean ± SEM (n=5) (**P*<0.05, student's t-test).

Together, my data demonstrate an early and progressive loss of LMPP/MPP4 cells with aging that may be initiated independently of alterations in HSCs. Within aged LMPP/MPP4 cells, transcriptome and *in vitro* functional analyses at the single-cell level reveal a concurrent increase in cycling of aging LMPP/MPP4 with loss of lymphoid priming and differentiation potential. Impaired lymphoid differentiation potential of aged LMPP/MPP4 is not rescued by transplantation into a young bone marrow microenvironment, demonstrating cell-autonomous changes in the MPP compartment with aging. These results pinpoint an age and cellular compartment to focus further interrogation of the drivers of lymphoid cell loss with aging.

3.3 Examination of the role of *Kmt5a* in regulating lineage fate of lymphoid-primed multipotent progenitor cells (LMPP/MPP4)

3.3.1 *In vitro* lentiviral hairpin screen identifies *Kmt5a* as a candidate gene altering lineage-specific cell production from LMPP/MPP4 cells.

LMPP/MPP4 cells represent the most differentiated population in the hematopoietic hierarchy known to retain the potential to produce both myeloid and lymphoid lineage progeny *in vivo*. The specific epigenetic mechanisms governing cell fate commitment in LMPPs toward either the myeloid or lymphoid lineage remains poorly understood.

To determine if epigenetic factors influence the lineage differentiation of LMPP and MPP4 cells, I began analyzing existing transcriptome data to identify epigenetic factors that are differentially expressed between myeloid and lymphoid progenitor cells. The Gene Expression Commons Database (GEXC, www.gexc.riken.jp) is an open platform database that provides the dynamic range of each gene by meta-analysis of thousands of microarray data in many mouse and human hematopoietic cell types (Seita et al., 2012). Differential expression is based on a StepMiner algorithm (Sahoo et al., 2007) that fits a rising step function to the microarray expression data. The algorithm computes a threshold for each individual gene that divides the microarray data into low versus high expression based on each gene's individual dynamic range. I used this tool to identify transcripts that are differentially expressed between the myeloid and lymphoid progenitor cell types derived from LMPP, the GMP and the CLP, respectively. A total of 2776 genes were found to be differentially

expressed between the two cell types **(Figure 3.14)**. 1660 genes were upregulated in the GMP compared to the CLP, while 1116 were upregulated in the CLP compared to the GMP. These differentially expressed genes can be classified into 4 clusters. Clusters I (292 genes) and IV (824) are both more highly expressed in GMPs compared to CLPs. Cluster I has high expression in LMPPs and contains *Treml1* and *Il-6*, two transcripts known to regulate myeloid differentiation (Cohen et al., 1992; Won et al., 2015). Cluster IV has low expression in LMPPs including known myeloid transcription factors such as *Mpo* and *C/epbα* (Koleva et al., 2012; Tobler et al., 1988). Clusters II (1046 genes) and III (614 genes) are both more highly expressed in CLPs compared to GMPs. Cluster II has high expression in LMPPs and includes *Il-7r*, an essential lymphoid transcript (Corcoran et al., 1996). Cluster III, has low expression in LMPPs and includes genes involved in mature lymphoid differentiation such as *Dntt*. Consistent with previous literature that LMPPs are lymphoid primed (Greig et al., 2010), cluster II- transcripts that are lowly expressed in GMPS but highly expressed in CLPs and LMPPs- is the largest of the four subsets.

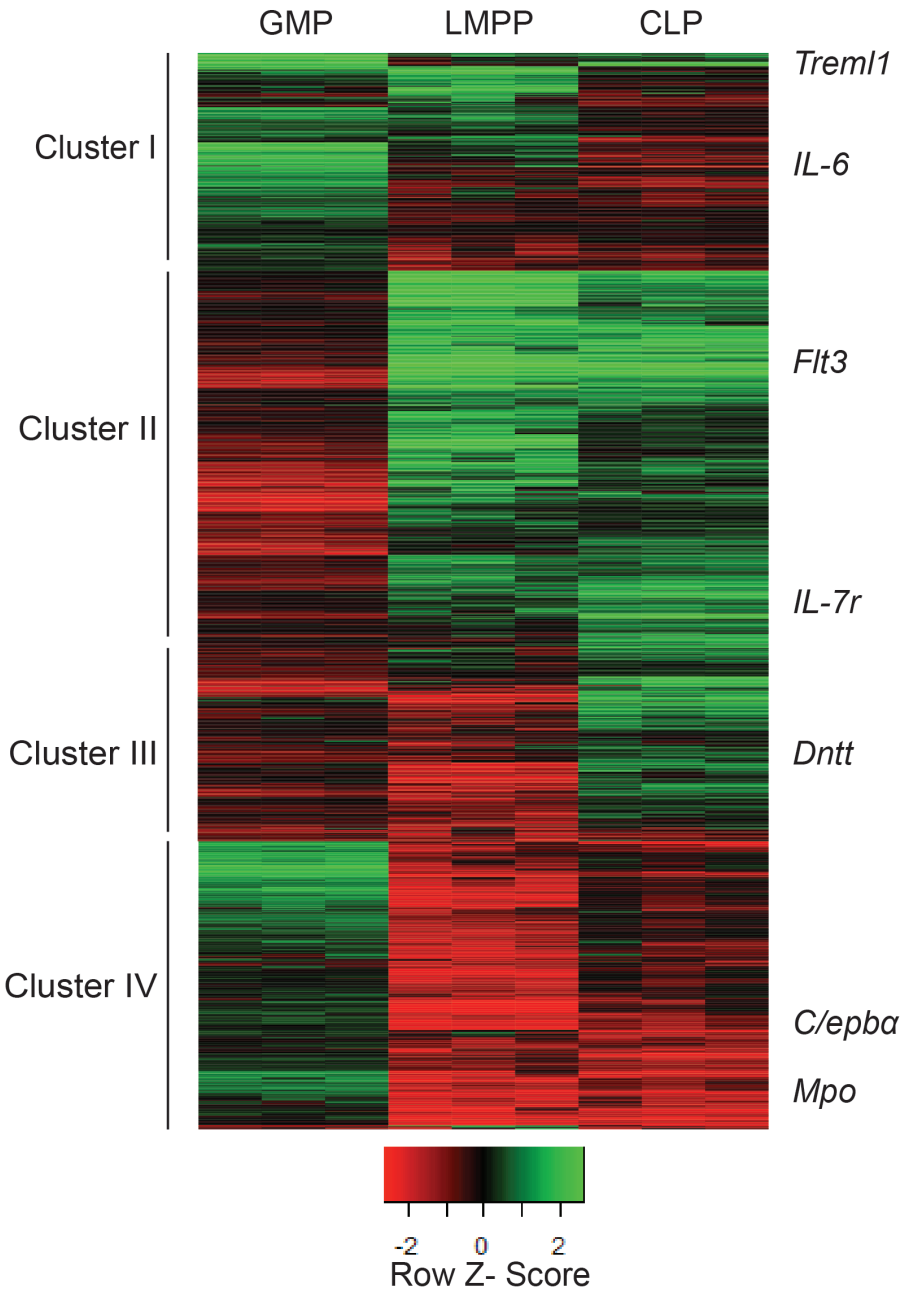

Figure 3.14 | Gene Expression Commons Database identifies four gene signatures of differentially expressed genes between the GMP and CLP.

To identify which of these differentially expressed genes had known roles in epigenetic regulatory processes, the gene list was annotated with GO terms using AmiGO 2 (The Gene Ontology Consortium, version 2.4.24) (Ashburner et al., 2000). Genes that were annotated with one of the 433 GO terms specifying epigenetic regulatory processes were then selected for further analysis. In total, of the 2776 differentially expressed genes, 86 overlapped with epigenetic GO term annotations and had a FDR value <0.05. In order to screen these candidate factors *in vitro,* I chose a lentiviral shRNA knockdown approach to modulate their expression. I narrowed our candidates based on commercially validated knockdown data (>75% knockdown of target expression in NIH-3T3 cells, Sigma). In addition, I included shRNA against *Crebbp* as a positive control due to its previously established indispensible role in hematopoietic differentiation (Rebel et al., 2002; Zimmer et al., 2011) as well as shRNA against *Setd7* due to its opposing epigenetic function to another candidate *Kdm5b* (Kim et al., 2015; Neff and Armstrong, 2013; Stewart et al., 2015) **(Table 3.2).**

Gene	Known Epigenetic Role	References	Differential Expression (GEXC) GMP	CLP
Crebbp	Histone acetyltransferase	(Bannister and Kouzarides, 1996)	No difference	No difference
Setd7	H3K4 methyltransferase	(Nishioka et al., 2002)	No difference	No difference
Atxn7l1	Histone acetyltransferase	(Helmlinger et al., 2004)	Upregulated	Downregulated
Cxxc1	Set1 methyltransferase complex	(Lee and Skalnik, 2005)	Upregulated	Downregulated
Kmt5a	H4K20 methyltransferase	(Rice et al., 2002)	Upregulated	Downregulated
Prdm16	H3K9 methyltransferase	(Pinheiro et al., 2012)	Upregulated	Downregulated
Suv39h2	H3K9 methyltransferase	(Rea et al., 2000)	Upregulated	Downregulated
Dach1	Recruits corepressors to chromatin	(Wu et al., 2009)	Upregulated	Downregulated
Tbl1x	HDAC3 complex	(Guenther et al., 2000)	Downregulated	Upregulated
Ncor2	Recruits HDAC complex	(Chen and Evans, 1995)	Downregulated	Upregulated
Myst4	Histone acetyltransferase	(McGraw et al., 2007)	Downregulated	Upregulated
Kdm5b	H3K4 demethylase	(Dey et al., 2008)	Downregulated	Upregulated
Ezh1	PRC2 complex	(Shen et al., 2008)	Downregulated	Upregulated
Ndn	Nuclear core protein complex	(Uetsuki et al., 1996)	Downregulated	Upregulated
Rnf40	H2B ubiquitin ligase	(Kari et al., 2011)	Downregulated	Upregulated
Atxn7l3	H2A and H2B deubiquitinase	(Atanassov et al., 2016)	Downregulated	Upregulated

Table 3.2 | Selected genes involved in epigenetic regulatory processes for *in vitro* lentiviral hairpin screening in LMPPs. Colors are based on epigenetic function: acetylation (green), methylation (blue), ubiquitination (orange), chromatin (pink).

Lentiviral shRNA pLKO.1 vectors targeting each of the 14 candidates were obtained from Sigma-Aldrich. To identify and isolate transduced cells carrying the shRNA, a GFP reporter cassette was cloned into the 3' end of CMV promoter region of each pLKO.1 vector (**Figure 3.15A).** Lentiviral supernatant was produced by co-transfection of each pLKO.1 vector with Rev, Tat, PM2, and VSVG viral packaging plasmids into HEK293T cells. To confirm the efficiency of knockdown, MEL (Murine erythroleukemia) cells were transduced with each of the viral supernatants and the level of expression of each target was compared to a non-targeting control via quantitative real-time PCR (qRT-PCR). At least 40% knockdown of target transcript expression was achieved from each hairpin **(Figure 3.15B).** I then began our screen using these confirmed lentiviral supernatants. 500 LMPP cells were isolated from the bone marrow of 8-10 week old C57BL/6J female mice and infected with lentiviral supernatant over 48 hours in liquid culture with the selected cytokines from Chapter 1. After 48 hours, the cells were harvested and half of the resulting cells were seeded into either a myelo-erythroid promoting CFU assay (M3434) or the preB-lymphoid promoting CFU assay (M3630) **(Figure 3.15C).**

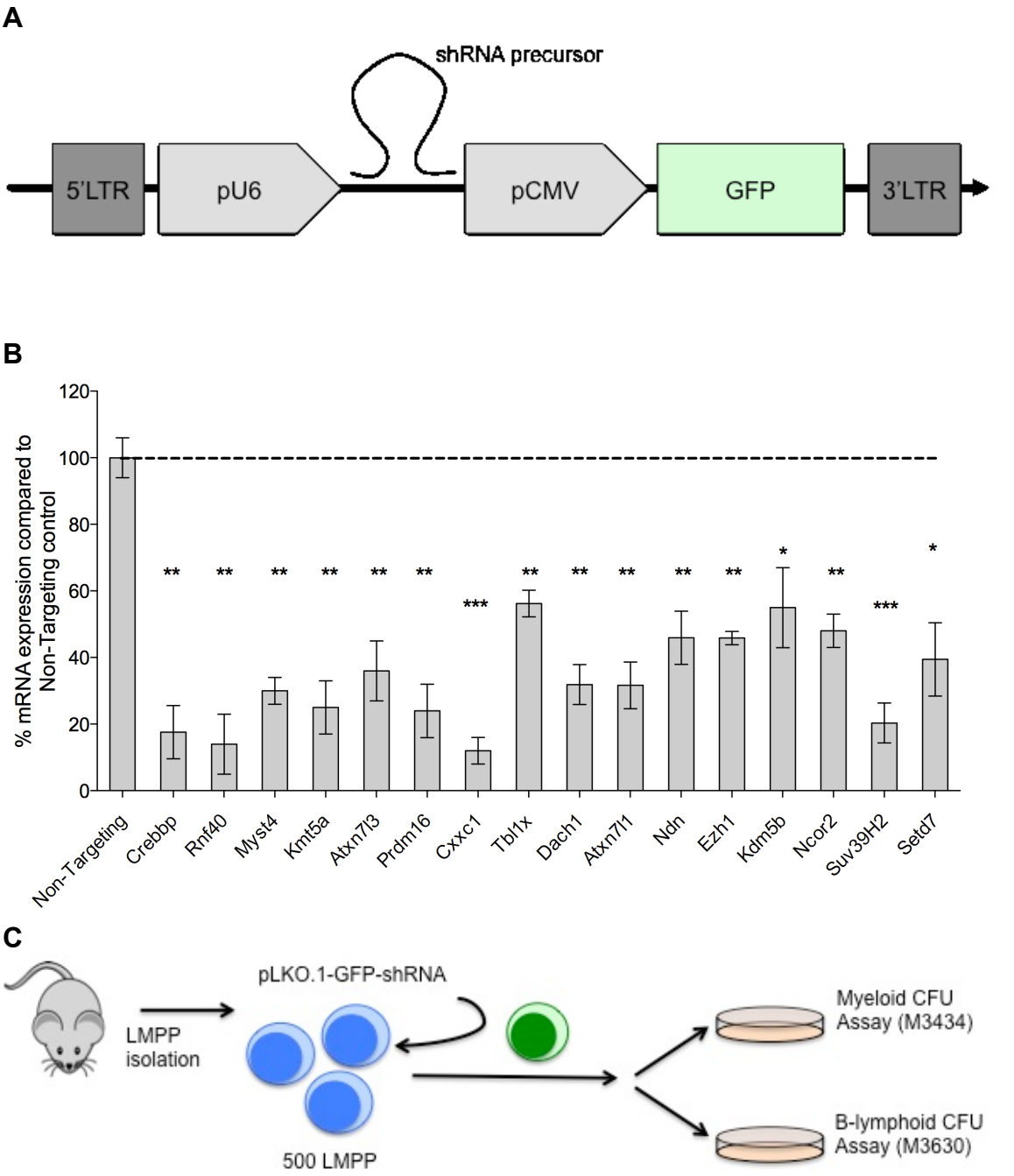

Figure 3.15 | Targeted knockdown approach for *in vitro* screening of candidate genes. (A) Schematic of the pLKO.1 vector including a GFP reporter cassette. **(B)** Level of transcript expression after knockdown with each shRNA measured by qRT–PCR in MEL cells. Bars represent mean ± SEM (n=2) (*P<0.05, **P<0.01, ***P<0.005 by unpaired t-test) **(C)** Experimental outline for *in vitro* shRNA screening of candidate genes using a clonal colony-forming unit (CFU assay).

Overall cloning efficiency was calculated as the total number of colonies arising out of both the myeloid and lymphoid assays as a percentage of the 500 input cells. Knockdown of the transcripts *Crebbp, Rnf40, Kmt5a*, *Cxxc1*, and *Ezh1* significantly altered the cloning efficiency of LMPPs compared to a non-targeting control shRNA **(Figure 3.16A)**. Knockdown of all these factors except for *Kmt5a* significantly impaired overall hematopoietic cell production from LMPPs, while knockdown of *Kmt5a* increased hematopoietic cell production compared to non-targeting control. In addition to overall cloning efficiency, we also examined the ratio of myeloid to lymphoid cell output. We discovered that knockdown of *Crebbp, Atxn7l3, Myst4, Rnf40*, *Kmt5a,* and *Suv39H2* significantly altered the ratio of myeloid to lymphoid differentiation compared to non-targeting control **(Figure 3.16B).** Knockdown of *Suv39h2* resulted in an increased ratio of lymphoid to myeloid cell production, while knockdown of *Crebbp, Atxn7l3, Myst4, Rnf40* or *Kmt5a* resulted in an increased ratio of myeloid to lymphoid cell production. As the knockdown of *Crebbp and Rnf40* exhibit significant loss of both myeloid and lymphoid lineage production, they are likely essential for viability or differentiation. *Kmt5a* was the only factor to produce a result in CFU expansion and myeloid lineage bias upon knockdown compared to non-targeting control.

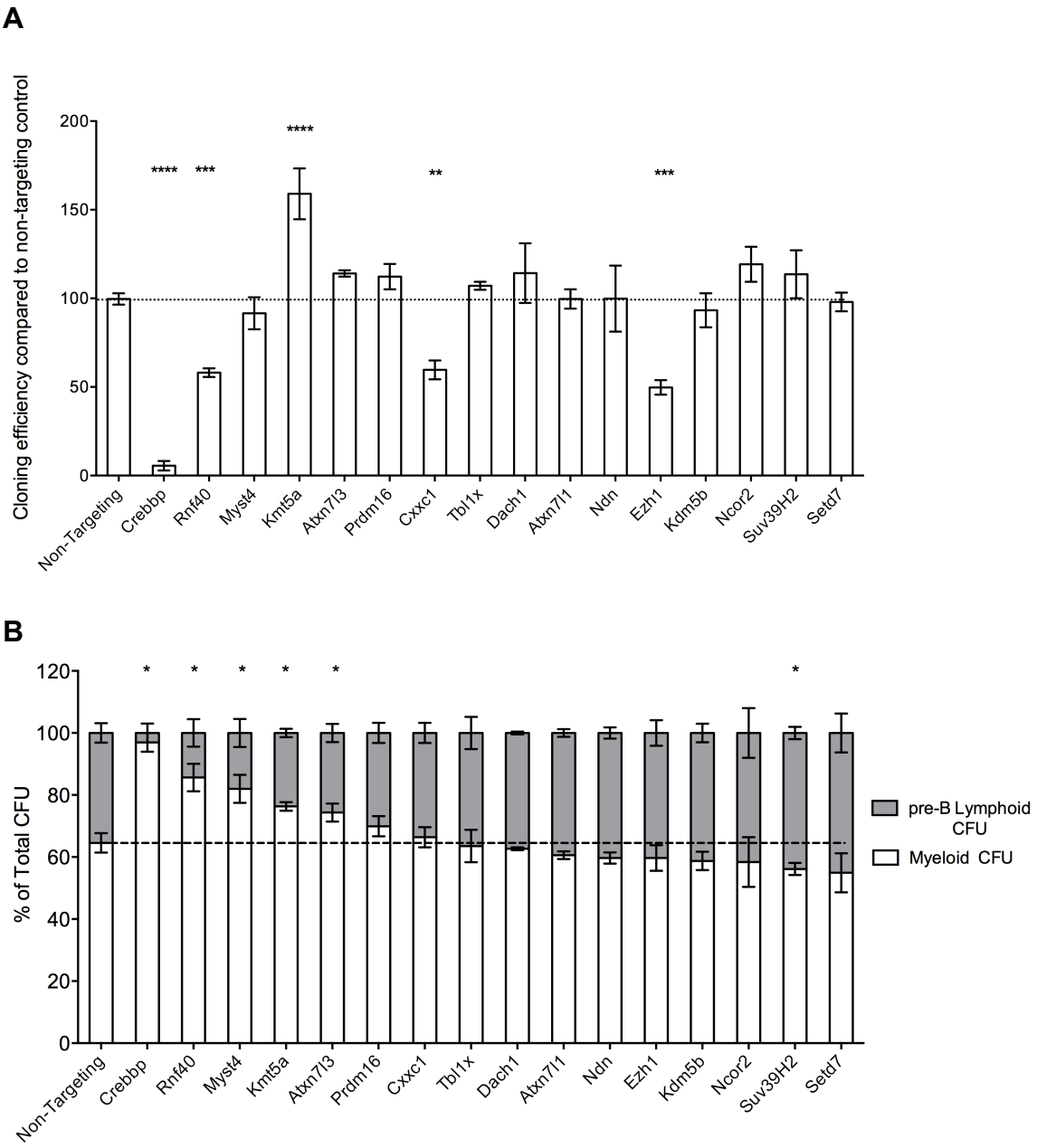

Figure 3.16 | *In vitro* shRNA screen identifies epigenetic factors altering hematopoietic cell production from LMPPs. (A) Total CFU cloning efficiency from 500 input LMPP cells after infection with target hairpin compared to non-targeting control (n=3) (***P*<0.01, ****P*<0.005, *****P*<0.001, unpaired student's t-test) **(B)** Frequency of total CFU arising from each lineage-promoting assay. Bars represent mean ± SEM (n=3) (**P*<0.05, unpaired student's t-test).

3.3.2 Knockdown of *Kmt5a* increases macrophage cell production from lymphoid-primed multipotent progenitors *in vitro*

To test the specificity and robustness of our shRNA targeting *Kmt5a,* I selected 2 additional independent shRNA hairpin constructs targeting *Kmt5a* in the pLKO.1 vector (Sigma). A mCherry fluorescent reporter cassette (Clontech) was cloned into these vectors to identify and isolate cells effectively transduced with the lentiviral hairpins. As *Kmt5a* has three known protein coding isoforms, hairpins were selected that targeted all isoforms **(Figure 3.17)**. One of these hairpins (1070) targets the same exon 7 as the hairpin used in the original screen (1074) while a second hairpin (1072) targets the 3'UTR of the *Kmt5a* transcript**.** Knockdown of *Kmt5a* was confirmed in MEL cells by analyzing *Kmt5a* expression via qRT-PCR compared to a non-targeting control. The highest level of knockdown of *Kmt5a* was seen using hairpins 1070 and 1072 at 72% ± 8.9 and 85% ± 9.1, respectively and were used for further studies **(Table 3.3).**

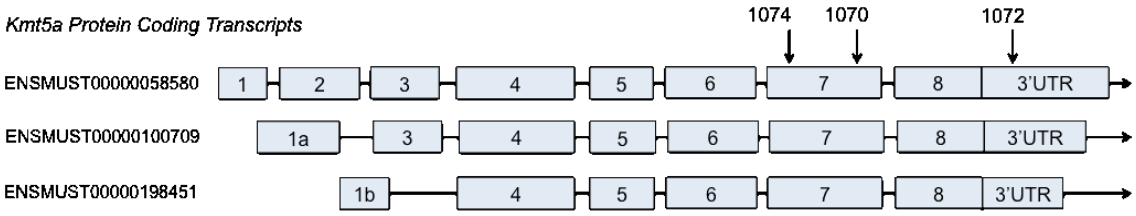

Figure 3.17 | Recognition target site of the three distinct hairpins selected to target *Kmt5a* transcripts. Arrows indicate the locations of the target sites within the *Kmt5a* transcript.

shRNA	Target Sequence	Transcript Region	% of *Kmt5a* Knockdown (KD)	Significant Compared to Non-Targeting Control
1070	TGGCTGCTACATGTACTAT	Exon 7	72 ± 8.9	*
1072	ACACTCACTCTTAGCTAA	3' UTR	85 ± 9.14	*
1074	AGGCATGAAGATTGATCT	Exon 7	66 ± 4.51	*

Table 3.3. | Knockdown efficiency of three independent shRNA hairpins targeting *Kmt5a* in MEL cells. Knockdown of *Kmt5a* was measured by RT-PCR compared to a non-targeting control (n=3) (*P<0.05).

To identify whether increase in myeloid CFU production observed in the primary screen could be replicated using 2 independent shRNAs, I performed knockdown of *Kmt5a* using hairpins 1070 and 1072. Primary MPP4 cells isolated from 2 month old C57BL/6J female mice were transduced with lentiviral supernatant for 48 hours, mCherry positive cells were sorted by FACS and 150 mCherry positive cells were plated into the myeloid-promoting CFU assay (M3434) **(Figure 3.18A).** After 48 hours, there was no significant difference seen in the proliferation between cells transduced with either *Kmt5a* hairpin or non-targeting control **(Figure 3.18B,C).** To interrogate whether knockdown alters proliferation during the 48 hour period, I examined mCherry expression via FACS and included a mock transduced control to aid in identification of mCherry positive expression. We observed that mCherry expression was not significantly different between cells transduced with either the non-targeting control or *Kmt5a* hairpins **(Figure 3.18D,E).** To confirm that *Kmt5a* had effectively been targeted in mCherry expressing cells, I analyzed *Kmt5a* expression in sorted mCherry positive cells using qRT-PCR. Cells positive for mCherry expression and transduced with *Kmt5a* hairpins exhibited significant knockdown of *Kmt5a* (78.3%±7.8 and 84.5%±9.2, respectively) versus the non-targeting control shRNA **(Figure 3.18F)**. Together, this data suggests that knockdown of *Kmt5a* has no significant effects on proliferation of MPP4 cells.

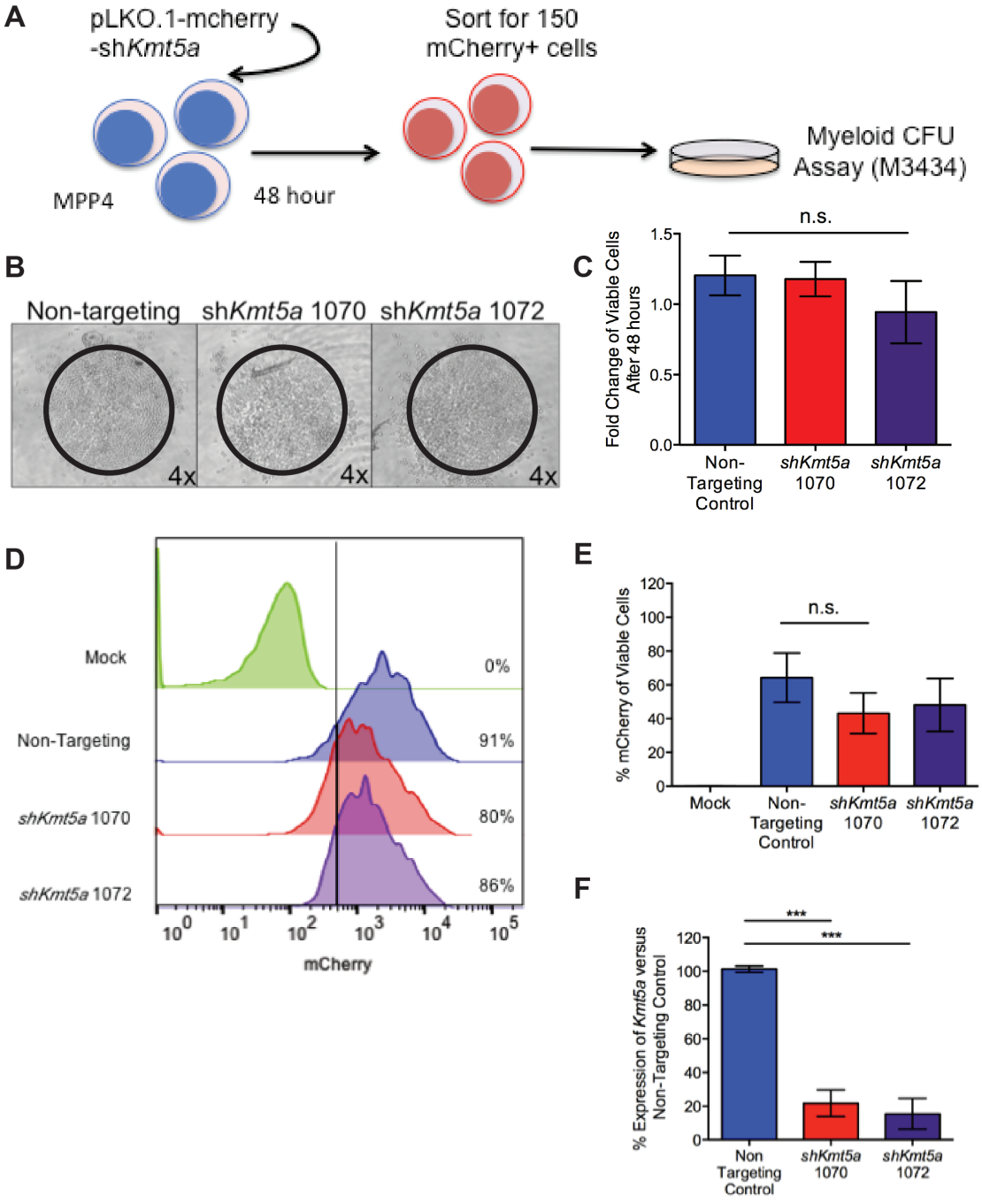

Figure 3.18 | Knockdown of *Kmt5a* has no significant effects on proliferation of MPP4 cells. (A) Experimental outline of CFU assay **(B)** Representative cells of infected with either non-targeting (NT) or 2 individual shRNA hairpins against *Kmt5a* (1070 and 1072) after 48 hours. Circles denote boundary of cellular growth in a single well. **(C)** Fold change of viable cells after 48 hours of MPP4 cells infected with either non-targeting or sh*Kmt5a* hairpins. **(D)** Representative FACS histogram of mCherry expression 48 hours post-knockdown of non-targeting, *Kmt5a* hairpins, and a mock-transduced control. Pre-gated on viable cells. **(E)** Percent of mCherry expression after 48 hours. Bars represent mean ± SEM (n=7). **(F)** qRT-PCR measuring level of *Kmt5a* expression of sorted mCherry positive cells 48 hours post-knockdown normalized to non-targeting control (n=3, ***P<0.005 by one-way ANOVA with Bonferroni adjusted post-hoc t-test)

Following transfer into the myeloid CFU assay, a significant increase in cloning efficiency was seen from cells infected with either the 1070 or 1072 hairpins **(Figure 3.19A)**. Additionally, knockdown of *Kmt5a* increased the macrophage colony forming output while no significant differences were seen in granulocyte or mixed myeloid colony types **(Figure 3.19B)**. Colony identification was confirmed by FACS analysis **(Figure 3.19C,D)**. The composition of bulk colonies derived from cells with hairpins against *Kmt5a* were significantly more macrophage compared to non-targeting control as measured by cell surface markers for macrophage (CD11b+/Gr-1-) and granulocyte (CD11b+/Gr-1+) **(Figure 3.19D)**. To confirm that the expanded myeloid colonies retained knockdown of *Kmt5a*, I performed quantitative real-time PCR to test for the expression of *Kmt5a* in isolated colonies. I found that knockdown of *Kmt5a* was sustained in the myeloid colonies of both hairpin conditions **(Figure 3.19E)**. My results demonstrate that knockdown of *Kmt5a* expands the myeloid colony-forming ability of LMPP and MPP4 cells, specifically producing a greater number of macrophage colonies.

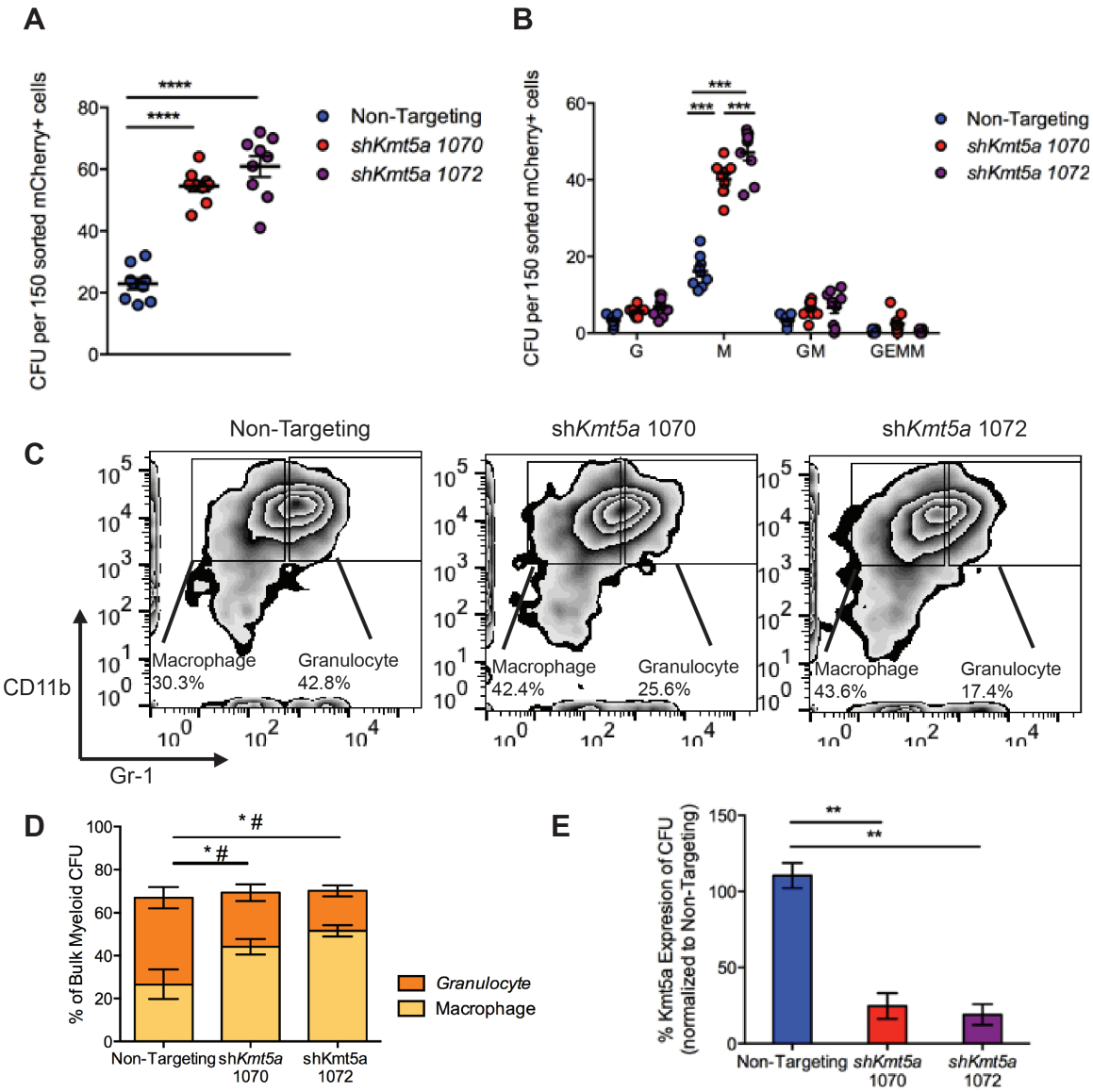

Figure 3.19 | Knockdown of *Kmt5a* promotes macrophage expansion from MPP4 cells in clonal *in vitro* assay. (A) Total colony-forming units (CFU) and **(B)** Individual myeloid colony-forming units (G- granulocyte, M- Macrophage, GM- Granulocyte-macrophage, GEMM- mixed myeloid) generated from 150 sorted mCherry positive infected with Non-targeting, sh*Kmt5a* 1070, and sh*Kmt5a* 1072 (n=7) (***P<0.005, ****P<0.001, one-way ANOVA with Bonferroni adjusted post-hoc t-test). **(C)** Representative FACS analysis of bulk myeloid colonies derived from cells infected with Non-targeting, sh*Kmt5a* 1070, and sh*Kmt5a* 1072 **(D)** Percentage of bulk myeloid colony expressing macrophage (CD11b) and granulocyte markers (Gr-1) (n=3, *P<0.05 macrophages, #P<0.05 granulocytes) **(E)** qRT-PCR measuring level of *Kmt5a* expression in bulk myeloid colonies normalized to colonies from NT control (n=3, **P<0.01, one-way ANOVA with Bonferroni adjusted post-hoc t-test)

To evaluate whether the myeloid expansion following knockdown of *Kmt5a* occurs independent of or at the expense of lymphoid differentiation, I used an OP9 co-culture system to assess lymphoid differentiation of MPP4 cells following *Kmt5a* knockdown **(Figure 3.20A)**. OP9 stromal cells have been shown to induce B-lymphoid differentiation *in vitro* from hematopoietic stem and progenitor cells, which can be analyzed by FACS for lymphoid and myeloid cell surface markers (Pietras et al., 2015b). MPP4 cells were transduced with *Kmt5a* hairpins or non-targeting control and placed on top of 1000 pre-seeded GFP OP9 cells. After 72 hours, 100 mCherry positive cells were sorted and replated on fresh OP9 cells. Knockdown of *Kmt5a* after 72 hours shows no significant changes in number of viable cells assessed by DAPI staining **(Figure 3.20B).**

After 17 days in culture, production from cells infected with either the non-targeting control or the sh*Kmt5a* hairpins is mainly myeloid and mainly lymphoid after 20 days in culture as observed by FACS analysis using markers for lymphoid (CD19) and myeloid (CD11b). **(Figure 3.20C,D)**. While there is a slight expansion of myeloid production seen at day 17 from the cells infected with the sh*Kmt5a* hairpins compared to the non-targeting control, these changes are non-significant **(Figure 3.20C).** In addition, there are no significant changes in lymphoid output between non-targeting and *Kmt5a* hairpins **(Figure 3.20C).** To evaluate whether the observations of the OP9 assay were due to knockdown, I measured *Kmt5a* expression at both day 17 and day 20 **(Figure 3.20E).** At both time points there is significant knockdown observed from either myeloid or

lymphoid cells produced from MPP4 cells infected with sh*Kmt5a* hairpins suggesting that the myeloid expansion seen in the CFU assay is independent of lymphoid differentiation.

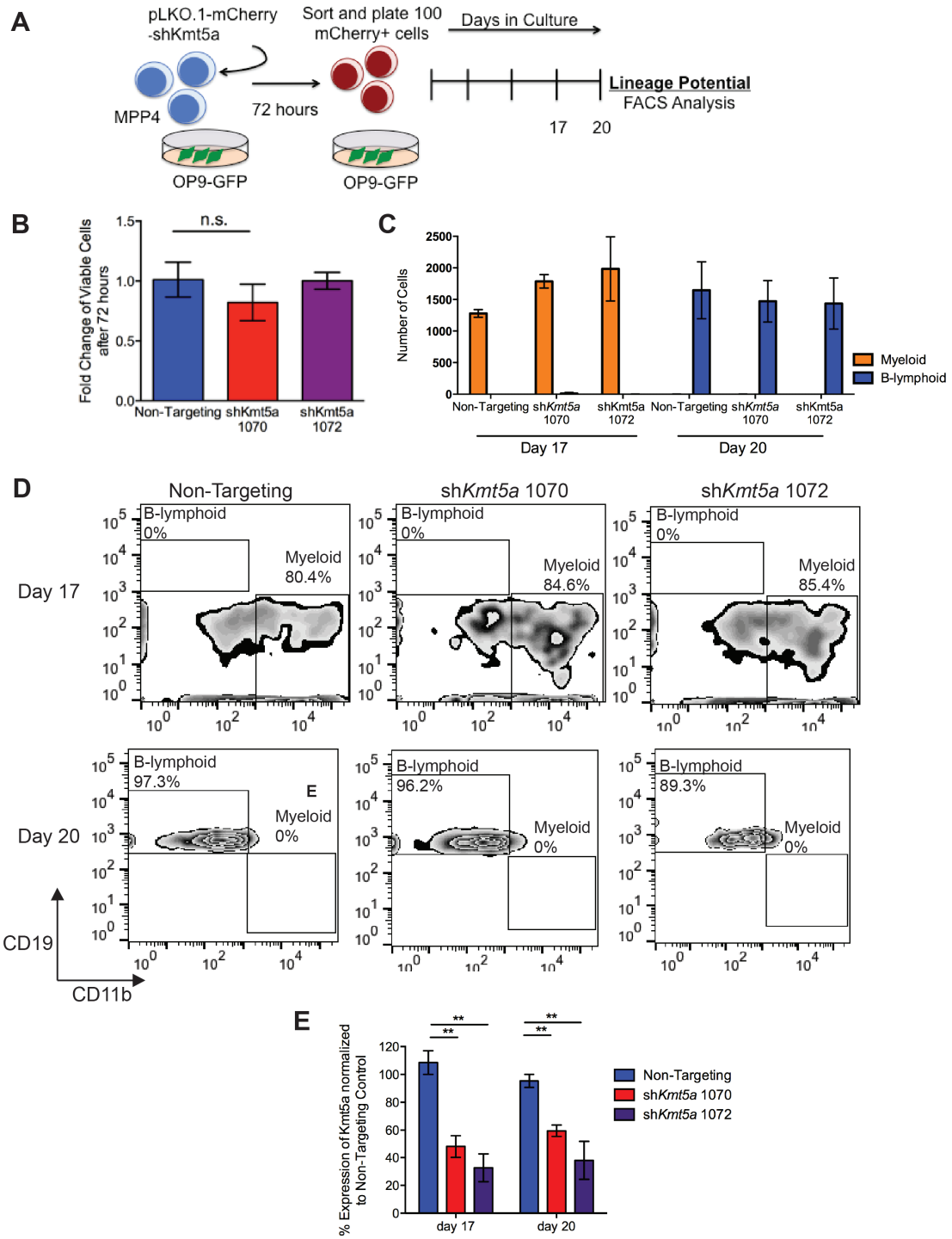

Figure 3.20 | Knockdown of *Kmt5a* does not alter lymphoid differentiation from MPP4 cells *in vitro*. (A) Experimental outline of OP-9 stromal co-culture experiment **(B)** Fold change in viable cells after 72 hours of MPP4 cells infected with either non-targeting or *Kmt5a* hairpins **(C)** Number of B-lymphoid and myeloid cells after 17 and 20 days in OP9 co-culture condition analyzed by FACS analysis using markers for lymphoid (CD19) and myeloid (CD11b). Bars represent mean ± SEM (n=3). **(D)** Representative FACS analysis of lineage output at day 17 and 20 of non-targeting (left), sh*Kmt5a* 1070 (middle), and sh*Kmt5a* 1072 (right). **(E)** Expression of *Kmt5a* compared to Non-targeting control at day 17 and 20. Bars represent mean ± SEM (n=2, ***P*<0.01, student's unpaired t-test).

3.3.3 Overexpression of *Kmt5a* expands granulocyte cell production from lymphoid-primed multipotent progenitors *in vitro*

To assess the phenotype caused by *Kmt5a* overexpression and whether this would result in the converse phenotype observed upon *Kmt5a* knockdown, I cloned the full-length *Kmt5a* cDNA ORF (Origene) into a lentiviral expression plasmid containing a GFP reporter, generated lentiviral supernatant, and utilized supernatant to transduce MPP4 cells. I sorted, after 48 hours, 150 GFP+ cells infected with either the empty vector or *Kmt5a* overexpression construct and then plated them into myeloid methylcellulose media (M3434). The overexpression of *Kmt5a* was observed to increase the total myeloid colony output **(Figure 3.21A)** compared to the empty vector control. In addition, I observed increased granulocyte-only and mixed granulocyte-macrophage colony types, while no significant difference was seen in macrophage-only or GEMM colony types **(Figure 3.21B).** Colony morphology was confirmed by FACS analysis **(Figure 3.21C,D).** The composition of bulk colonies derived from cells with overexpression of *Kmt5a* were slightly increased in granulocyte content compared to empty control as measured by cell surface markers for macrophage (CD11b+/Gr-1-) and granulocyte (CD11b+/Gr-1+) (granulocyte P=0.22, macrophage P=0.12) **(Figure 3.21D)**.

To identify if this expansion was independent of lymphoid differentiation, I used the OP9 co-culture to read out lymphoid output of MPP4 cells after infection **(Figure 3.21E,F).** Similar to knockdown data, I observe no alterations in

lymphoid differentiation at day 20 after knockdown. To evaluate whether the observations of the OP9 assay were due to overexpression of *Kmt5a*, I measured *Kmt5a* expression after 20 days in culture **(Figure 3.21G).** There is increase in expression of *Kmt5a* observed from mature cells types produced from MPP4 cells infected with *Kmt5a* overexpression suggesting that the myeloid expansion seen in the CFU assay is independent of lymphoid differentiation. Taken together, my observations suggest that increased *Kmt5a* expression results in enhanced granulocyte production, while reduced *Kmt5a* expression promotes enhanced macrophage production from MPP4 cells.

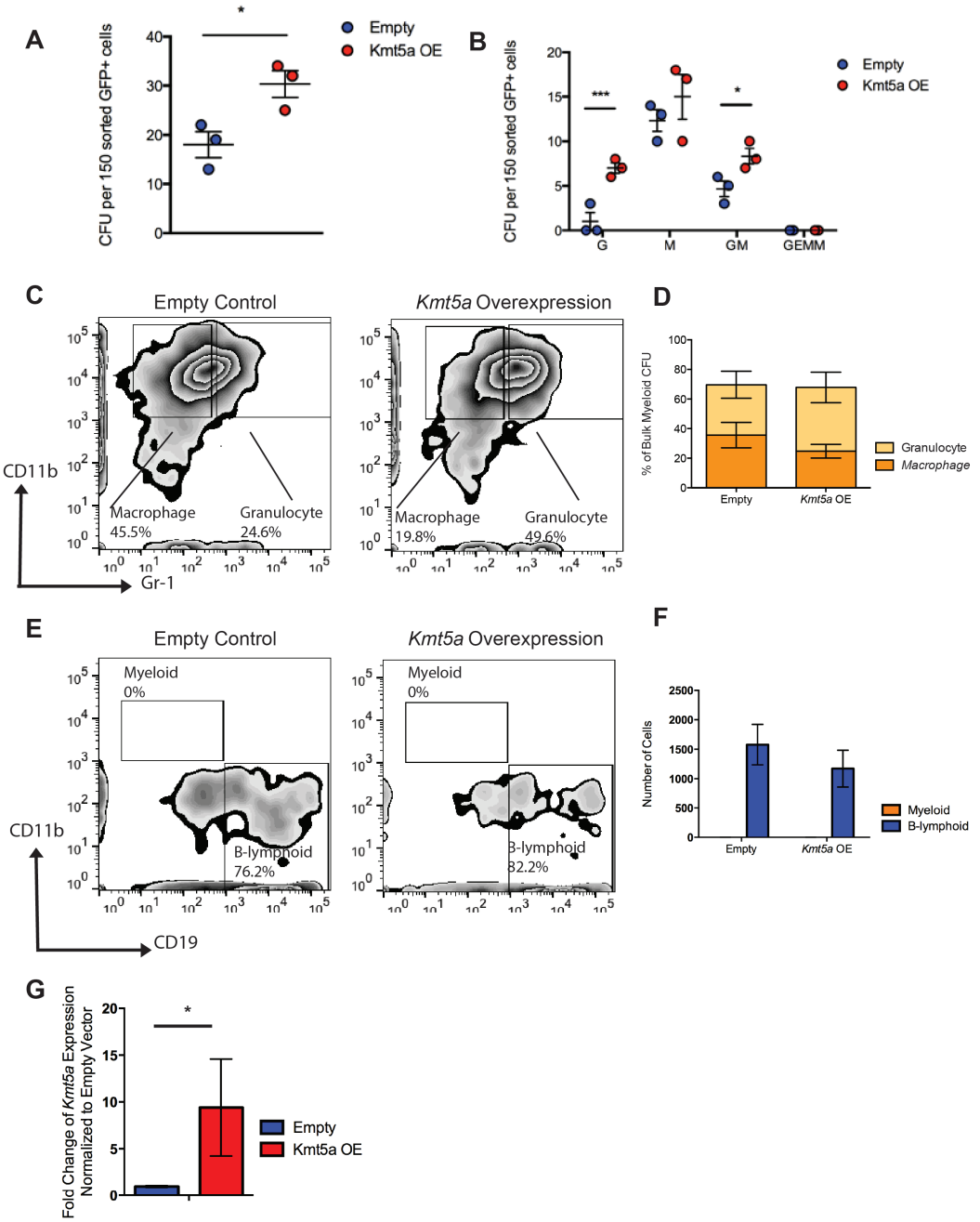

Figure 3.21 | Overexpression of *Kmt5a* promotes granulocyte differentiation from MPP4 cells *in vitro*. **(A)** Total colony-forming units (CFU) and **(B)** Individual myeloid colony-forming units generated from 150 sorted GFP positive cells from MPP4 cells infected with either empty vector or *Kmt5a* overexpression (OE) vector. Bars represent the mean ± SEM (n=3, **P*<0.05, ****P*<0.005, unpaired student t-test). **(C)** Representative FACS analysis of bulk myeloid colonies derived from cells infected with Empty or *Kmt5a* overexpression. **(D)** Percentage of bulk myeloid colony expressing macrophage (CD11b) and granulocyte markers (Gr-1). Bars represent mean ± SEM (n=3). **(E)** Representative FACS analysis of lineage output at day 20 of Empty (left), *Kmt5a* overexpression (right). **(F)** Number of B-lymphoid and myeloid cells after 20 days in OP9 co-culture condition analyzed by FACS analysis using markers for lymphoid (CD19) and myeloid (CD11b). Bars represent mean ± SEM (n=3)**. (G)** Expression of *Kmt5a* compared to empty control at day 20. Bars represent mean ± SEM (n=2, **P*<0.05, unpaired student's t-test).

3.3.4 Overexpression of Lysine 376 methylation-insensitive *p53* in MPP4 cells does not phenocopy myeloid expansion induced by *Kmt5a* knockdown

Although classically known as an H4K20 histone methyltransferase, the KMT5A enzyme is also capable of methylating non-histone proteins such as P53 at residue K376 (Shi et al., 2007). My goal was to assess whether the macrophage CFU expansion phenotype observed upon knockdown of *Kmt5a* in MPP4 cells is mediated through a reduction of P53K376 methylation. I designed an overexpression experiment to investigate if reduction in P53K376 methylation phenocopied the myeloid expansion we observed with *Kmt5a* knockdown. **(Figure 3.22A)**. I used site-directed mutagenesis to create a *p53* construct that produces P53 protein unable to be methylated by *Kmt5a* by a conversion of lysine residue 376 to arginine **(Figure 3.22B)**. I then overexpressed this construct or, as a control, a wild-type construct of *p53* in MPP4 cells and sorted, after 48 hours, 150 GFP+ empty, *p53* wild-type, or $p53^{K376R}$ -expressing cells, and then plated them into myeloid methylcellulose media (M3434). The overexpression of wild-type *p53* significantly impairs myeloid differentiation while overexpression of the K376R mutant exhibits no significant differences in total **(Figure 3.22C)** or lineage-specific myeloid differentiation compared to empty vector control **(Figure 3.22D).** While there is a difference in the total number of colonies between the wild type and methylation-insensitive *p53,* there are no lineage-specific differences between them.

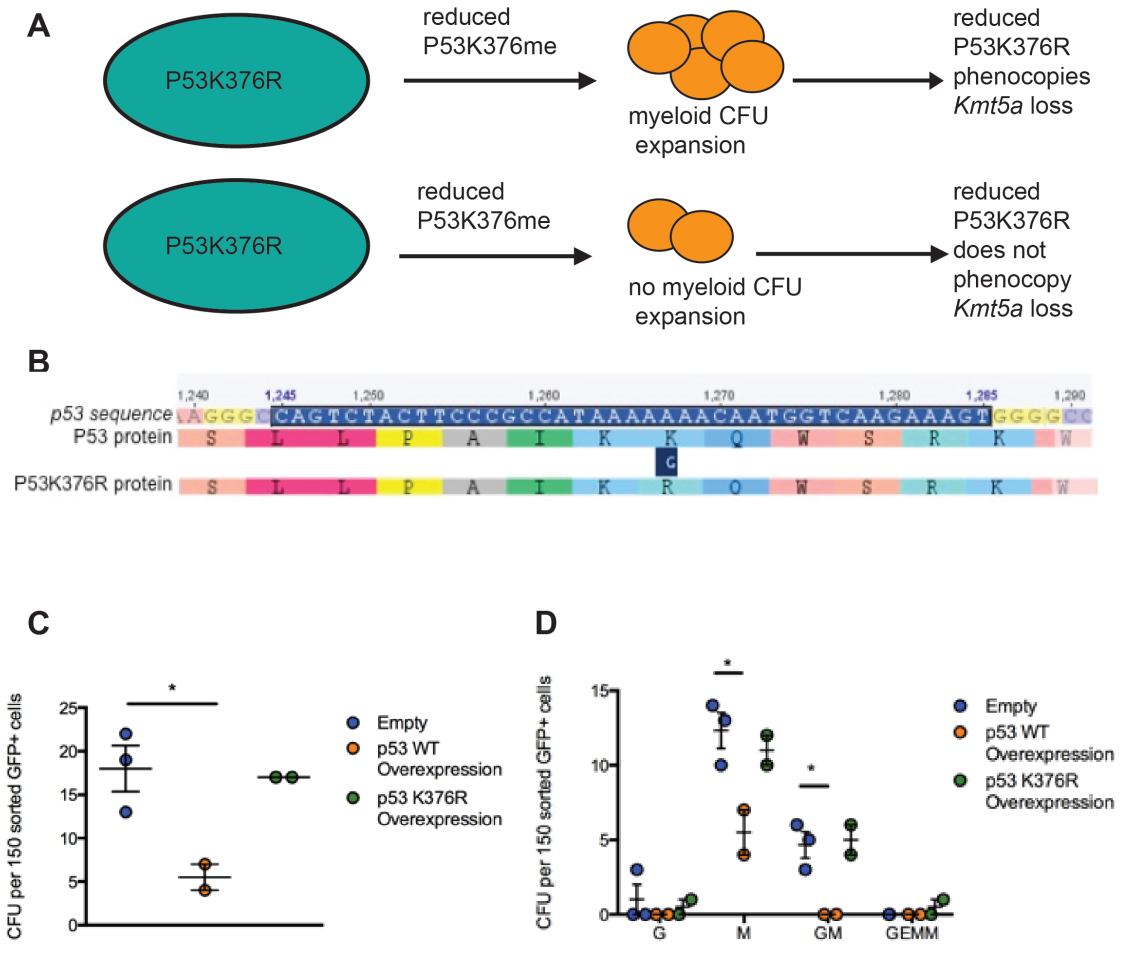

Figure 3.22 | Overexpression of Lysine 376 methylation-insensitive *p53* in lymphoid-primed multipotent progenitors does not phenocopy loss of *Kmt5a*. **(A)** Experimental model of the role of P53K376 methylation in *Kmt5a* knockdown-induced myeloid expansion. **(B)** Site-directed mutagenesis of lysine 376 induces a lysine to arginine mutation **(C)** Total colony-forming unit and **(D)** Individual myeloid colony-forming units generated from 150 GFP+ sorted cells transduced with empty vector, *p53* wild-type, or $p53^{K376R}$ overexpression constructs (n=3) (**P*<0.05, student's unpaired t-test).

CHAPTER 4: DISCUSSION

In vitro assays can be utilized to assess functional alterations in multipotent progenitor cells

Despite the robustness of the well-defined, highly utilized myeloid methylcellulose assay for assessing the myeloid differentiation potential of hematopoietic stem and progenitor cells, its application in defining cell fate from these multipotent cells remains limited. With increasing technological developments, the hematopoietic field has revised the classical hierarchy of hematopoiesis to a model highlighting the multiple potentials of progenitor cells **(Figure 4.1)**. HSCs can differentiate into three progenitor populations that are primed but not restricted to distinct lineages. Incorporating multiple accepted staining strategies (Adolfsson et al., 2005; Akashi et al., 2000; Pietras et al., 2015a; Wilson et al., 2008), I found that the lymphoid primed multipotent progenitor populations MPP4 and LMPP are highly overlapping. In fact all cells defined as LMPP are also MPP4 cells with high Flk2 expression. In my studies, both populations are used and show similar results and trends. However, small differences in significance are likely due to the LMPP population being a more highly defined subset of MPP4.

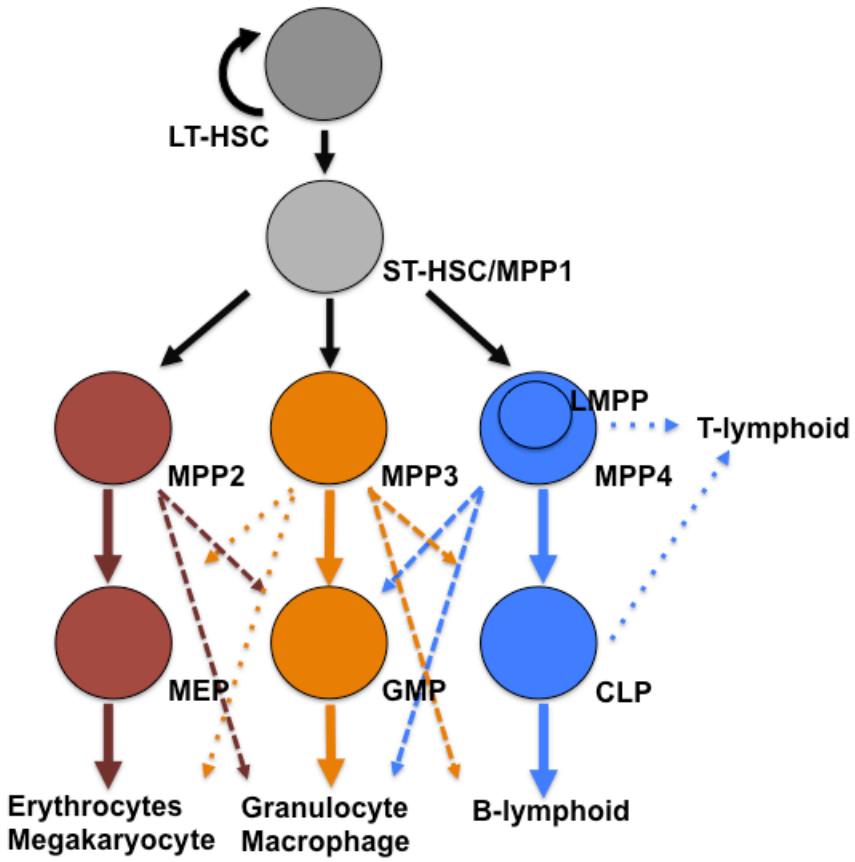

Figure 4.1 | Integrative model of multipotent progenitor populations. Based on gating strategies MPPs can be separated into three distinct populations derived from the ST-HSC (also termed MPP1). MPP2 cells predominantly generates megakaryocyte-erythroid cells, MPP3 predominantly generates granulocyte–macrophage cell types and MPP4 predominantly generates B-lymphoid cell types. LMPP, a population defined by an alternate gating strategy, lies within the MPP4 population. Solid arrows represent dominant lineage output while dashed arrows represent cell potentials that are less robust.

As multipotent stem and progenitor cells have the capacity to differentiate into both myeloid and B-lymphoid cells, a thorough examination of cell potential includes assays to concurrently read out both of these lineage potentials. A recognized assay to determine lymphoid potential is the OP9 assay (Pietras et al., 2015a), which I have optimized in our laboratory for the purposes of assessing both myeloid and lymphoid potential from a population of LMPP cells. Importantly, I found this assay to be consistent with the results of *in vivo* transplantation of LMPP cells with respect to the dynamics of lineage cell production. However, it currently remains unclear whether the late emerging B-lymphoid cells are produced from slowly dividing lymphoid progenitors or if they are produced from myeloid cells that shift toward lymphoid cells. Future experiments using progenitor and stem cell surface markers will help identify progenitor dynamics and how they contribute to production of mature cell types in the OP9 culture system. Due to its dynamic nature, the OP9 assay cannot ascertain the multiple lineage potentials of a single cell because the readout is terminal and the timing of peaks for myeloid and lymphoid production is different.

The lack of a single-cell or clonal assay system to interrogate the *de novo* lymphoid and myeloid/lymphoid bipotency of multipotent progenitor cells has remained a barrier in the field. To address this limitation, I developed a stroma-free, *in vitro* system to interrogate both lymphoid and myeloid differentiation potential, enabling not only a high-throughput system to characterize multilineage

output of progenitor cells but also a method to identify lineage potential of single lymphoid-primed multipotent progenitor cells.

The commercial methylcellulose assay M3630 includes the growth factor IL-7 to promote the differentiation of progenitor cells towards the B-lymphoid lineage. However, *de novo* lymphoid-primed multipotent progenitors do not produce any mature colony cell types in this media. Therefore, IL-7 alone cannot promote *in vitro* hematopoietic differentiation from LMPP/MPP4 cells. *De novo* CLPs are able to produce CFU-preB in M3630, suggesting that unmodified M3630 media assays lymphoid-restricted, not lineage-primed progenitors. With the addition of SCF and Flt3L to the media, two factors observed to increase the multilineage differentiation of stem cells (Kent et al., 2008; Lyman et al., 1994), it was expected that the cloning efficiency of these cells would increase. Due to the high cell surface marker expression of Flt3 in LMPP cells, the increase in colonies would be expected mainly in the CFU-preB colony type. While the addition of these factors to M3630 did increase cloning efficiency of *de novo* LMPP/MPP cells, the increase was observed mostly in macrophage colonies. A 48 hour culture with a combination of factors- IL-3, IL-6, IL-7, SCF, and LIF- followed by plating in M3630 supplemented with Flt3L and SCF was able to produce CFU-preB colonies from LMPP/MPP4 cells. Interestingly, using the single cell assay, I was able to resolve that a majority of single LMPP/MPP4 cells were dual potent, producing both macrophage and pre-B colony types. There also exists LMPP/MPP4 cells that produce only myeloid or only lymphoid colonies *in vitro*. A

majority of *in vitro* studies of multipotent progenitors have focused on the myeloid methylcellulose or the lymphoid OP9 assay to identify the lineage potential of progenitor cells, likely underestimating the prevalence and importance of cells with dual myeloid and lymphoid potential. Although single cell transplants with LMPP/MPP4 cells are not feasible due to their limited self-renewal, *in vivo* barcoding and tracking experiments could identify if these dual potent and unipotent classes of LMPP/MPP4 cells exist *in vivo*. If these subsets of LMPP/MPP4 cells do exist *in vivo*, identifying additional cell surface markers to distinguish them could provide insight to their specific contributions to hematopoietic cell production.

I have utilized this assay along with single cell transcriptome profiling to specifically characterize the cellular and molecular alterations in aging LMPP cells. In future studies by our group and other groups, this assay will facilitate biochemical or targeted genetic screens to study multipotent progenitor cell fate decisions in blood cancer, regeneration, immune dysfunction, or aging.

LMPP/MPP4 cells are important and early contributors to age-associated lineage skewing

The contribution and importance of multipotential hematopoietic progenitor cells to age-induced decline in hematopoietic function and predisposition to myeloid malignancy were previously unclear. The majority of studies in the literature examining aging of hematopoietic stem and progenitor cells have focused on the

HSCs as drivers of phenotypic alterations associated with aging. Recent lineage tracing studies have revealed that the multipotent progenitor compartment contributes more significantly to steady-state adult hematopoiesis than HSC cells (Busch et al., 2015; Sun et al., 2014b), suggesting that they may have an underappreciated role in driving or contributing to hematopoietic aging. Here, I have determined that age-associated myeloid lineage skewing is reflected in the composition of the multipotential progenitor cell pool. Within this pool, lymphoid-primed LMPP/MPP4 cells were specifically and significantly depleted compared to other myeloid and erythroid-primed multipotent progenitor populations. In addition to the depletion of this population, LMPP/MPP4 cells in aged mice exhibited loss of quiescence at both the cellular and molecular level. This increase in cycling LMPPs with aging considered alongside to previous HSC studies that observed an increase in quiescence (Beerman et al., 2014; Flach et al., 2014), suggests that LMPP cells may contribute more to the mature hematopoietic cell production than HSCs during aging. The progressive decline in frequency and total numbers of LMPP/MPP4 cells occurs prior to cellular composition changes in the myeloid-biased, lymphoid-biased, and balanced HSC subsets, suggesting that a population other than the HSC (either an intermediate hematopoietic progenitor population or a neighboring bone marrow microenvironment population) contributes to the loss of LMPP/MPP4 cells in aging.

Utilizing the single cell assay, I have determined LMPP/MPP4 cells exhibit clonal alterations in lineage potential with aging. There is an increase with aging of LMPP and MPP4 cells with granulocyte-restricted potential and a decrease in cells with dual macrophage and B-lymphoid differentiation potential **(Figure 4.2A)**. This shift in clonal composition is consistent with myeloid-biased hematopoietic cell production associated with aging. In addition the loss of B-lymphoid producing clones is consistent with the decreased transcriptional lymphoid priming in aging LMPP cells. These data suggest a shift in composition of the LMPP and MPP4 population with aging, with specific depletion of cells as they commit to the macrophage and/or preB lineages as early as 8 months of age, suggesting that loss of macrophage and B cell-restricted progenitors is initiated early in the process of aging.

Additionally, aging LMPP cells exhibit a transcriptional enrichment of *Myc* target genes, suggesting that these cells are susceptible to *Myc* transformation. Increased expression or aberrant activation of *Myc* target genes plays an important role in leukemogenesis (Delgado and Leon, 2010). Critical for the balance of self-renewal and differentiation in HSCs, enforced *Myc* expression in mice leads to a loss of HSCs due to reduced self-renewal and an increase in proliferation of progenitor cells and differentiation (Wilson et al., 2004). LMPP cells exhibiting this aberrant gene signature could gain a clonal proliferative advantage over the lifetime of an individual. If these *Myc*-deregulated clones are correlated to myeloid-restricted LMPP cells, they may directly contribute to

myeloid-biased hematopoietic production observed in aging. Furthermore, they may be directly implicated in tumor initiation and the increased risk of Acute Myeloid Leukemia observed in aging. Future studies tracking development and expansion of different lineage-primed clones of LMPP cells as well as their susceptibility to additional genomic or epigenomic alterations will determine whether these can be classified as clones directly implicated in aging-associated leukemia or other hematopoietic cancers.

While my work supports the concept that age-induced alterations in lymphoid production can be caused by skewed selection and/or differentiation of long-lived progenitor cells (Busch et al., 2015), observed changes in the number of LMPP and MPP4 cells with aging suggests that these alterations are initiated in a cell type earlier than the LMPP and also independent of cellular composition changes in lineage-biased HSC subsets. It is possible that the aging microenvironment contributes external signals responsible for the loss of lymphoid primed multipotent progenitor cells. While many studies have investigated the aging microenvironment, many of these are in the context of transplantation, a procedure that has been shown to dramatically alter the structural and cellular composition of the niche (Cao et al., 2011; Capilla-Gonzalez et al., 2014). Future work defining microenvironment alterations that contribute to multipotential progenitor population changes will be necessary in identifying if the specific reduction of LMPP and MPP4 cells with aging is due to external cues from neighboring bone marrow microenvironment populations or intrinsic alterations induced by aging.

Epigenetic regulation of cell fate of LMPP/MPP4 cells through the histone methyltransferase *Kmt5a*

A targeted shRNA lentiviral screen of epigenetic factors using the clonal cell fate assay that I established identified five factors- *Crebbp*, *Atxn7l3*, *Rnf40*, *Myst4*, and *Kmt5a*- important for regulating the myeloid and lymphoid cellular output from LMPP cells. Upon further investigation of *Kmt5a,* using both CFU and stromal co-culture assays, the alterations observed were confined to the myeloid compartment. Knockdown of *Kmt5a* in LMPP/MPP4 cells promoted an expansion of macrophage-restricted progenitor cells, while overexpression of *Kmt5a* promoted granulocyte-restricted and granulocyte-macrophage progenitor cells **(Figure 4.2B)**. Future investigations into the functional alterations induced by loss or overexpression of *Kmt5a* will focus on *in vivo* multilineage engraftment. The clonal CFU assay represents a snapshot of mature lineage outcomes of a population, while *in vivo* transplantation will identify if the myeloid expansion seen by modulation of *Kmt5a* is due to alterations in the dynamics of myeloid differentiation. Although a conditional knockout model exists for *Kmt5a (Oda et al., 2009),* there currently exists no LMPP- or MPP4- specific promoter-driven Cre recombinase model to limit the knockout to these populations; therefore, to investigate the *in vivo* role of *Kmt5a* specifically in LMPP/MPP4 cells, transplantation assays remain necessary.

To address the molecular mechanisms by which *Kmt5a* might be regulating the lineage outcome of LMPP/MPP4 cells, we focused on the non-histone methylation function of the Kmt5a protein. Evidence that the dynamics of the protein methylation function of Kmt5a is faster than the histone methylation function suggested that the alterations in P53 methylation may contribute greater to the phenotypes observed with *Kmt5a* knockdown than H4K20me1 alterations (Black et al., 2012; Shi et al., 2007). Investigation of the role of P53 in hematopoiesis has been limited to the HSC population. P53 is primarily expressed in HSCs and regulates their quiescence and self-renewal (Liu et al., 2009). *P53*-deficient HSCs are highly proliferative yet are impaired in their repopulation capability compared to wild-type controls, implying that reduced P53 activity compromises the functional fitness of HSCs (Chen et al., 2008; TeKippe et al., 2003). However, total bone marrow cells from *p53*-null mice outcompete wild-type bone marrow cells, indicating the role of P53 in progenitor cells may be different from that observed in the HSC population (Akala et al., 2008).

Overexpression of a K376 methylation-insensitive P53 yielded no differences in myeloid colony production compared to the control. If the myeloid expansion seen with knockdown of *Kmt5a* is due to the loss of methylation of P53, we would expect that the methylation-insensitive *p53* would phenocopy the *Kmt5a* shRNA knockdown results and produce more macrophage colonies compared to the empty vector; however, no expansion is seen. These results suggest that the macrophage expansion observed upon knockdown of *Kmt5a* is not mediated

through methylation of P53K376. Overexpression of the wild-type *p53* did result in a significant decrease in myeloid colony production of all lineage types compared to the empty control. While overexpression of the mutant *p53* does show an increase in myeloid colony production compared to the overexpression of the wild-type *p53,* the expansion is seen in all myeloid lineage types, suggesting that while p53 methylation may regulate hematopoietic production from MPP4 cells, it does not mediate the lineage-specific production observed by modulation of *Kmt5a*. A caveat to this model is the use of overexpression constructs enables endogenous P53 to be methylated by KMT5A. Excess P53 caused by overexpression of either the wild-type or mutant construct may be degraded, confounding the phenotype observed. To clarify the role of P53 methylation in hematopoietic production, isolating MPP4 cells from *p53*-null mice would enable only the overexpressed P53, wild-type or mutant, to be present in the cell. By removing the endogenous protein, the phenotype will be driven primarily by the differences in P53 methylation status. In addition to P53, KMT5A has more recently been found to monomethylate other non-histone proteins such as PCNA (Hamamoto et al., 2015; Takawa et al., 2012). Future experiments outside the scope of this thesis will investigate monomethylation of H4K20 or PCNA as a mediator of *Kmt5a* knockdown or overexpression phenotypes to determine the precise mechanisms regulating myeloid lineage output from lymphoid-primed multipotent progenitors.

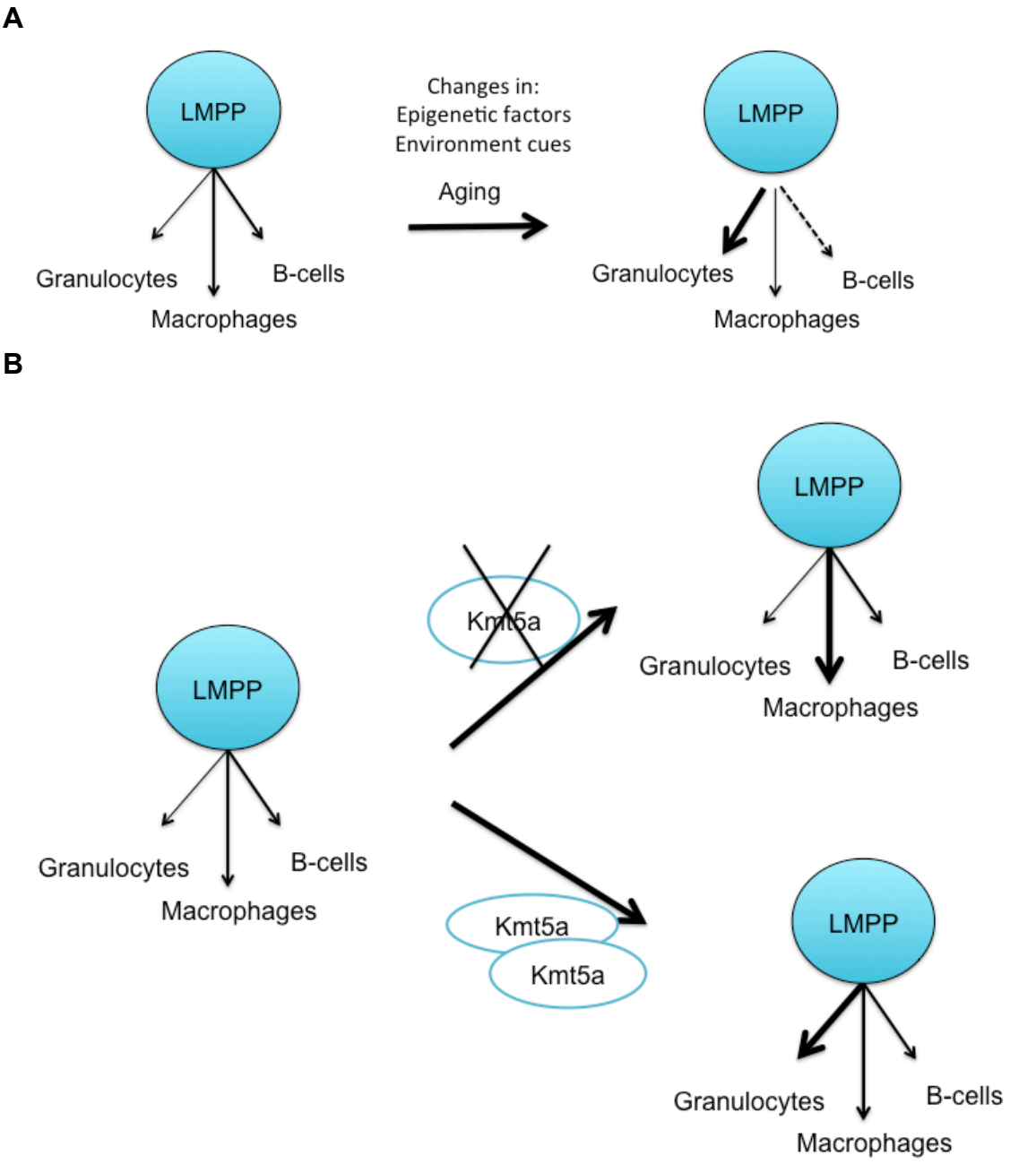

Figure 4.2 | Alterations in cellular outcome from lymphoid-primed multipotent progenitors. **(A)** In aging, multiple factors including alterations in environmental signals or epigenetic factors, such as *Kmt5a,* cause an increase in granulocyte production at the expense of B-lymphoid production. **(B)** Knockdown of *Kmt5a* in LMPP cells results in an expansion of macrophage cell production, while overexpression of *Kmt5a* in LMPP cells results in an increase of granulocyte production.

Functional plasticity of progenitor cells: implications in aging and development of novel therapeutics

While FACS phenotypic analysis is the most robust method to isolate specific stem and progenitors populations, there remains some disconnect between cell surface marker definition of a population and its true functional potential. A recent study has shown that GMP cells retain some of the lymphoid priming signature seen in LMPP cells, but the lymphoid priming signature is not retained in mature lymphoid or myeloid cells (Ng et al., 2009). Additionally, GMP cells can produce lymphoid cells *in vitro*, but have limited *in vivo* production of lymphoid cells (Richie Ehrlich et al., 2011). The goal of the differential expression performed between the CLP and GMP was to find transcriptional differences between functionally myeloid-restricted and functionally lymphoid-restricted progenitors. Including the GMP as a myeloid-restricted progenitor may have underestimated the transcriptional signatures that control lineage specification and restriction, specifically towards lymphopoiesis. Instead, I may have limited the analysis to two progenitor cell types that are functionally different *in vivo*, but are transcriptionally much more similar than previously thought and have overlapping cell fate potentials. A more appropriate population to perform this differential expression is the CFU-GM which is functionally myeloid-restricted *in vivo and in vitro* (Douay et al., 1986; Moore, 2009); however, the cell surface markers to specifically distinguish these progenitors from the GMP population or more mature myeloid progenitors is still unknown.

The overlapping transcriptional profile of GMPs and CLPs and the ability of myeloid GMPs to produce lymphoid cells *in vitro* highlights that there is a certain level of plasticity in lineage potential from multipotent progenitors. Furthermore, the restriction of GMP cells to myeloid cellular output *in vivo,* combined with my own observations of lineage output of LMPP cells in different *in vitro* assay conditions, suggests the microenvironment of stem and progenitor cells can override transcriptional programming and can influence their cellular outcome. Extracellular signals and growth factors in the OP9 assay promote lymphoid differentiation of GMP and LMPP cells from expression of shared lymphoid priming transcripts. However, *in vivo* microenvironmental cues not only promote differentiation from myeloid-associated transcript expression in GMPs but also restrict their output to myeloid cell types. There are a limited number of growth factors and supplements that can be added to *in vitro* assays, thus the microenvironment may directly contribute to differences observed between *in vitro* and *in vivo* functional assays of lineage potential from progenitor cells. The sensitivity of progenitor cells to adapt to cues in their microenvironment likely enables them to adequately respond to the highly dynamic demands of the hematopoietic system.

The disconnect between phenotypic definition, transcriptional priming, and functional lineage potential can be further observed in aging hematopoiesis. While we isolate HSC and progenitor populations based on cell surface markers defined by cells from young mice, we observe functional differences in the aging

hematopoietic stem and progenitor cells. Specifically, aging HSC cells lose homing capacity, self-renewal, and become more myeloid-biased suggesting it becomes functionally similar to MPP/MPP3 cells (Rossi et al., 2005). However, the expression of the CD150 marker used to distinguish stem cells from progenitor cells increases (Kiel et al., 2005). Similarly, phenotypic LMPP/MPP4 cells are functionally similar to MPP/MPP3 cells in aging. It is possible that current cell surface markers are not appropriate for aging cell populations and that different sets of cell surface markers define true functional populations in older mice. In order to find these true functional populations, extensive single cell *in vivo* studies with index sorting of multiple cell surface markers would be necessary.

Furthermore, exploring alterations in the aging microenvironment should be extensively studied to identify the extent to which the hematopoietic niche contributes to the cellular fate of aging stem and multipotent progenitors. There is mounting evidence in favor of aging-induced microenvironmental changes contributing to hematopoietic defects (Bethel et al., 2013; Ergen et al., 2012). Previous studies have observed rejuvenating effects of old HSCs transplanted into young recipients (Conboy et al., 2005). While I observe intrinsic alterations of LMPP/MPP4 cells driving age-related phenotypes, contributions from the microenvironment are not necessarily mutually exclusive. A complete model of lymphoid primed multipotent progenitor aging may include both intrinsic and extrinsic signals. Transplanting LMPP/MPP4 cells from a young donor into an

aged recipient could identify if an aged microenvironment deleteriously affects the lineage output of these lymphoid primed progenitor cells. If these external signals can be identified and controlled, it may be possible to alter the stringency of “myeloid-restricted” or “lymphoid-restricted” progenitors. We may be able to take advantage of the flexibility of progenitor cells and reverse the progenitor-level effects of age-associated lineage skewing by not only reversing myeloid-biased production from aged LMPP/MPP4 cells but also enabling the traditionally-labeled GMP myeloid progenitor to make more lymphoid cells to compensate for the reduction of LMPP/MPP4 cells observed in aging. The advantage of using external cues or epigenetic therapies to modify cellular fates is their transient nature; a signal can be added or removed during times of acute hematopoietic stress such as bone marrow transplantation-induced regeneration conditions. This work highlights the importance of further studying the multipotent progenitor population to take advantage of its contribution to multilineage hematopoietic cell production and to open possible avenues of modifying cellular outcomes from progenitors to reduce recovery times, reduce graft-versus-host disorder, or decrease susceptibility to co-infections from suppressed immune systems, and reverse age-associated hematopoietic decline in the elderly.

Bibliography

Abbas, T., E. Shibata, J. Park, S. Jha, N. Karnani, and A. Dutta. 2010. CRL4(Cdt2) regulates cell proliferation and histone gene expression by targeting PR-Set7/Set8 for degradation. *Molecular cell* 40:9-21.

Adolfsson, J., R. Mansson, N. Buza-Vidas, A. Hultquist, K. Liuba, C.T. Jensen, D. Bryder, L. Yang, O.J. Borge, L.A. Thoren, K. Anderson, E. Sitnicka, Y. Sasaki, M. Sigvardsson, and S.E. Jacobsen. 2005. Identification of Flt3+ lympho-myeloid stem cells lacking erythro-megakaryocytic potential a revised road map for adult blood lineage commitment. *Cell* 121:295-306.

Aggarwal, R., J. Lu, V.J. Pompili, and H. Das. 2012. Hematopoietic stem cells: transcriptional regulation, ex vivo expansion and clinical application. *Curr Mol Med* 12:34-49.

Akala, O.O., I.K. Park, D. Qian, M. Pihalja, M.W. Becker, and M.F. Clarke. 2008. Long-term haematopoietic reconstitution by Trp53-/-p16Ink4a-/-p19Arf-/- multipotent progenitors. *Nature* 453:228-232.

Akashi, K., D. Traver, T. Miyamoto, and I.L. Weissman. 2000. A clonogenic common myeloid progenitor that gives rise to all myeloid lineages. *Nature* 404:193-197.

Akunuru, S., and H. Geiger. 2016. Aging, Clonality, and Rejuvenation of Hematopoietic Stem Cells. *Trends Mol Med* 22:701-712.

Alam, I., D. Goldeck, A. Larbi, and G. Pawelec. 2013. Aging affects the proportions of T and B cells in a group of elderly men in a developing country--a pilot study from Pakistan. *Age (Dordr)* 35:1521-1530.

Allis, C.D., S.L. Berger, J. Cote, S. Dent, T. Jenuwien, T. Kouzarides, L. Pillus, D. Reinberg, Y. Shi, R. Shiekhattar, A. Shilatifard, J. Workman, and Y. Zhang. 2007. New nomenclature for chromatin-modifying enzymes. *Cell* 131:633-636.

Aravind, L., S. Abhiman, and L.M. Iyer. 2011. Natural history of the eukaryotic chromatin protein methylation system. *Prog Mol Biol Transl Sci* 101:105-176.

Arrowsmith, C.H., C. Bountra, P.V. Fish, K. Lee, and M. Schapira. 2012. Epigenetic protein families: a new frontier for drug discovery. *Nat Rev Drug Discov* 11:384-400.

Asai, T., Y. Liu, N. Bae, and S.D. Nimer. 2011. The p53 tumor suppressor protein regulates hematopoietic stem cell fate. *J Cell Physiol* 226:2215-2221.

Ashburner, M., C.A. Ball, J.A. Blake, D. Botstein, H. Butler, J.M. Cherry, A.P. Davis, K. Dolinski, S.S. Dwight, J.T. Eppig, M.A. Harris, D.P. Hill, L. Issel-Tarver, A. Kasarskis, S. Lewis, J.C. Matese, J.E. Richardson, M. Ringwald, G.M. Rubin, and G. Sherlock. 2000. Gene ontology: tool for the unification of biology. The Gene Ontology Consortium. *Nat Genet* 25:25-29.

Atanassov, B.S., R.D. Mohan, X. Lan, X. Kuang, Y. Lu, K. Lin, E. McIvor, W. Li, Y. Zhang, L. Florens, S.D. Byrum, S.G. Mackintosh, T. Calhoun-Davis, E. Koutelou, L. Wang, D.G. Tang, A.J. Tackett, M.P. Washburn, J.L. Workman, and S.Y. Dent. 2016. ATXN7L3 and ENY2 Coordinate Activity of Multiple H2B

Deubiquitinases Important for Cellular Proliferation and Tumor Growth. *Mol Cell* 62:558-571.
Bannister, A.J., and T. Kouzarides. 1996. The CBP co-activator is a histone acetyltransferase. *Nature* 384:641-643.
Barker, J., and C.M. Verfaillie. 2000. A novel in vitro model of early human adult B lymphopoiesis that allows proliferation of pro-B cells and differentiation to mature B lymphocytes. *Leukemia* 14:1614-1620.
Beck, D.B., H. Oda, S.S. Shen, and D. Reinberg. 2012. PR-Set7 and H4K20me1: at the crossroads of genome integrity, cell cycle, chromosome condensation, and transcription. *Genes Dev* 26:325-337.
Beerman, I., D. Bhattacharya, S. Zandi, M. Sigvardsson, I.L. Weissman, D. Bryder, and D.J. Rossi. 2010. Functionally distinct hematopoietic stem cells modulate hematopoietic lineage potential during aging by a mechanism of clonal expansion. *Proc Natl Acad Sci U S A* 107:5465-5470.
Beerman, I., C. Bock, B.S. Garrison, Z.D. Smith, H. Gu, A. Meissner, and D.J. Rossi. 2013. Proliferation-dependent alterations of the DNA methylation landscape underlie hematopoietic stem cell aging. *Cell Stem Cell* 12:413-425.
Beerman, I., J. Seita, M.A. Inlay, I.L. Weissman, and D.J. Rossi. 2014. Quiescent hematopoietic stem cells accumulate DNA damage during aging that is repaired upon entry into cell cycle. *Cell Stem Cell* 15:37-50.
Bellantuono, I., A. Aldahmash, and M. Kassem. 2009. Aging of marrow stromal (skeletal) stem cells and their contribution to age-related bone loss. *Biochim Biophys Acta* 1792:364-370.
Bender, J.G., K.L. Unverzagt, P.B. Maples, Y. Mehrotra, J. Mellon, D.E. Van Epps, and C.C. Stewart. 1992. Functional characterization of mouse granulocytes and macrophages produced in vitro from bone marrow progenitors stimulated with interleukin 3 (IL-3) or granulocyte-macrophage colony-stimulating factor (GM-CSF). *Exp Hematol* 20:1135-1140.
Benetti, R., S. Gonzalo, I. Jaco, G. Schotta, P. Klatt, T. Jenuwein, and M.A. Blasco. 2007. Suv4-20h deficiency results in telomere elongation and derepression of telomere recombination. *J Cell Biol* 178:925-936.
Bertrand, J.Y., S. Giroux, A. Cumano, and I. Godin. 2005. Hematopoietic stem cell development during mouse embryogenesis. *Methods Mol Med* 105:273-288.
Bethel, M., B.R. Chitteti, E.F. Srour, and M.A. Kacena. 2013. The changing balance between osteoblastogenesis and adipogenesis in aging and its impact on hematopoiesis. *Curr Osteoporos Rep* 11:99-106.
Birbrair, A., and P.S. Frenette. 2016. Niche heterogeneity in the bone marrow. *Ann N Y Acad Sci* 1370:82-96.
Black, J.C., C. Van Rechem, and J.R. Whetstine. 2012. Histone lysine methylation dynamics: establishment, regulation, and biological impact. *Mol Cell* 48:491-507.
Bleul, C.C., R.C. Fuhlbrigge, J.M. Casasnovas, A. Aiuti, and T.A. Springer. 1996. A highly efficacious lymphocyte chemoattractant, stromal cell-derived factor 1 (SDF-1). *J Exp Med* 184:1101-1109.

Bocker, M.T., I. Hellwig, A. Breiling, V. Eckstein, A.D. Ho, and F. Lyko. 2011. Genome-wide promoter DNA methylation dynamics of human hematopoietic progenitor cells during differentiation and aging. *Blood* 117:e182-189.

Boehm, T., and C.C. Bleul. 2006. Thymus-homing precursors and the thymic microenvironment. *Trends Immunol* 27:477-484.

Bottardi, S., A. Aumont, F. Grosveld, and E. Milot. 2003. Developmental stage-specific epigenetic control of human beta-globin gene expression is potentiated in hematopoietic progenitor cells prior to their transcriptional activation. *Blood* 102:3989-3997.

Bradley, T.R., and G.S. Hodgson. 1979. Detection of primitive macrophage progenitor cells in mouse bone marrow. *Blood* 54:1446-1450.

Bradley, T.R., and D. Metcalf. 1966. The growth of mouse bone marrow cells in vitro. *Aust J Exp Biol Med Sci* 44:287-299.

Broske, A.M., L. Vockentanz, S. Kharazi, M.R. Huska, E. Mancini, M. Scheller, C. Kuhl, A. Enns, M. Prinz, R. Jaenisch, C. Nerlov, A. Leutz, M.A. Andrade-Navarro, S.E. Jacobsen, and F. Rosenbauer. 2009. DNA methylation protects hematopoietic stem cell multipotency from myeloerythroid restriction. *Nat Genet* 41:1207-1215.

Bunting, S., R. Widmer, T. Lipari, L. Rangell, H. Steinmetz, K. Carver-Moore, M.W. Moore, G.A. Keller, and F.J. de Sauvage. 1997. Normal platelets and megakaryocytes are produced in vivo in the absence of thrombopoietin. *Blood* 90:3423-3429.

Busch, K., K. Klapproth, M. Barile, M. Flossdorf, T. Holland-Letz, S.M. Schlenner, M. Reth, T. Hofer, and H.R. Rodewald. 2015. Fundamental properties of unperturbed haematopoiesis from stem cells in vivo. *Nature* 518:542-546.

Cao, X., X. Wu, D. Frassica, B. Yu, L. Pang, L. Xian, M. Wan, W. Lei, M. Armour, E. Tryggestad, J. Wong, C.Y. Wen, W.W. Lu, and F.J. Frassica. 2011. Irradiation induces bone injury by damaging bone marrow microenvironment for stem cells. *Proc Natl Acad Sci U S A* 108:1609-1614.

Capilla-Gonzalez, V., H. Guerrero-Cazares, J.M. Bonsu, O. Gonzalez-Perez, P. Achanta, J. Wong, J.M. Garcia-Verdugo, and A. Quinones-Hinojosa. 2014. The subventricular zone is able to respond to a demyelinating lesion after localized radiation. *Stem Cells* 32:59-69.

Carlyle, J.R., A.M. Michie, C. Furlonger, T. Nakano, M.J. Lenardo, C.J. Paige, and J.C. Zuniga-Pflucker. 1997. Identification of a novel developmental stage marking lineage commitment of progenitor thymocytes. *J Exp Med* 186:173-182.

Carmel, R. 2001. Anemia and aging: an overview of clinical, diagnostic and biological issues. *Blood Rev* 15:9-18.

Centore, R.C., C.G. Havens, A.L. Manning, J.M. Li, R.L. Flynn, A. Tse, J. Jin, N.J. Dyson, J.C. Walter, and L. Zou. 2010. CRL4(Cdt2)-mediated destruction of the histone methyltransferase Set8 prevents premature chromatin compaction in S phase. *Molecular cell* 40:22-33.

Challen, G.A., N.C. Boles, S.M. Chambers, and M.A. Goodell. 2010. Distinct hematopoietic stem cell subtypes are differentially regulated by TGF-beta1. *Cell Stem Cell* 6:265-278.

Chambers, S.M., C.A. Shaw, C. Gatza, C.J. Fisk, L.A. Donehower, and M.A. Goodell. 2007. Aging hematopoietic stem cells decline in function and exhibit epigenetic dysregulation. *PLoS Biol* 5:e201.

Chen, J., F.M. Ellison, K. Keyvanfar, S.O. Omokaro, M.J. Desierto, M.A. Eckhaus, and N.S. Young. 2008. Enrichment of hematopoietic stem cells with SLAM and LSK markers for the detection of hematopoietic stem cell function in normal and Trp53 null mice. *Exp Hematol* 36:1236-1243.

Cho, R.H., H.B. Sieburg, and C.E. Muller-Sieburg. 2008. A new mechanism for the aging of hematopoietic stem cells: aging changes the clonal composition of the stem cell compartment but not individual stem cells. *Blood* 111:5553-5561.

Choi, E.S., M.M. Hokom, J.L. Nichol, A. Hornkohl, and P. Hunt. 1995. Functional human platelet generation in vitro and regulation of cytoplasmic process formation. *C R Acad Sci III* 318:387-393.

Cohen, A., D. Petsche, T. Grunberger, and M.H. Freedman. 1992. Interleukin 6 induces myeloid differentiation of a human biphenotypic leukemic cell line. *Leuk Res* 16:751-760.

Conboy, I.M., M.J. Conboy, A.J. Wagers, E.R. Girma, I.L. Weissman, and T.A. Rando. 2005. Rejuvenation of aged progenitor cells by exposure to a young systemic environment. *Nature* 433:760-764.

Congdon, L.M., S.I. Houston, C.S. Veerappan, T.M. Spektor, and J.C. Rice. 2010. PR-Set7-mediated monomethylation of histone H4 lysine 20 at specific genomic regions induces transcriptional repression. *J Cell Biochem* 110:609-619.

Corcoran, A.E., F.M. Smart, R.J. Cowling, T. Crompton, M.J. Owen, and A.R. Venkitaraman. 1996. The interleukin-7 receptor alpha chain transmits distinct signals for proliferation and differentiation during B lymphopoiesis. *Embo J* 15:1924-1932.

Coskun, S., H. Chao, H. Vasavada, K. Heydari, N. Gonzales, X. Zhou, B. de Crombrugghe, and K.K. Hirschi. 2014. Development of the fetal bone marrow niche and regulation of HSC quiescence and homing ability by emerging osteolineage cells. *Cell Rep* 9:581-590.

Coulombel, L. 2004. Identification of hematopoietic stem/progenitor cells: strength and drawbacks of functional assays. *Oncogene* 23:7210-7222.

Cumano, A., K. Dorshkind, S. Gillis, and C.J. Paige. 1990. The influence of S17 stromal cells and interleukin 7 on B cell development. *Eur J Immunol* 20:2183-2189.

Dahl, R., J.C. Walsh, D. Lancki, P. Laslo, S.R. Iyer, H. Singh, and M.C. Simon. 2003. Regulation of macrophage and neutrophil cell fates by the PU.1:C/EBPalpha ratio and granulocyte colony-stimulating factor. *Nat Immunol* 4:1029-1036.

Delgado, M.D., and J. Leon. 2010. Myc roles in hematopoiesis and leukemia. *Genes Cancer* 1:605-616.

Dey, B.K., L. Stalker, A. Schnerch, M. Bhatia, J. Taylor-Papidimitriou, and C. Wynder. 2008. The histone demethylase KDM5b/JARID1b plays a role in cell fate decisions by blocking terminal differentiation. *Mol Cell Biol* 28:5312-5327.

Dorshkind, K., E. Montecino-Rodriguez, and R.A. Signer. 2009. The ageing immune system: is it ever too old to become young again? *Nat Rev Immunol* 9:57-62.

Dorssers, L., H. Burger, F. Bot, R. Delwel, A.H. Geurts van Kessel, B. Lowenberg, and G. Wagemaker. 1987. Characterization of a human multilineage-colony-stimulating factor cDNA clone identified by a conserved noncoding sequence in mouse interleukin-3. *Gene* 55:115-124.

Douay, L., N.C. Gorin, J.Y. Mary, E. Lemarie, M. Lopez, A. Najman, J. Stachowiak, M.C. Giarratana, C. Baillou, C. Salmon, and et al. 1986. Recovery of CFU-GM from cryopreserved marrow and in vivo evaluation after autologous bone marrow transplantation are predictive of engraftment. *Exp Hematol* 14:358-365.

Dykstra, B., S. Olthof, J. Schreuder, M. Ritsema, and G. de Haan. 2011. Clonal analysis reveals multiple functional defects of aged murine hematopoietic stem cells. *J Exp Med* 208:2691-2703.

Dzierzak, E., and N.A. Speck. 2008. Of lineage and legacy: the development of mammalian hematopoietic stem cells. *Nat Immunol* 9:129-136.

Ergen, A.V., N.C. Boles, and M.A. Goodell. 2012. Rantes/Ccl5 influences hematopoietic stem cell subtypes and causes myeloid skewing. *Blood* 119:2500-2509.

Ferguson-Smith, A.C., Y.F. Chen, M.S. Newman, L.T. May, P.B. Sehgal, and F.H. Ruddle. 1988. Regional localization of the interferon-beta 2/B-cell stimulatory factor 2/hepatocyte stimulating factor gene to human chromosome 7p15-p21. *Genomics* 2:203-208.

Fernandez, K.S., and P.A. de Alarcon. 2013. Development of the hematopoietic system and disorders of hematopoiesis that present during infancy and early childhood. *Pediatr Clin North Am* 60:1273-1289.

Flach, J., S.T. Bakker, M. Mohrin, P.C. Conroy, E.M. Pietras, D. Reynaud, S. Alvarez, M.E. Diolaiti, F. Ugarte, E.C. Forsberg, M.M. Le Beau, B.A. Stohr, J. Mendez, C.G. Morrison, and E. Passegue. 2014. Replication stress is a potent driver of functional decline in ageing haematopoietic stem cells. *Nature* 512:198-202.

Fraga, M.F., E. Ballestar, M.F. Paz, S. Ropero, F. Setien, M.L. Ballestar, D. Heine-Suner, J.C. Cigudosa, M. Urioste, J. Benitez, M. Boix-Chornet, A. Sanchez-Aguilera, C. Ling, E. Carlsson, P. Poulsen, A. Vaag, Z. Stephan, T.D. Spector, Y.Z. Wu, C. Plass, and M. Esteller. 2005. Epigenetic differences arise during the lifetime of monozygotic twins. *Proc Natl Acad Sci U S A* 102:10604-10609.

Franceschi, C., M. Capri, D. Monti, S. Giunta, F. Olivieri, F. Sevini, M.P. Panourgia, L. Invidia, L. Celani, M. Scurti, E. Cevenini, G.C. Castellani, and S. Salvioli. 2007. Inflammaging and anti-inflammaging: a systemic perspective on aging and longevity emerged from studies in humans. *Mech Ageing Dev* 128:92-105.

Friedman, A.D. 2002. Transcriptional regulation of granulocyte and monocyte development. *Oncogene* 21:3377-3390.

Gekas, C., and T. Graf. 2013. CD41 expression marks myeloid-biased adult hematopoietic stem cells and increases with age. *Blood* 121:4463-4472.

Goldberg, A.D., C.D. Allis, and E. Bernstein. 2007. Epigenetics: a landscape takes shape. *Cell* 128:635-638.

Goronzy, J.J., W.W. Lee, and C.M. Weyand. 2007. Aging and T-cell diversity. *Exp Gerontol* 42:400-406.

Greig, K.T., C.A. de Graaf, J.M. Murphy, M.R. Carpinelli, S.H. Pang, J. Frampton, B.T. Kile, D.J. Hilton, and S.L. Nutt. 2010. Critical roles for c-Myb in lymphoid priming and early B-cell development. *Blood* 115:2796-2805.

Guenther, M.G., W.S. Lane, W. Fischle, E. Verdin, M.A. Lazar, and R. Shiekhattar. 2000. A core SMRT corepressor complex containing HDAC3 and TBL1, a WD40-repeat protein linked to deafness. *Genes Dev* 14:1048-1057.

Hamamoto, R., V. Saloura, and Y. Nakamura. 2015. Critical roles of non-histone protein lysine methylation in human tumorigenesis. *Nat Rev Cancer* 15:110-124.

Hamilton, B.K., L. Rybicki, J. Dabney, L. McLellan, H. Haddad, L. Foster, D. Abounader, M. Kalaycio, R. Sobecks, R. Dean, H. Duong, B.T. Hill, B.J. Bolwell, and E.A. Copelan. 2014. Quality of life and outcomes in patients60 years of age after allogeneic hematopoietic cell transplantation. *Bone Marrow Transplant* 49:1426-1431.

Han, S., K. Yang, Z. Ozen, W. Peng, E. Marinova, G. Kelsoe, and B. Zheng. 2003. Enhanced differentiation of splenic plasma cells but diminished long-lived high-affinity bone marrow plasma cells in aged mice. *J Immunol* 170:1267-1273.

Harker, L.A., L.K. Roskos, U.M. Marzec, R.A. Carter, J.K. Cherry, B. Sundell, E.N. Cheung, D. Terry, and W. Sheridan. 2000. Effects of megakaryocyte growth and development factor on platelet production, platelet life span, and platelet function in healthy human volunteers. *Blood* 95:2514-2522.

Harrison, D.E. 1980. Competitive repopulation: a new assay for long-term stem cell functional capacity. *Blood* 55:77-81.

Helmlinger, D., S. Hardy, S. Sasorith, F. Klein, F. Robert, C. Weber, L. Miguet, N. Potier, A. Van-Dorsselaer, J.M. Wurtz, J.L. Mandel, L. Tora, and D. Devys. 2004. Ataxin-7 is a subunit of GCN5 histone acetyltransferase-containing complexes. *Hum Mol Genet* 13:1257-1265.

Houston, S.I., K.J. McManus, M.M. Adams, J.K. Sims, P.B. Carpenter, M.J. Hendzel, and J.C. Rice. 2008. Catalytic function of the PR-Set7 histone H4 lysine 20 monomethyltransferase is essential for mitotic entry and genomic stability. *J Biol Chem* 283:19478-19488.

Hu, M., D. Krause, M. Greaves, S. Sharkis, M. Dexter, C. Heyworth, and T. Enver. 1997. Multilineage gene expression precedes commitment in the hemopoietic system. *Genes Dev* 11:774-785.

Huang, J., J. Dorsey, S. Chuikov, L. Perez-Burgos, X. Zhang, T. Jenuwein, D. Reinberg, and S.L. Berger. 2010. G9a and Glp methylate lysine 373 in the tumor suppressor p53. *J Biol Chem* 285:9636-9641.

Iwasaki, H., S. Mizuno, Y. Arinobu, H. Ozawa, Y. Mori, H. Shigematsu, K. Takatsu, D.G. Tenen, and K. Akashi. 2006. The order of expression of transcription factors directs hierarchical specification of hematopoietic lineages. *Genes Dev* 20:3010-3021.

Jones, R.J., J.E. Wagner, P. Celano, M.S. Zicha, and S.J. Sharkis. 1990. Separation of pluripotent haematopoietic stem cells from spleen colony-forming cells. *Nature* 347:188-189.

Jordan, C.T., J.P. McKearn, and I.R. Lemischka. 1990. Cellular and developmental properties of fetal hematopoietic stem cells. *Cell* 61:953-963.
Jorgensen, S., I. Elvers, M.B. Trelle, T. Menzel, M. Eskildsen, O.N. Jensen, T. Helleday, K. Helin, and C.S. Sorensen. 2007. The histone methyltransferase SET8 is required for S-phase progression. *J Cell Biol* 179:1337-1345.
Jorgensen, S., G. Schotta, and C.S. Sorensen. 2013. Histone H4 lysine 20 methylation: key player in epigenetic regulation of genomic integrity. *Nucleic Acids Res* 41:2797-2806.
Karachentsev, D., K. Sarma, D. Reinberg, and R. Steward. 2005. PR-Set7-dependent methylation of histone H4 Lys 20 functions in repression of gene expression and is essential for mitosis. *Genes Dev* 19:431-435.
Kari, V., A. Shchebet, H. Neumann, and S.A. Johnsen. 2011. The H2B ubiquitin ligase RNF40 cooperates with SUPT16H to induce dynamic changes in chromatin structure during DNA double-strand break repair. *Cell Cycle* 10:3495-3504.
Kent, D., M. Copley, C. Benz, B. Dykstra, M. Bowie, and C. Eaves. 2008. Regulation of hematopoietic stem cells by the steel factor/KIT signaling pathway. *Clin Cancer Res* 14:1926-1930.
Kiel, M.J., O.H. Yilmaz, T. Iwashita, C. Terhorst, and S.J. Morrison. 2005. SLAM family receptors distinguish hematopoietic stem and progenitor cells and reveal endothelial niches for stem cells. *Cell* 121:1109-1121.
Kim, J.D., E. Kim, S. Koun, H.J. Ham, M. Rhee, M.J. Kim, and T.L. Huh. 2015. Proper Activity of Histone H3 Lysine 4 (H3K4) Methyltransferase Is Required for Morphogenesis during Zebrafish Cardiogenesis. *Mol Cells* 38:580-586.
Kim, M., H.B. Moon, and G.J. Spangrude. 2003. Major age-related changes of mouse hematopoietic stem/progenitor cells. *Ann N Y Acad Sci* 996:195-208.
Kodama, H., M. Nose, S. Niida, and S. Nishikawa. 1994. Involvement of the c-kit receptor in the adhesion of hematopoietic stem cells to stromal cells. *Exp Hematol* 22:979-984.
Koleva, R.I., S.B. Ficarro, H.S. Radomska, M.J. Carrasco-Alfonso, J.A. Alberta, J.T. Webber, C.J. Luckey, G. Marcucci, D.G. Tenen, and J.A. Marto. 2012. C/EBPalpha and DEK coordinately regulate myeloid differentiation. *Blood* 119:4878-4888.
Kondo, M., I.L. Weissman, and K. Akashi. 1997. Identification of clonogenic common lymphoid progenitors in mouse bone marrow. *Cell* 91:661-672.
Kowalczyk, M.S., I. Tirosh, D. Heckl, T.N. Rao, A. Dixit, B.J. Haas, R.K. Schneider, A.J. Wagers, B.L. Ebert, and A. Regev. 2015. Single-cell RNA-seq reveals changes in cell cycle and differentiation programs upon aging of hematopoietic stem cells. *Genome Res* 25:1860-1872.
Laslo, P., C.J. Spooner, A. Warmflash, D.W. Lancki, H.J. Lee, R. Sciammas, B.N. Gantner, A.R. Dinner, and H. Singh. 2006. Multilineage transcriptional priming and determination of alternate hematopoietic cell fates. *Cell* 126:755-766.
Lee, J.H., and D.G. Skalnik. 2005. CpG-binding protein (CXXC finger protein 1) is a component of the mammalian Set1 histone H3-Lys4 methyltransferase complex, the analogue of the yeast Set1/COMPASS complex. *J Biol Chem* 280:41725-41731.

Lemischka, I.R., D.H. Raulet, and R.C. Mulligan. 1986. Developmental potential and dynamic behavior of hematopoietic stem cells. *Cell* 45:917-927.
Levine, A.J. 1997. p53, the cellular gatekeeper for growth and division. *Cell* 88:323-331.
Li, Z., F. Nie, S. Wang, and L. Li. 2011. Histone H4 Lys 20 monomethylation by histone methylase SET8 mediates Wnt target gene activation. *Proceedings of the National Academy of Sciences of the United States of America* 108:3116-3123.
Liang, Y., G. Van Zant, and S.J. Szilvassy. 2005. Effects of aging on the homing and engraftment of murine hematopoietic stem and progenitor cells. *Blood* 106:1479-1487.
Liu, W., B. Tanasa, O.V. Tyurina, T.Y. Zhou, R. Gassmann, W.T. Liu, K.A. Ohgi, C. Benner, I. Garcia-Bassets, A.K. Aggarwal, A. Desai, P.C. Dorrestein, C.K. Glass, and M.G. Rosenfeld. 2010. PHF8 mediates histone H4 lysine 20 demethylation events involved in cell cycle progression. *Nature* 466:508-512.
Liu, Y., S.E. Elf, T. Asai, Y. Miyata, G. Sashida, G. Huang, S. Di Giandomenico, A. Koff, and S.D. Nimer. 2009. The p53 tumor suppressor protein is a critical regulator of hematopoietic stem cell behavior. *Cell Cycle* 8:3120-3124.
Loder, F., B. Mutschler, R.J. Ray, C.J. Paige, P. Sideras, R. Torres, M.C. Lamers, and R. Carsetti. 1999. B cell development in the spleen takes place in discrete steps and is determined by the quality of B cell receptor-derived signals. *J Exp Med* 190:75-89.
Lu, X., M.D. Simon, J.V. Chodaparambil, J.C. Hansen, K.M. Shokat, and K. Luger. 2008. The effect of H3K79 dimethylation and H4K20 trimethylation on nucleosome and chromatin structure. *Nat Struct Mol Biol* 15:1122-1124.
Lyman, S.D., L. James, L. Johnson, K. Brasel, P. de Vries, S.S. Escobar, H. Downey, R.R. Splett, M.P. Beckmann, and H.J. McKenna. 1994. Cloning of the human homologue of the murine flt3 ligand: a growth factor for early hematopoietic progenitor cells. *Blood* 83:2795-2801.
Lynch, H.E., G.L. Goldberg, A. Chidgey, M.R. Van den Brink, R. Boyd, and G.D. Sempowski. 2009. Thymic involution and immune reconstitution. *Trends Immunol* 30:366-373.
Malik, J., M. Getman, and L.A. Steiner. 2015. Histone methyltransferase Setd8 represses Gata2 expression and regulates erythroid maturation. *Molecular and cellular biology* 35:2059-2072.
Mansson, R., A. Hultquist, S. Luc, L. Yang, K. Anderson, S. Kharazi, S. Al-Hashmi, K. Liuba, L. Thoren, J. Adolfsson, N. Buza-Vidas, H. Qian, S. Soneji, T. Enver, M. Sigvardsson, and S.E. Jacobsen. 2007. Molecular evidence for hierarchical transcriptional lineage priming in fetal and adult stem cells and multipotent progenitors. *Immunity* 26:407-419.
McCulloch, E.A., L. Siminovitch, and J.E. Till. 1964. Spleen-Colony Formation in Anemic Mice of Genotype Ww. *Science* 144:844-846.
McCulloch, E.A., and J.E. Till. 1964. Proliferation of Hemopoietic Colony-Forming Cells Transplanted into Irradiated Mice. *Radiat Res* 22:383-397.

McGraw, S., G. Morin, C. Vigneault, P. Leclerc, and M.A. Sirard. 2007. Investigation of MYST4 histone acetyltransferase and its involvement in mammalian gametogenesis. *BMC Dev Biol* 7:123.
Mercer, E.M., Y.C. Lin, C. Benner, S. Jhunjhunwala, J. Dutkowski, M. Flores, M. Sigvardsson, T. Ideker, C.K. Glass, and C. Murre. 2011. Multilineage priming of enhancer repertoires precedes commitment to the B and myeloid cell lineages in hematopoietic progenitors. *Immunity* 35:413-425.
Milite, C., A. Feoli, M. Viviano, D. Rescigno, A. Cianciulli, A.L. Balzano, A. Mai, S. Castellano, and G. Sbardella. 2016. The emerging role of lysine methyltransferase SETD8 in human diseases. *Clin Epigenetics* 8:102.
Mocchegiani, E., and M. Malavolta. 2004. NK and NKT cell functions in immunosenescence. *Aging Cell* 3:177-184.
Moore, M.A. 2009. Stem cell proliferation: Ex vivo and in vivo observations. *Stem Cells* 15:
Morita, Y., H. Ema, and H. Nakauchi. 2010. Heterogeneity and hierarchy within the most primitive hematopoietic stem cell compartment. *J Exp Med* 207:1173-1182.
Morrison, S.J., A.M. Wandycz, K. Akashi, A. Globerson, and I.L. Weissman. 1996. The aging of hematopoietic stem cells. *Nat Med* 2:1011-1016.
Nahi, H., G. Selivanova, S. Lehmann, L. Mollgard, S. Bengtzen, H. Concha, A. Svensson, K.G. Wiman, M. Merup, and C. Paul. 2008. Mutated and non-mutated TP53 as targets in the treatment of leukaemia. *Br J Haematol* 141:445-453.
Neff, T., and S.A. Armstrong. 2013. Recent progress toward epigenetic therapies: the example of mixed lineage leukemia. *Blood* 121:4847-4853.
Nemeth, M.J., M.R. Kirby, and D.M. Bodine. 2006. Hmgb3 regulates the balance between hematopoietic stem cell self-renewal and differentiation. *Proc Natl Acad Sci U S A* 103:13783-13788.
Ng, S.Y., T. Yoshida, J. Zhang, and K. Georgopoulos. 2009. Genome-wide lineage-specific transcriptional networks underscore Ikaros-dependent lymphoid priming in hematopoietic stem cells. *Immunity* 30:493-507.
Nijnik, A., L. Woodbine, C. Marchetti, S. Dawson, T. Lambe, C. Liu, N.P. Rodrigues, T.L. Crockford, E. Cabuy, A. Vindigni, T. Enver, J.I. Bell, P. Slijepcevic, C.C. Goodnow, P.A. Jeggo, and R.J. Cornall. 2007. DNA repair is limiting for haematopoietic stem cells during ageing. *Nature* 447:686-690.
Nishikawa, S., M. Nakasato, N. Takakura, M. Ogawa, and H. Kodama. 1994. Stromal cell-dependent bone marrow culture with a nearly protein-free defined medium. *Immunol Lett* 40:163-169.
Nishioka, K., S. Chuikov, K. Sarma, H. Erdjument-Bromage, C.D. Allis, P. Tempst, and D. Reinberg. 2002. Set9, a novel histone H3 methyltransferase that facilitates transcription by precluding histone tail modifications required for heterochromatin formation. *Genes Dev* 16:479-489.
Notta, F., S. Zandi, N. Takayama, S. Dobson, O.I. Gan, G. Wilson, K.B. Kaufmann, J. McLeod, E. Laurenti, C.F. Dunant, J.D. McPherson, L.D. Stein, Y. Dror, and J.E. Dick. 2016. Distinct routes of lineage development reshape the human blood hierarchy across ontogeny. *Science* 351:aab2116.

Oda, H., M.R. Hubner, D.B. Beck, M. Vermeulen, J. Hurwitz, D.L. Spector, and D. Reinberg. 2010. Regulation of the histone H4 monomethylase PR-Set7 by CRL4(Cdt2)-mediated PCNA-dependent degradation during DNA damage. *Mol Cell* 40:364-376.

Oda, H., I. Okamoto, N. Murphy, J. Chu, S.M. Price, M.M. Shen, M.E. Torres-Padilla, E. Heard, and D. Reinberg. 2009. Monomethylation of histone H4-lysine 20 is involved in chromosome structure and stability and is essential for mouse development. *Mol Cell Biol* 29:2278-2295.

Or, R., A. Abdul-Hai, and A. Ben-Yehuda. 1998. Reviewing the potential utility of interleukin-7 as a promoter of thymopoiesis and immune recovery. *Cytokines Cell Mol Ther* 4:287-294.

Pang, W.W., E.A. Price, D. Sahoo, I. Beerman, W.J. Maloney, D.J. Rossi, S.L. Schrier, and I.L. Weissman. 2011. Human bone marrow hematopoietic stem cells are increased in frequency and myeloid-biased with age. *Proc Natl Acad Sci U S A* 108:20012-20017.

Paul, F., Y. Arkin, A. Giladi, D.A. Jaitin, E. Kenigsberg, H. Keren-Shaul, D. Winter, D. Lara-Astiaso, M. Gury, A. Weiner, E. David, N. Cohen, F.K. Lauridsen, S. Haas, A. Schlitzer, A. Mildner, F. Ginhoux, S. Jung, A. Trumpp, B.T. Porse, A. Tanay, and I. Amit. 2015. Transcriptional Heterogeneity and Lineage Commitment in Myeloid Progenitors. *Cell* 163:1663-1677.

Pelanda, R., and R.M. Torres. 2012. Central B-cell tolerance: where selection begins. *Cold Spring Harb Perspect Biol* 4:a007146.

Pesavento, J.J., H. Yang, N.L. Kelleher, and C.A. Mizzen. 2008. Certain and progressive methylation of histone H4 at lysine 20 during the cell cycle. *Molecular and cellular biology* 28:468-486.

Pietras, E.M., D. Reynaud, Y.A. Kang, D. Carlin, F.J. Calero-Nieto, A.D. Leavitt, J.M. Stuart, B. Gottgens, and E. Passegue. 2015a. Functionally Distinct Subsets of Lineage-Biased Multipotent Progenitors Control Blood Production in Normal and Regenerative Conditions. *Cell Stem Cell* 17:35-46.

Pietras, E.M., D. Reynaud, Y.A. Kang, D. Carlin, F.J. Calero-Nieto, A.D. Leavitt, J.M. Stuart, B. Gottgens, and E. Passegue. 2015b. Functionally Distinct Subsets of Lineage-Biased Multipotent Progenitors Control Blood Production in Normal and Regenerative Conditions (vol 17, pg 35, 2015). *Cell Stem Cell* 17:246-246.

Pinheiro, I., R. Margueron, N. Shukeir, M. Eisold, C. Fritzsch, F.M. Richter, G. Mittler, C. Genoud, S. Goyama, M. Kurokawa, J. Son, D. Reinberg, M. Lachner, and T. Jenuwein. 2012. Prdm3 and Prdm16 are H3K9me1 methyltransferases required for mammalian heterochromatin integrity. *Cell* 150:948-960.

Ploemacher, R.E., J.P. van der Sluijs, J.S. Voerman, and N.H. Brons. 1989. An in vitro limiting-dilution assay of long-term repopulating hematopoietic stem cells in the mouse. *Blood* 74:2755-2763.

Purton, L.E., and D.T. Scadden. 2007. Limiting factors in murine hematopoietic stem cell assays. *Cell Stem Cell* 1:263-270.

Qian, C., and M.M. Zhou. 2006. SET domain protein lysine methyltransferases: Structure, specificity and catalysis. *Cell Mol Life Sci* 63:2755-2763.

Quentmeier, H., H.G. Drexler, D. Fleckenstein, M. Zaborski, A. Armstrong, J.E. Sims, and S.D. Lyman. 2001. Cloning of human thymic stromal lymphopoietin

(TSLP) and signaling mechanisms leading to proliferation. *Leukemia* 15:1286-1292.
Randall, T.D., and I.L. Weissman. 1997. Phenotypic and functional changes induced at the clonal level in hematopoietic stem cells after 5-fluorouracil treatment. *Blood* 89:3596-3606.
Rea, S., F. Eisenhaber, D. O'Carroll, B.D. Strahl, Z.W. Sun, M. Schmid, S. Opravil, K. Mechtler, C.P. Ponting, C.D. Allis, and T. Jenuwein. 2000. Regulation of chromatin structure by site-specific histone H3 methyltransferases. *Nature* 406:593-599.
Rebel, V.I., A.L. Kung, E.A. Tanner, H. Yang, R.T. Bronson, and D.M. Livingston. 2002. Distinct roles for CREB-binding protein and p300 in hematopoietic stem cell self-renewal. *Proc Natl Acad Sci U S A* 99:14789-14794.
Reed, S.M., and D.E. Quelle. 2014. p53 Acetylation: Regulation and Consequences. *Cancers (Basel)* 7:30-69.
Reya, T., S.J. Morrison, M.F. Clarke, and I.L. Weissman. 2001. Stem cells, cancer, and cancer stem cells. *Nature* 414:105-111.
Reynaud, D., I.A. Demarco, K.L. Reddy, H. Schjerven, E. Bertolino, Z. Chen, S.T. Smale, S. Winandy, and H. Singh. 2008. Regulation of B cell fate commitment and immunoglobulin heavy-chain gene rearrangements by Ikaros. *Nat Immunol* 9:927-936.
Rice, J.C., K. Nishioka, K. Sarma, R. Steward, D. Reinberg, and C.D. Allis. 2002. Mitotic-specific methylation of histone H4 Lys 20 follows increased PR-Set7 expression and its localization to mitotic chromosomes. *Genes Dev* 16:2225-2230.
Richie Ehrlich, L.I., T. Serwold, and I.L. Weissman. 2011. In vitro assays misrepresent in vivo lineage potentials of murine lymphoid progenitors. *Blood* 117:2618-2624.
Rossi, D.J., D. Bryder, J.M. Zahn, H. Ahlenius, R. Sonu, A.J. Wagers, and I.L. Weissman. 2005. Cell intrinsic alterations underlie hematopoietic stem cell aging. *Proc Natl Acad Sci U S A* 102:9194-9199.
Rossi, D.J., C.H. Jamieson, and I.L. Weissman. 2008. Stems cells and the pathways to aging and cancer. *Cell* 132:681-696.
Rothenberg, E.V., J.E. Moore, and M.A. Yui. 2008. Launching the T-cell-lineage developmental programme. *Nat Rev Immunol* 8:9-21.
Sahin, E., and R.A. Depinho. 2010. Linking functional decline of telomeres, mitochondria and stem cells during ageing. *Nature* 464:520-528.
Sahoo, D., D.L. Dill, R. Tibshirani, and S.K. Plevritis. 2007. Extracting binary signals from microarray time-course data. *Nucleic Acids Res* 35:3705-3712.
Sanjuan-Pla, A., I.C. Macaulay, C.T. Jensen, P.S. Woll, T.C. Luis, A. Mead, S. Moore, C. Carella, S. Matsuoka, T. Bouriez Jones, O. Chowdhury, L. Stenson, M. Lutteropp, J.C. Green, R. Facchini, H. Boukarabila, A. Grover, A. Gambardella, S. Thongjuea, J. Carrelha, P. Tarrant, D. Atkinson, S.A. Clark, C. Nerlov, and S.E. Jacobsen. 2013. Platelet-biased stem cells reside at the apex of the haematopoietic stem-cell hierarchy. *Nature* 502:232-236.
Schmitt, T.M., and J.C. Zuniga-Pflucker. 2002. Induction of T cell development from hematopoietic progenitor cells by delta-like-1 in vitro. *Immunity* 17:749-756.

Schotta, G., M. Lachner, K. Sarma, A. Ebert, R. Sengupta, G. Reuter, D. Reinberg, and T. Jenuwein. 2004. A silencing pathway to induce H3-K9 and H4-K20 trimethylation at constitutive heterochromatin. *Genes Dev* 18:1251-1262.

Schotta, G., R. Sengupta, S. Kubicek, S. Malin, M. Kauer, E. Callen, A. Celeste, M. Pagani, S. Opravil, I.A. De La Rosa-Velazquez, A. Espejo, M.T. Bedford, A. Nussenzweig, M. Busslinger, and T. Jenuwein. 2008. A chromatin-wide transition to H4K20 monomethylation impairs genome integrity and programmed DNA rearrangements in the mouse. *Genes Dev* 22:2048-2061.

Scott, E.W., M.C. Simon, J. Anastasi, and H. Singh. 1994. Requirement of transcription factor PU.1 in the development of multiple hematopoietic lineages. *Science* 265:1573-1577.

Scott, L.M., C.I. Civin, P. Rorth, and A.D. Friedman. 1992. A novel temporal expression pattern of three C/EBP family members in differentiating myelomonocytic cells. *Blood* 80:1725-1735.

Seifert, H., B. Mohr, C. Thiede, U. Oelschlagel, U. Schakel, T. Illmer, S. Soucek, G. Ehninger, and M. Schaich. 2009. The prognostic impact of 17p (p53) deletion in 2272 adults with acute myeloid leukemia. *Leukemia* 23:656-663.

Seita, J., D. Sahoo, D.J. Rossi, D. Bhattacharya, T. Serwold, M.A. Inlay, L.I. Ehrlich, J.W. Fathman, D.L. Dill, and I.L. Weissman. 2012. Gene Expression Commons: an open platform for absolute gene expression profiling. *PLoS One* 7:e40321.

Shen, X., Y. Liu, Y.J. Hsu, Y. Fujiwara, J. Kim, X. Mao, G.C. Yuan, and S.H. Orkin. 2008. EZH1 mediates methylation on histone H3 lysine 27 and complements EZH2 in maintaining stem cell identity and executing pluripotency. *Mol Cell* 32:491-502.

Shi, X., I. Kachirskaia, H. Yamaguchi, L.E. West, H. Wen, E.W. Wang, S. Dutta, E. Appella, and O. Gozani. 2007. Modulation of p53 function by SET8-mediated methylation at lysine 382. *Mol Cell* 27:636-646.

Stewart, M.H., M. Albert, P. Sroczynska, V.A. Cruickshank, Y. Guo, D.J. Rossi, K. Helin, and T. Enver. 2015. The histone demethylase Jarid1b is required for hematopoietic stem cell self-renewal in mice. *Blood* 125:2075-2078.

Subramanian, A., H. Kuehn, J. Gould, P. Tamayo, and J.P. Mesirov. 2007. GSEA-P: a desktop application for Gene Set Enrichment Analysis. *Bioinformatics* 23:3251-3253.

Subramanian, A., P. Tamayo, V.K. Mootha, S. Mukherjee, B.L. Ebert, M.A. Gillette, A. Paulovich, S.L. Pomeroy, T.R. Golub, E.S. Lander, and J.P. Mesirov. 2005. Gene set enrichment analysis: a knowledge-based approach for interpreting genome-wide expression profiles. *Proceedings of the National Academy of Sciences of the United States of America* 102:15545-15550.

Sudo, K., H. Ema, Y. Morita, and H. Nakauchi. 2000. Age-associated characteristics of murine hematopoietic stem cells. *J Exp Med* 192:1273-1280.

Sun, D., M. Luo, M. Jeong, B. Rodriguez, Z. Xia, R. Hannah, H. Wang, T. Le, K.F. Faull, R. Chen, H. Gu, C. Bock, A. Meissner, B. Gottgens, G.J. Darlington, W. Li, and M.A. Goodell. 2014a. Epigenomic profiling of young and aged HSCs reveals concerted changes during aging that reinforce self-renewal. *Cell Stem Cell* 14:673-688.

Sun, J., A. Ramos, B. Chapman, J.B. Johnnidis, L. Le, Y.J. Ho, A. Klein, O. Hofmann, and F.D. Camargo. 2014b. Clonal dynamics of native haematopoiesis. *Nature* 514:322-327.

Sutherland, H.J., C.J. Eaves, A.C. Eaves, W. Dragowska, and P.M. Lansdorp. 1989. Characterization and partial purification of human marrow cells capable of initiating long-term hematopoiesis in vitro. *Blood* 74:1563-1570.

Takawa, M., H.S. Cho, S. Hayami, G. Toyokawa, M. Kogure, Y. Yamane, Y. Iwai, K. Maejima, K. Ueda, A. Masuda, N. Dohmae, H.I. Field, T. Tsunoda, T. Kobayashi, T. Akasu, M. Sugiyama, S. Ohnuma, Y. Atomi, B.A. Ponder, Y. Nakamura, and R. Hamamoto. 2012. Histone lysine methyltransferase SETD8 promotes carcinogenesis by deregulating PCNA expression. *Cancer Res* 72:3217-3227.

TeKippe, M., D.E. Harrison, and J. Chen. 2003. Expansion of hematopoietic stem cell phenotype and activity in Trp53-null mice. *Exp Hematol* 31:521-527.

Tobler, A., C.W. Miller, K.R. Johnson, M.E. Selsted, G. Rovera, and H.P. Koeffler. 1988. Regulation of gene expression of myeloperoxidase during myeloid differentiation. *J Cell Physiol* 136:215-225.

Trowbridge, J.J., J.W. Snow, J. Kim, and S.H. Orkin. 2009. DNA methyltransferase 1 is essential for and uniquely regulates hematopoietic stem and progenitor cells. *Cell Stem Cell* 5:442-449.

Tsang, J.C., Y. Yu, S. Burke, F. Buettner, C. Wang, A.A. Kolodziejczyk, S.A. Teichmann, L. Lu, and P. Liu. 2015. Single-cell transcriptomic reconstruction reveals cell cycle and multi-lineage differentiation defects in Bcl11a-deficient hematopoietic stem cells. *Genome Biol* 16:178.

Tuljapurkar, S.R., T.R. McGuire, S.K. Brusnahan, J.D. Jackson, K.L. Garvin, M.A. Kessinger, J.T. Lane, O.K. BJ, and J.G. Sharp. 2011. Changes in human bone marrow fat content associated with changes in hematopoietic stem cell numbers and cytokine levels with aging. *J Anat* 219:574-581.

Uetsuki, T., K. Takagi, H. Sugiura, and K. Yoshikawa. 1996. Structure and expression of the mouse necdin gene. Identification of a postmitotic neuron-restrictive core promoter. *J Biol Chem* 271:918-924.

Uyemura, K., S.C. Castle, and T. Makinodan. 2002. The frail elderly: role of dendritic cells in the susceptibility of infection. *Mech Ageing Dev* 123:955-962.

van Os, R., L.M. Kamminga, and G. de Haan. 2004. Stem cell assays: something old, something new, something borrowed. *Stem Cells* 22:1181-1190.

Van Zant, G., and Y. Liang. 2012. Concise review: hematopoietic stem cell aging, life span, and transplantation. *Stem Cells Transl Med* 1:651-657.

Vilagos, B., M. Hoffmann, A. Souabni, Q. Sun, B. Werner, J. Medvedovic, I. Bilic, M. Minnich, E. Axelsson, M. Jaritz, and M. Busslinger. 2012. Essential role of EBF1 in the generation and function of distinct mature B cell types. *J Exp Med* 209:775-792.

Wagner, W., S. Bork, P. Horn, D. Krunic, T. Walenda, A. Diehlmann, V. Benes, J. Blake, F.X. Huber, V. Eckstein, P. Boukamp, and A.D. Ho. 2009. Aging and replicative senescence have related effects on human stem and progenitor cells. *PLoS One* 4:e5846.

Wagner, W., P. Horn, S. Bork, and A.D. Ho. 2008. Aging of hematopoietic stem cells is regulated by the stem cell niche. *Exp Gerontol* 43:974-980.

West, L.E., and O. Gozani. 2011. Regulation of p53 function by lysine methylation. *Epigenomics* 3:361-369.
West, L.E., S. Roy, K. Lachmi-Weiner, R. Hayashi, X. Shi, E. Appella, T.G. Kutateladze, and O. Gozani. 2010. The MBT repeats of L3MBTL1 link SET8-mediated p53 methylation at lysine 382 to target gene repression. *J Biol Chem* 285:37725-37732.
Whitfield, M.L., G. Sherlock, A.J. Saldanha, J.I. Murray, C.A. Ball, K.E. Alexander, J.C. Matese, C.M. Perou, M.M. Hurt, P.O. Brown, and D. Botstein. 2002. Identification of genes periodically expressed in the human cell cycle and their expression in tumors. *Molecular biology of the cell* 13:1977-2000.
Wilson, A., E. Laurenti, G. Oser, R.C. van der Wath, W. Blanco-Bose, M. Jaworski, S. Offner, C.F. Dunant, L. Eshkind, E. Bockamp, P. Lio, H.R. Macdonald, and A. Trumpp. 2008. Hematopoietic stem cells reversibly switch from dormancy to self-renewal during homeostasis and repair. *Cell* 135:1118-1129.
Wilson, A., M.J. Murphy, T. Oskarsson, K. Kaloulis, M.D. Bettess, G.M. Oser, A.C. Pasche, C. Knabenhans, H.R. Macdonald, and A. Trumpp. 2004. c-Myc controls the balance between hematopoietic stem cell self-renewal and differentiation. *Genes Dev* 18:2747-2763.
Won, K.J., S.W. Park, S. Lee, I.K. Kong, J.I. Chae, B. Kim, E.J. Lee, and D.K. Kim. 2015. A New Triggering Receptor Expressed on Myeloid Cells (TREM) Family Member, TLT-6, is Involved in Activation and Proliferation of Macrophages. *Immune Netw* 15:232-240.
Wu, K., S. Katiyar, A. Witkiewicz, A. Li, P. McCue, L.N. Song, L. Tian, M. Jin, and R.G. Pestell. 2009. The cell fate determination factor dachshund inhibits androgen receptor signaling and prostate cancer cellular growth. *Cancer Res* 69:3347-3355.
Wu, L. 2006. T lineage progenitors: the earliest steps en route to T lymphocytes. *Curr Opin Immunol* 18:121-126.
Xing, Z., M.A. Ryan, D. Daria, K.J. Nattamai, G. Van Zant, L. Wang, Y. Zheng, and H. Geiger. 2006. Increased hematopoietic stem cell mobilization in aged mice. *Blood* 108:2190-2197.
Yahata, T., T. Takanashi, Y. Muguruma, A.A. Ibrahim, H. Matsuzawa, T. Uno, Y. Sheng, M. Onizuka, M. Ito, S. Kato, and K. Ando. 2011. Accumulation of oxidative DNA damage restricts the self-renewal capacity of human hematopoietic stem cells. *Blood* 118:2941-2950.
Yin, Y., V.C. Yu, G. Zhu, and D.C. Chang. 2008. SET8 plays a role in controlling G1/S transition by blocking lysine acetylation in histone through binding to H4 N-terminal tail. *Cell cycle* 7:1423-1432.
Yu, N., P. Huangyang, X. Yang, X. Han, R. Yan, H. Jia, Y. Shang, and L. Sun. 2013. microRNA-7 suppresses the invasive potential of breast cancer cells and sensitizes cells to DNA damages by targeting histone methyltransferase SET8. *The Journal of biological chemistry* 288:19633-19642.
Zimmer, S.N., Q. Zhou, T. Zhou, Z. Cheng, S.L. Abboud-Werner, D. Horn, M. Lecocke, R. White, A.V. Krivtsov, S.A. Armstrong, A.L. Kung, D.M. Livingston, and V.I. Rebel. 2011. Crebbp haploinsufficiency in mice alters the bone marrow

microenvironment, leading to loss of stem cells and excessive myelopoiesis. *Blood* 118:69-79.

Zohren, F., G.P. Souroullas, M. Luo, U. Gerdemann, M.R. Imperato, N.K. Wilson, B. Gottgens, G.L. Lukov, and M.A. Goodell. 2012. The transcription factor Lyl-1 regulates lymphoid specification and the maintenance of early T lineage progenitors. *Nat Immunol* 13:761-769.